

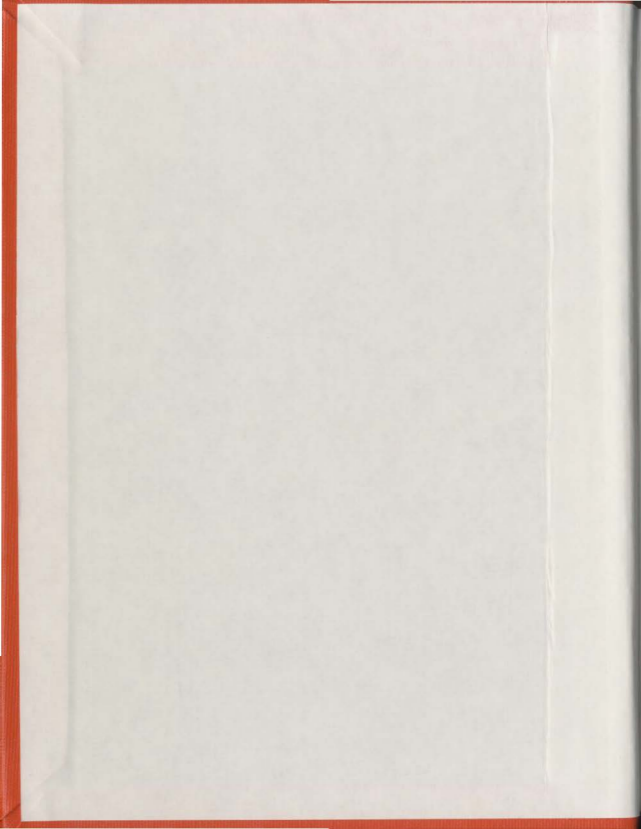
EFFECT OF THE LOSS OF TETHER  
STIFFNESS ON THE BEHAVIOR OF  
A TENSION LEG PLATFORM

CENTRE FOR NEWFOUNDLAND STUDIES

TOTAL OF 10 PAGES ONLY  
MAY BE XEROXED

(Without Author's Permission)

NITINDRA R. JOGLEKAR



CONF





## CANADIAN THESES ON MICROFICHE

I.S.B.N.

## THESES CANADIENNES SUR MICROFICHE



National Library of Canada  
Collections Development Branch

Canadian Theses on  
Microfiche Service

Ottawa, Canada  
K1A 0N4

Bibliothèque nationale du Canada  
Direction du développement des collections

Service des thèses canadiennes  
sur microfiche

### NOTICE

The quality of this microfiche is heavily dependent upon the quality of the original thesis submitted for microfilming. Every effort has been made to ensure the highest quality of reproduction possible.

If pages are missing, contact the university which granted the degree.

Some pages may have indistinct print especially if the original pages were typed with a poor typewriter ribbon or if the university sent us a poor photocopy.

Previously copyrighted materials (journal articles, published tests, etc.) are not filmed.

Reproduction in full or in part of this film is governed by the Canadian Copyright Act, R.S.C. 1970, c. C-30. Please read the authorization forms which accompany this thesis.

THIS DISSERTATION  
HAS BEEN MICROFILMED  
EXACTLY AS RECEIVED

### AVIS

La qualité de cette microfiche dépend grandement de la qualité de la thèse soumise au microfilmage. Nous avons tout fait pour assurer une qualité supérieure de reproduction.

Si il manque des pages, veuillez communiquer avec l'université qui a conféré le grade.

La qualité d'impression de certaines pages peut laisser à désirer, surtout si les pages originales ont été dactylographiées à l'aide d'un ruban usé ou si l'université nous a fait parvenir une photocopie de mauvaise qualité.

Les documents qui font déjà l'objet d'un droit d'auteur (articles de revue, examens publiés, etc.) ne sont pas microfilmés.

La reproduction, même partielle, de ce microfilm est soumise à la Loi canadienne sur le droit d'auteur, SRC 1970, c. C-30. Veuillez prendre connaissance des formules d'autorisation qui accompagnent cette thèse.

LA THÈSE A ÉTÉ  
MICROFILMÉE TELLE QUE  
NOUS L'AVONS RECUE

**EFFECT OF THE LOSS OF TETHER STIFFNESS  
ON THE BEHAVIOR OF A TENSION LEG PLATFORM**

BY

© Nitindra R. Joglekar, B.Tech. (Hons)

A Thesis submitted to the School of Graduate Studies  
in partial fulfillment of the requirements  
for the degree of  
Master of Engineering

Faculty of Engineering and Applied Science  
Memorial University of Newfoundland

August, 1984

St. John's

Newfoundland

Canada

## ABSTRACT

A numerical model for the hydrodynamic analysis of a Tension Leg Platform has been implemented using strip theory. A computer algorithm has been developed using beam elements for a large displacement nonlinear analysis of the cable network.

A parametric study of the platform motion response and tension variations has been made for cases of loss in the cable stiffness. It has been shown that if the total tension remains constant, the surge motion will not be affected but the heave and pitch motions will be increased and tether tensions will vary significantly. The tether tensions are affected by the lateral cable dynamics.

ACKNOWLEDGEMENT

The author wishes to express his sincere gratitude to Dr. M. Booton for his supervision, support and encouragement during the entire course of this work. Sincere thanks are due to Dr. G. R. Peters, Dean of Engineering and Applied Sciences and Dr. T. R. Chari, Associate Dean of Engineering and Applied Sciences for their encouragement.

The author is indebted to Dr. F. A. Aldrich, Dean of Graduate studies for awarding a university fellowship for the past two years.

The author wishes to extend his deep appreciation to Dr. A. S. J. Swamidas, visiting Research fellow, Dr. K. Munaswamy, post doctoral fellow and Mr. A. Allievi, fellow graduate student for their valuable suggestions and helpful discussions and to Levinia Vatcher for the typing of the manuscript.



iv

CONTENTS

	<u>Page</u>
ABSTRACT	ii
ACKNOWLEDGEMENT	iii
LIST OF TABLES	vi
LIST OF FIGURES	vii
NOMENCLATURE	ix
CHAPTER 1 INTRODUCTION	1
1.1 Background	1
1.2 Objectives	2
CHAPTER 2 LITERATURE REVIEW	3
2.1 Environmental Loads and Response	3
2.2 Modelling of the Tether	7
CHAPTER 3 THE TENSION LEG PLATFORM	10
3.1 The Design Philosophy	10
3.2 General Description	11
3.3 The Tether System	13
CHAPTER 4 PROBLEM FORMULATION	16
4.1 Introduction	16
4.2 Linear Model	17
4.2.1 The Constituent Forces	17
4.2.2 The Equation of Motion	19
4.2.3 Tether Stiffness Model	20
4.3 Nonlinear Model	22
4.3.1 Assumptions	22
4.3.2 The Finite Element Model	24
4.3.3 The Time Integration Scheme	26
4.4 Numerical Analysis	29
CHAPTER 5 ANALYSIS OF THE RESULTS	33
5.1 Introduction	33
5.2 Validation	33
5.3 Parametric Studies	35
5.4 Discussion	39
CHAPTER 6 CONCLUSION	44
BIBLIOGRAPHY	46
APPENDIX A HYDRODYNAMIC ANALYSIS	91
APPENDIX B THE STIFFNESS COMPUTATION	96

	<u>Page</u>
APPENDIX C INPUT AND OUTPUT OF THE PROGRAMMES	100
APPENDIX D LISTING OF TLP1	107
APPENDIX E LISTING OF TLP2	127

LIST OF TABLES

<u>NO.</u>	<u>TITLE</u>	<u>PAGE</u>
1	Comparison of computed results with data presented by Kirk and Etok (1979)	50
2	A parametric study of surge response amplitude operators	51
3	A parametric study of heave response amplitude operators	52
4	A parametric study of the pitch response amplitude operators	53
5	A parametric study of the tension response amplitude operators on the aft side	54
6	A parametric study of the tension response amplitude operators on the forward side	55

LIST OF FIGURES

<u>No.</u>	<u>Title</u>	<u>Page</u>
1	Overall view of TLP with key dimensions	56
2	Schematic representation of planar motions	57
3	Natural frequencies of a Tension Leg Platform	57
4	Details of the mooring system	58
5	Mooring compartment	59
6	The linear model	60
7	The finite element model	61
8	Definition sketches	62
9	Tether Model	63
10	Flow chart of linear analysis algorithm	64
11	Flow chart of nonlinear analysis algorithm	65
12	Elastic stiffness matrix of a beam element	66
13	Surge force versus frequency	67
14	Heave force versus frequency	68
15	Pitching moment versus frequency	69
16	Displacement versus time	70
17	Surge displacement versus time: Parametric study	71
18	Heave displacement versus time: Parametric study	72
19	Pitch motion versus time: Parametric study	73
20	Tension aft versus time: Parametric study	74
21	Tension forward versus time: Parametric study	75
22	Effect of wave height on tension history: Parametric study	76

<u>NO.</u>	<u>TITLE</u>	<u>PAGE</u>
23	Effect of wave frequency on tension history: Parametric study	77
24	Surge response amplitude operator versus time: A case study	78
25	Heave response amplitude operator versus time: A case study	79
26	Pitch response amplitude operator versus time: A case study	80
27	Surge displacement versus time: A case study	81
28	Heave displacement versus time: A case study	82
29	Pitch motion versus time: A case study	83
30	Tension response amplitude operator versus time period aft starboard side	84
31	Tension response amplitude operator versus time period for aft port side	85
32	Tension response amplitude operator versus time period for forward port side	86
33	Tension response amplitude operator versus time periods for forward starboard side	87
34	Tension aft versus elapsed time	88
35	Tension forward versus elapsed time	89

NOMENCLATURE

OXYZ	The global frame of reference fixed at the initial position of center of gravity
$\bar{r}_k$	Displacement vector ( $k=1,2,\dots,6$ refer to surge, sway, heave, roll, pitch and yaw respectively)
$t_0$	Starting time
$t$	Elapsed time
$\tau$	Time increment
$\omega$	Circular frequency of wave
$K$	Wave number
$a_0$	Amplitude of incident wave
$a$	Water depth
$\beta$	Direction of propagation of incident waves with respect to positive X axis
$g$	Acceleration due to gravity
$i$	$\sqrt{-1}$
$\phi$	complex velocity potential
$\psi$	complex velocity potential, function of space co-ordinates only
oxyz	local frame of reference for an element as defined in Fig. 8(b)
$\rho$	density of water
$V$	Volume of immersed body
$\underline{B}(x_b, y_b, z_b)$	Global coordinates of the bottom of the cable at any time $t$
$\underline{G}(x_g, y_g, z_g)$	Global co-ordinates of the center of gravity at any time $t$
$\underline{O}(x_0, y_0, z_0)$	Global co-ordinates of the bottom of the cable at any time $t$

$[m_{ij}]$	mass matrix
$[a_{ij}]$	added mass matrix
$[b_{ij}]$	damping co-efficient matrix
$[c_{ij}]$	hydrostatic restoring coefficient matrix
$\{R\}$	inertia vector
$\dot{R}$	$dR/dt$
$\ddot{r}$	$dr/dt$
$\ddot{r}$	$d^2r/dt^2$
$\{R_a\}$	exciting force vector
$\{R_s\}$	Restoring force vector
$\delta_{kj}$	if $k=j$ or 0 if $k \neq j$
$S$	surface area of the hull
$n$	normal vector
$\mu_1$	$\cosh(x+d)/\cosh(kz)$
$[K_{ij}]$	Cable stiffness matrix
$T$	Equilibrium tension in the cable
$L$	length of the cable/element
$E$	Young's modulus
$A$	Area of crosssection of the cable
$[K_E]$	Elastic stiffness matrix of the cable/element
$[K_G]$	Geometric stiffness matrix of the cable/element
$V_1, V_2$	Axial displacements of a plane truss element
$\theta_1; \theta_2$	Rotations of a plane truss element
$C_{DL}$	Equivalent linear drag coefficient

$C_{DQ}$	Quadratic drag coefficient
$u_0$	Amplitude of the periodic fluid velocity
$[C_{kj}]$	Total restoring force matrix
$F_k$	Amplitude of the forcing function
$S_j$	Amplitude of the $j$ th mode of motion
$K_1, K_2$	Stiffnesses at end 1 and 2
$d_1, d_2$	Deflections at end 1 and 2
$D$	Total force of buoyancy
$W$	Total weight of the structure
$P$	Total pretension
$L, X$	Distances defined in Fig. 9(a)
$d_0(dx, dy, dz)$	Displacement of point $0$
$dT$	Change in cable tension
$dL$	Change in length of cable
$N$	Number of degrees of freedom



## CHAPTER 1

INTRODUCTION1.1 Background

Drilling for oil, over the past 40 years has moved from land and near shore sites to structures in water depths in excess of 1500 meters, and into harsher environments full of waves, currents, wind, seaquakes and icebergs. Central to this development is the design of an inexpensive, but reliable facility, from which oil extraction may proceed.

In shallow waters, the choice is generally a fixed platform, whose fundamental period is well below the peak period of the exciting sea-states. With the increase of water depth, the structure's natural period increases and it is susceptible to resonance, resulting in large displacements and stresses. The cost of fixed structures also increases exponentially with the increase of water depth.

In order to overcome these problems, compliant structures have been developed. These structures exhibit motion under loading, which generally leads to reduced loading. There are many varieties of compliant structures, but the most widely favoured types are the Semisubmersible, the Guyed Tower, and currently the Tension Leg Platform (TLP).

The Tension Leg Platform is designed on the Principle of Excess Buoyancy. It seeks to achieve a measure of steadiness by pulling vertically upwards a set of cables attached firmly to the sea-bed. In effect it functions like a pendulum hung upside down.

The first of such platforms, the Triton, was produced almost 20 years ago. The development of the concept has come a long way since then, and the first commercial production facility of this type, the Hutton TLP, will shortly be operational in the North Sea.

## 1.2 Objectives

This thesis is concerned with the loss of stiffness in any tether, and the study of its effects on the platform response. Hydrodynamic interaction will be taken into account using the drag and inertia effects and the added mass concept. The tethers are first modelled as linear springs attached to a lumped model of the topside, with six degrees of freedom, to obtain the response in the frequency domain. Subsequently, the nonlinear effects caused by the large displacements will be studied using a Finite Element idealization of the system in the time domain.

The aim of the study is to ascertain the characteristic changes in the behaviour of the system due to the loss of tether stiffness.

CHAPTER 2  
LITERATURE REVIEW

2.1 Environmental Loads and the Response of  
a Tension Leg Platform

Methods of environmental response and analysis, which have been applied in the design of floating bodies and other compliant platforms and semisubmersibles, provide a sound basis for the analysis of the motion response of a Tension Leg Platform.

The hydrodynamics of the platform can be determined by the following two models.

The first model is based on the classical hydrodynamic theory, wherein a solution to the Laplace equation is sought in the fluid domain, subject to the prevailing boundary conditions. These conditions include the kinematic boundary condition on the free surface and on the body surface itself, a constant pressure dynamic condition derived from the rigid body equations of motion and the far field condition. A solution scheme of this type has been suggested among others, by Faltinsen and Michelson (1974), by the so-called three dimensional singularity distribution technique.

The second approach is less exact, but is readily adaptable for structures, such as space frames. The hydrodynamic properties of each member are estimated either

experimentally or by using Strip theory. This formulation is in effect identical to the analysis suggested by Morison et al. (1951). The basis of assembly, termed as hydrodynamic synthesis, is the assumption that the hydrodynamic forces on the assembled structure equal the summation of the forces acting on the individual members. Some of the earliest work, such as the motion analysis of semisubmersibles by Burke (1970) and Hooft (1971), follow this approach.

The hydrodynamic synthesis technique for the prediction of the motion response and tension variation in the tethers was first proposed by Paulling and Horton (1970), for a linearized model of a Tension Leg Platform in regular and irregular waves, and the computed results were shown to be in good agreement with some experimental findings.

Nonlinear effects, which were neglected in the previous analysis, were considered by Paulling (1974) in a time domain analysis. It was suggested that nonlinearities may be caused by things, such as:

- i. non-linear terms in the rotational equations of motion.
- ii. finite amplitude waves
- iii. nonlinear drag forces

The results included both transient and steady state responses which were computed using the Runge-Kutta technique for time integration.

The possibility of dynamic instabilities at critical wave frequencies and subharmonic oscillations at cross seas has been demonstrated by Rainey (1978). These have generated great interest, especially amongst the British researchers, who have carried out a number of experimental studies.

The resonance problem for tethers in deeper waters has been discussed by Roren and Steinwik (1977). They have used the three dimensional singularity distribution technique for the hydrodynamic analysis.

The nonlinear analysis carried out by Natwig and Pendered (1977) uses the Newmark as well as the Newton-Raphson Method for the time integration. They have concluded that the linear methods give reliable results if the mean drift forces are included.

Albrecht et al. (1978) have presented algorithms for linear and nonlinear analyses. They have also discussed tether dynamics and considered the cases of inclined tethers.

A comparison of linear and nonlinear analysis has been presented by Denise and Heaf (1979). They have commented on the range of validity of each analysis and brought out the fact that the most significant nonlinear effect is caused by the large displacements in the geometry of the tethers. Other effects, such as the buoyancy in the

splash zone and viscous forces, are of lesser consequence. The geometric nonlinearity also considerably influences the tensions in the tethers.

Ashford and Wood (1978) have investigated various numerical integration schemes and have concluded that no one scheme is best suited for the solution. Therefore, the choice of the scheme should be made according to the nature of the model.

The state of the art was quite well established by the late seventies. Most published work in the recent years can be categorized as:

(i) Literature dealing with the design aspects, such as the work of Capanoglu (1979), Liu et al. (1980), Chou et al. (1980), Mercier et al. (1980), Tetlow et al. (1982), Ellis et al. (1982), Lloyd et al. (1983).

(ii) Literature dealing with the platform motion analysis, a majority among these report experimental investigations, such as the work of Yoshida et al. (1981), Faltinsen et al. (1982), Katayama (1982), Lyons et al. (1983) and Dunsire and Owen (1984).

The current trend in the analysis seems to be focused on detailed investigation of specific problems. A combination of various hydrodynamic models have been studied. If the platform has larger pontoons close to the water surface, the interaction effects, neglected in the Morison's

equation, will be significant. The viscous effects are more significant in the slender members, and they cannot be accounted for in the potential flow analysis. A synthesis of the two models gives the best results, as reported by Standing (1979).

In a recent article Dillingham (1984) has described the model scale simulation of a TLP, the research areas of particular interest in the current model tests and made recommendations for future tests.

## 2.2 Modelling of the Tether System

Most of the available literature deals with models, the tethers being represented by linear springs.

The analytical transmission line solution was employed by Hong (1974) to predict the behavior of the lightly tensioned taut ropes attached to oceanographic buoys.

Albrecht et al. (1978) have presented a detailed treatment of the nonlinearities caused by large deformations in a quasistatic study of a Finite Element model of the mooring system.

The analysis of Richardson and Pinto (1979) is based on tethers modelled as heavy catenaries, which give a simple closed form solution.

The research group at University College, London has developed the analytical solutions in a systematic manner. Jeffries and Patel (1981) have carried out a comparison of various mathematical models of the tether system. They have used an analytical model, the linear modal analysis and the Finite Element model for this comparison. Only the Finite Element model can cater for the nonlinearities. Patel and Lynch (1983) have presented a mathematical model of the coupled dynamics of a Tension Leg Platform and the lateral dynamics of its tethers. This study investigates the effects of water depth, surface platform mass, and the tether mass per unit length on the tether displacement and the bending strength, as well as on the resulting platform motion. It has been shown that, while the tether dynamics do not affect the platform motions, the platform motions affect the tether dynamics considerably.

Keysor and Mott (1971) report that the offshore industry has in the past used frequency measurement technique for the estimation of the cable tensions.

State of the art of the vibration analysis of fixed offshore platforms, where shifts in the resonant frequencies are used to study the loss of tether stiffness, for the purpose of integrity monitoring is well established.

Most of the reviewed literature considered the tethers to have equal stiffness. The investigation carried



out by Yoshida et al. (1978) studied the effects of snap loads on a taut moored platform. A current investigation at the Harriot-Watt University, UK is aimed at a comprehensive model tests programme, that covers the study of the effects of tether failure, including redistribution of loads and change in the structure's performance.

A theoretical analysis for modelling the loss of tether stiffness and its effects on the platform behavior has not been reported in the open literature.

## CHAPTER 3

THE TENSION LEG PLATFORM3.1 The Design Philosophy

The Tension Leg Platform is a floating structure that has been connected to the anchor/foundation fixed at the sea-bed by vertical mooring lines. These tethers virtually eliminate the vertical plane motions of heave, pitch and roll, while the lateral motions of sway, surge and yaw are considerably reduced. An excess of buoyancy over the platform weight keeps the mooring lines taut at all times. A majority of the force of buoyancy is provided by the columns at the corners and the connecting horizontal pontoons, all of which are collectively termed as the hull. A schematic representation of the forces and the movement of the platform is shown in Fig. 2.

In reality, the platform is a continuous mechanical system with an infinite number of free vibration modes and frequencies. The six displacements mentioned above are only an approximation of some of the true modes of the continuous system. These 6 modes are described as the principal modes to distinguish them from the secondary modes, which are closely related to the so-called tether dynamics, that is, the vibration of tethers within themselves.

Figure 3 shows the natural frequencies in

comparison with exciting sea-state energy, and it should readily be clear that the platform is designed so as to avoid resonance.

The primary design objectives are:

- (i) to provide the space and support for all the functional requirements in the development of the oil field.
- (ii) to obtain moderate wave, wind and current forces and response.
- (iii) to minimize the weight and maximize the payload.
- (iv) to achieve watertight partitions to withstand partial damage.
- (v) to achieve stability during transit and routine maintenance.
- (vi) to provide easy access for work and inspection.

### 3.2 General Description

The development of a new technology is greatly enhanced by its specific application to one real project. All the studies prior to the design of the Hutton TLP necessarily included several alternative solutions. Factors, such as environmental conditions, water depth and soil properties have led to a configuration choice which is likely to become a model for the future generation of platforms. This design, shown in Fig. 1, is described as follows.

The hull structure of the Hutton TLP consists of cylindrical columns and rectangular pontoons. The ring stiffened columns have a series of watertight flats to limit flooding. They house a system for anchoring the Tension Legs and transferring their loads to the shell of the columns and the the column-pontoon node. At sea level, where the possibility of collision damage is most severe, a double-skin construction is used to provide a secondary path for the loads on the columns.

The pontoons, rectangular in section, are constructed of orthogonally stiffened plates, using web frames and longitudinals, and provide a rigid joint. The joint is subjected to axial and bending loads and also provides an additional way of resisting the Tension Leg crossloads.

The deck provides the workspace for the topside facilities and consists of a grillage of 12.5 meters deep bulkheads, into which modular pallets are placed at the main, mezzanine and weather deck levels to form an integrated structure.)

The hull and the decks are fabricated separately and mated in shallow water, after which they are towed to the site and are installed with the help of the mooring system.

Though the structure is similar in configuration to semisubmersible drilling rigs, the following features are

distinctive:

- (i) the portion of buoyancy provided by the columns, compared with that provided by the pontoons is much greater in a Tension Leg Platform. This is done to minimize the tension leg loads, rather than the induced heave motions.
- (ii) the overall depth is much greater than that of a semisubmersible. This is done to avoid the high slam in the case of a high tide together with a high wave.
- (iii) diagonal bracings are avoided to reduce complex joints.

### 3.3 The Mooring System

The Hutton TLP is a permanent installation in the sense that it will be operational in all but most adverse environmental conditions and is functionally equivalent to a fixed platform. Fig. 4(a) shows a typical tension leg. The sixteen tension legs provide a flexible connection between the hull and the foundation and can withstand high cyclic loads, which may vary between 0 and 2400 tonnes. During their 20 years of design life the legs will be subjected to  $10^8$  load reversals.

At the upper end (Fig. 4(b)), the load will be transferred to the hull through a load block, into a locking collar of the tension adjustment assembly, which passes the

load to the cross load bearing (CLB). Below the CLB there are 11 elements each approximately 9.5 meters long, and with a maximum yield strength of  $795 \text{ N/mm}^2$  (Fig. 4(c)). The bottom of the leg has the anchor connector (Fig. 4(d)), which is a device for attaching the leg to the template on the seabed. This connector is activated by the force of gravity and locks itself in. It can be removed from the deck remotely with a hydraulic device.

Both ends of the tension leg have elastomeric flexjoints, which allow free rotation up to 18.5 degrees.

The deployment of the leg is undertaken from the mooring compartment (Fig. 5), which is located in the upper part of the column. The leg elements are stored here prior to installation. The compartment houses specially developed mechanical handling equipments. These are used for installation and removal of the leg elements.

The tether system installation is carried out in calm weather. The platform is temporarily moored with the help of an eight point catenary mooring system. A single leg element in each corner is assembled and lowered, along with the connecting assembly. The succeeding elements are added on till the lower end reaches 5 meters above the seabed. The motion compensator on each leg is then stroked fully to raise each leg by about 10 meters. Finally, the anchor connectors are stabbed into the templates. At this stage, the

compensators account for the vessel's motions. A nominal tension is applied to each leg to check for locking and the check valves on the compensators are closed. When the heave motion is fully suppressed, the platform is pulled down to its operating draft with the help of hydraulic jacks. The load plates are now locked and the platform is partially deballasted. The platform is now in the TLP mode. The remaining 12 elements are now lowered with the help of a polar crane. Once all the elements are in position, the platform is deballasted to its operational draft.

As for the redundancy of the system, any two tethers at each corner can take the design load if the remaining tethers in the cluster are not functional. There is a provision for retracting any of the tethers temporarily for inspection. Even the unthinkable failure of all the tethers in a corner would not be progressive, although the platform would be in jeopardy, unless its center of gravity is moved towards the untethered corner.

Load cells in each corner are used to continuously monitor the tension in the tether and these values are used for onboard load distribution.

CHAPTER 4  
PROBLEM FORMULATION

4.1 Introduction

The objective of this formulation is to develop mathematical models to study the effect of the loss of tether stiffness on the behavior of a Tension Leg Platform.

It is apparent that a damaged structure will have different motion characteristics from those of an intact structure. The usual assumptions pertaining to the restoring force computations, must therefore be modified to cater for the uneven tether stiffnesses. The study has been carried out in two stages.

First a frequency domain analysis is carried out with the assumption that the system behaves linearly. Strictly speaking, this analysis has a limited validity, but it serves as an indicator of the nature of the changes. The structure is modelled as a lumped mass with  $\beta$  degrees of freedom. A schematic diagram of this model is shown in Fig. 6. Essentially, this formulation follows a strip theory approach to study the tension variations and the motion responses.

It has been shown that the geometric nonlinearity caused by the large deformations influences the platform behavior as well as the tension history significantly (Denise



and Heaf, 1979). A large displacement nonlinear model is developed for a time domain analysis. The hydrodynamic properties are derived from the previous model. The platform is modelled as a 3-dimensional network of beam elements with 45 nodes and 249 degrees of freedom. This model is shown in Fig. 7.

## 4.2 Linear Analysis

### 4.2.1 The constitutive forces

Consider a rigid floating body oscillating about a state of rest in response to excitation by long crested linear waves. An inertial system of coordinates OXYZ attached to the equilibrium position of the center of gravity is defined, and the motion is denoted by  $r_k$  for the  $k^{\text{th}}$  degree of freedom, as shown in Fig. 8(a). The problem posed here deals with the fluid motion induced by small amplitude oscillations of the object as well as the fluid motion associated with the interaction of the object with a train of incoming waves. The theoretical basis of the formulation along with detailed derivations has been presented by Høoft (1970, 1971) for a semisubmersible assuming potential flow. This formulation has been adopted here with certain minor modifications. The salient features of this formulation along with the implicit assumptions are discussed in

Appendix A. The modification proposed in regard to tether stiffness modelling is presented in the next section.

On the basis of the afore-mentioned formulation, it is inferred that the platform motion in waves is caused by reaction to the external disturbances. The 3 parts of the reactive force are

- (i) forces in phase with the acceleration (Inertial forces)
- (ii) forces in phase with the velocity (Damping forces)
- (iii) forces proportional to the displacement (Restoring forces)

The wave excitation forces on the body are approximated by two parts:

- (i) The undisturbed pressure force (also known as the Proudé-Krylov force), which is the force that arises from the pressure over hull in a wave that has not been disturbed by the hull.
- (ii) The inertia force, which arises from the acceleration of the added mass of the hull in a wave that has not been disturbed by the hull.

The potential flow solution neglects the viscous effects, which are of significant magnitude. The viscous forces are therefore included additionally as proposed by Paulling (1971). The viscous part is usually assumed to be a quadratic function of the velocity by analogy to the case of

steady flow. For the present analysis, the quadratic drag is replaced by an "equivalent linear drag force". The equivalent linear drag coefficient  $C_{DL}$  is given by,

$$C_{DL} = \frac{8}{3\pi} u_0 C_{DQ}$$

where  $C_{DQ}$  is the quadratic drag coefficient and  $u_0$  is the amplitude of the periodic fluid velocity.

The last of the constituent forces is the restoring force introduced by the tether system. This force is proportional to the displacement and is attributed to the components of anchor line tensions tending to restore the structure following a small displacement.

#### 4.2.2 The Equation of Motion

The equation of motion in the simplified form results from equating the reactive forces with the excitation forces.

$$\sum_{j=1}^6 (m_{kj} + a_{kj}) \ddot{r}_j + b_{kj} \dot{r}_j + c_{kj} r_j = F_k \exp(i\omega t) \quad k=1, 2, \dots, 6 \quad (4.1)$$

where

$F_k \exp(i\omega t)$  = Hydrodynamic excitation force

$[m_{kj}]$  = Mass/Inertia matrix

$[a_{kj}]$  = added Mass matrix

$[b_{kj}]$  = Damping coefficient matrix

$[C_{kj}]$  = Restoring force matrix

$\omega$  = Circular frequency of excitation

In order to reduce the coupled second order differential equations to a set of linear complex equations, it is necessary to assume harmonic motions. Substituting  $r_j = s_j \exp(i\omega t)$

$$\sum_{j=1}^6 \{-\omega^2 (m_{kj} + a_{kj}) + i\omega b_{kj} + c_{kj}\} s_j = F_k$$

where  $s_j$  is the amplitude of the  $j$ th mode of motion. The equation of motion, is solved for  $s_j$ .

#### 4.2.3 The Tether Stiffness Model

##### Calculation of the Equilibrium Tensions

Fig. 9(a) shows the planar configuration of a Tension Leg Platform with the tethers modelled as linear springs of unequal stiffness  $K_1$  and  $K_2$ . At equilibrium their respective deflections are  $d_1$  and  $d_2$ . The total force of buoyancy is  $D$ , acting at the center of buoyancy ( $X$  units from tether with stiffness  $K_1$ ). The total weight  $W$  is acting at the midpoint between the two tethers (or  $L/2$  units from the tether with stiffness  $K_1$ ). It is the total underwater volume which remains constant. The total pretension is  $P$ , so that

$$P = D - W$$

The equilibrium equations are,

$$K_1 \cdot d_1 + K_2 \cdot d_2 = P \quad (4.2)$$

$$K1 \cdot d1 \cdot X = K2 \cdot d2 \cdot (L' - X) - W \cdot (X - L'/2) \quad \dots (4.3)$$

This problem is statically indeterminate in  $X$ ,  $d1$  and  $d2$ . From the geometry depicted in Fig. 9(b), the deflection at  $X$  is

$$dx = d1 + (d2 - d1) \cdot X/L' \quad (4.4)$$

The deflection at  $X$  is caused by the translation of the body and rotational motion about the midpoint, so that

$$dx = P(1/K1 + K2) + 4' \cdot (X' - L'/2)^2 / (K1 - K2)L'^2 \quad \dots (4.5)$$

from (4.4) and (4.5)

$$\frac{L'^2}{4} (K1 - K2) (d1 \cdot L' + (\frac{d2 - d1}{PL}) - \frac{1}{K1 + K2}) - 9(\frac{L'}{2} - X)^2 = 0 \quad \dots (4.6)$$

Equations 4.2, 4.3, and 4.6 are solved iteratively for  $X$ ,  $d1$  and  $d2$ . This principle is further applied to the other plane to arrive at the 3-dimensional equilibrium.

#### Cable Stiffness Matrix

Cables are assumed to be weightless, taut and of linear stiffness. The model includes the elastic stiffness due to the extension of the cable as well as "the pendulum" stiffness due to the pretension in the cable under lateral displacement.

The configuration of a typical cable has been shown in Fig. 9(c). Consider a cable fixed at the point  $B(x_b, y_b, z_b)$  with its other end attached to a moving structure at the

point  $O(x_0, y_0, z_0)$ . The motion of the structure is about the point  $OG(x_g, y_g, z_g)$ . If the point of attachment moves by a small distance  $dO(dx, dy, dz)$ , the force on the structure to the first order is

$$dT = -T dO + \left( \frac{EA - T}{L^2} \right) dL (B - O) \quad (4.7)$$

where

- $T$  = Pretension
- $L$  = Length
- $E$  = Young's modulus
- $A$  = Area of crosssection
- $dL$  = Change in length

It can be shown from Eqn. 4.7 that the  $j$ th component of the displacement  $r_j$  at  $OG$  will cause forces given by

$$dT_i = \sum_{j=1}^6 -K_{ij} r_j \quad \text{for } i=1,2,\dots,6 \quad (4.8)$$

where  $K_{ij}$  is the stiffness due to the cable.

The detailed stiffness matrix was derived and the final equations are presented in Appendix B.

### 4.3 Nonlinear Analysis

#### 4.3.1 The Equation of Motion

It has been shown by Albrecht et al. (1978) that in the time-domain analysis a formulation of the equation of motion based on an impulse response function, which yields frequency independent added mass coefficients and retardation

functions, has to be used. Generally, the equations of motion for a multi degree of freedom system read

$$\sum_{k=1}^N [m_{kj} + a_{kj}](\ddot{r}) + [b_{kj}](\dot{r}) + (F_{restoring}(r)) =$$

$$F(r, \dot{r}, r, t)$$

(4.9)

where

$[m_{kj}]$  = Mass/Inertia matrix

$[a_{kj}]$  = Added mass matrix

$[b_{kj}]$  = Damping matrix

$(F_{restoring}(r))$  = Restoring force vector

$(F(r, \dot{r}, r, t))$  = Exciting force vector

and  $\{r\}$ ,  $\{\dot{r}\}$ ,  $\{\ddot{r}\}$  are the displacement, velocity and acceleration vectors respectively. The number of degrees of freedom is  $N$ , which includes both the rigid and elastic degrees of freedom.

There are a number of nonlinear terms which may appear in Eqn. 4.9. Denise and Heaf (1979) have shown that among the various nonlinear effects, the variation in the restoring force due to large displacements is the most influential factor governing the tension response of the tethers as well as the motion of the platform.

The hydrodynamic properties, that is, the added mass, damping and the wave induced excitation forces are calculated using a formulation similar to the linear model.

The theoretical basis and assumptions made for this formulation are discussed in Appendix A. However, the load vector in the nonlinear formulation has to be computed at each step, because it is dependent on the instantaneous position of the platform.

The restoring force vector has contributions from the hydrostatic force, the elastic stiffness of the tethers as well as the geometric stiffness of the tether system.

The discretization of the continuum is carried out using the finite element model. The concept of finite element in time dimension is employed for the solution of the equation of motion by an iterative numerical scheme.

#### 4.3.2 The Finite Element Model

For the large displacement dynamic response calculation of the tether network the finite element model is employed. The advantage of this model lies not only in the facility to incorporate all the parameters affecting the system, but also in the high degree of reliability of the results.

Fig. 7 shows line diagram of the finite element model.

The tethers are modelled as beam elements with 12 degrees of freedom (three translational and three rotational at each end). The end nodes of each tether are hinged. This model incorporates the variation in the tether



properties and tension along the length as well as the computation of the contributions due to elastic and geometric stiffness. The model has the capability of incorporating the excitation caused by vortex shedding at tethers, and exact current and wave forces on the tethers. These effects are not included in the present analysis. The response of the tether network is stiffness dominated.

The topside is modelled as a lumped rigid mass having six degrees of freedom. The motions at the top are transferred to the nodes 2 through 5. Since an accurate estimation of the first derivative of the exciting force is not available, the motion of the topside is solved using the Wilson- $\theta$  algorithm, given by Bathe and Wilson (1976). Thus the topside configuration is a rigid body model of the platform hull and its motions are inertia dominated.

It has been brought out in the discussion of the nonlinear stiffness formulation (see Appendix B) that the larger the number of elements in any tether, the greater is the accuracy of the formulated geometric stiffness. However, the larger number of elements lead to larger requirements of computer time for the analysis. The system was first modelled with larger number of elements (40), and subsequently the number of elements was reduced to (25). This helped in a 66% saving in the computer time while affecting the accuracy of the results marginally.

#### 4.3.3 The Time Integration Scheme

Argyris et al. (1973) have derived the concept of the application of finite element methodology for the time step integration of nonlinear cable networks. The equation of motion (4.9) is rewritten as

$$\{\ddot{r}\} = \{\dot{R}a\} - \{\dot{R}s\} - [b] \{\dot{r}\} \quad (4.10)$$

and

$$\{\dot{r}\} = \{\dot{R}a\} - \{\dot{R}s\} - [b] \{r\} \quad (4.11)$$

where

$\{R\}$  = Inertia force vector

$\{Ra\}$  = Exciting force vector

$\{Rs\}$  = Restoring force vector

$[b]$  = Damping matrix

$\{r\}$  = Displacement vector

The superscript "." denotes the derivative with respect to time. If the inertia force is assumed to be a cubic function of time, it has been shown by Argyris that

$$\begin{aligned} \{\ddot{r}_1\} &= \{\ddot{r}_0 + \frac{m^{-1}}{12} (6\dot{R}_0 + \tau\ddot{R}_0 + 6\dot{R}_1 - \tau\ddot{R}_1)\} \\ &= \{\ddot{r}_0 + \dot{d}r\} \quad \dots (4.12) \end{aligned}$$

$$\begin{aligned} \{\dot{r}_1\} &= \{\dot{r}_0 + (\tau\ddot{r}_0 + \frac{2m^{-1}}{60} (2\dot{R}_0 + 3\tau\ddot{R}_0 + 9\dot{R}_1))\} \\ &= \{\dot{r}_0 + \dot{d}r\} \quad \dots (4.13) \end{aligned}$$

and

$$\{r\} = \{m\}^{-1} \{R_1\} \quad (4.1)$$

where the subscript "0" indicates the value of the variable at the beginning of a time step and the subscript "1" indicates the value of the variable after a time step ( $\tau$ ) and  $\{m\}$  is the equivalent mass matrix (the sum of mass and added mass matrix). An iterative solution scheme is adopted for the solution of the initial value problem using Eqns. 4.12, 4.13 and 4.14. For the first estimate the values  $\{R_1\}$  and  $\{R_1\}$  are approximated as

$$\{R_1\} = \{R_0 + \tau R_0\}$$

$$\{R_1\} = \{R_0\}$$

Strictly speaking, the kinematically equivalent mass and damping matrices are changing with the geometry, but they are assumed to be constant.

The choice of the scheme of integration is closely linked to the nature of the problem in terms of numerical stability and desired accuracy. The ideal algorithm should also have the minimum requirement of computer time and memory.

The algorithm of finite elements in time integration is best suited for the present analysis because of the following reasons:

- (i) The equation of motion in the present.

formulation assumes the added mass matrix to be constant, whereas the stiffness matrices are position dependent. This method does not require an inversion of the stiffness matrix and just one inversion of the mass matrix, as against all the other methods in the literature, which call for the matrix inversion at every step.

(ii) The tether stiffness matrix has a large bandwidth. A scheme has been developed, as described in the next section, which does not require global assembly of the stiffness matrix and uses a column vector product of the stiffness and the displacement vector directly. This scheme saves on the total in-core memory requirement.

(iii) It has been shown by Argyris (1973) that this method in effect amounts to a 5<sup>th</sup> order interpolation of the displacement function and is more stable and accurate than most of the prevailing numerical integration schemes in nonlinear mechanics. Albrecht et al. (1978) have also established that methods which work directly are not suitable for the solution of nonlinear problems involving cable networks and have used this scheme for their analysis. In the computation of the motion response, the effect of the starting transient has been reduced by allowing the exciting term to build up gradually. This is accomplished by multiplying the force and moment terms by a tapering function. The first 2 cycles are ignored while presenting

the results, so that the effect of transient motion has been suppressed.

#### 4.4 Numerical Analysis

The linear analysis programme has been implemented directly from the equations discussed earlier. The flow chart is shown in Fig. 10. The damping force is dependent on the amplitude of velocity, and an initial velocity has to be assumed for the subsequent iterative solution. The convergence is quite fast and an accuracy of less than 3% has been specified as the error bound. A listing of a typical input scheme and the computer code (see TLPI.FOR) are attached in the appendices C and D.

The implementation of the nonlinear solution scheme is very involved. The most critical part of the numerical solution arises from the largely different values of mass and stiffness for the rigid body and the tether degrees of freedom. The displacement, velocity and acceleration terms associated with the soft degrees of freedom explode and the system is numerically unstable when the time integration scheme is used directly. It is essential to condense out the rigid degrees of freedom to avoid this instability. This has been achieved in two steps.

First the motion analysis of the topside is carried out by treating it as a rigid body. The displacements are

now transferred to the top nodes of the cable network and force matrix on the network is computed. Now the bottom nodes of the cable are assumed to be fixed and the lateral dynamics of the network is analyzed, in the second step.

The top nodes are condensed out by the so called Guyan reduction (see Guyan, 1965). Partitioning the equations of motion as

$$\begin{bmatrix} K_{cc} & K_{cr} \\ K_{rc} & K_{rr} \end{bmatrix} + \lambda \begin{bmatrix} m_{cc} & 0 \\ 0 & m_r \end{bmatrix} \begin{bmatrix} r_c \\ r_r \end{bmatrix} = \begin{bmatrix} F_c \\ F_r \end{bmatrix}$$

where the subscript c denotes the condensed degrees of freedom, and the subscript r denotes the retained degrees of freedom. Writing the first partitioned equation along with the damping terms as

$$(K_{cc} - w^2 m_{cc} + iwb_{cc})r_c + K_{cc} r_r = F_c \quad (4.15)$$

Eqn. 4.15 is rewritten so as to keep the inertia terms on the right-hand side

$$r_c = -(K_{cc} r_c + K_{cc} r_r) - b_{cc} r_r + F_c \quad (4.16)$$

$$r_c = -[K] (r_c) - b_{cc} r_r + F_c \quad (4.17)$$

on differentiating Eqn. 4.16

$$\dot{r}_c = -[K] (\dot{r}_c) - b_{cc} \dot{r}_r + \dot{F}_c \quad (4.18)$$

and similarly,

$$\dot{r}_r = -[K] (\dot{r}_r) - b_{rr} \dot{r}_r + \dot{F}_r \quad (4.19)$$

$$R_r = -[K] \{r_r\} - b_{rr} \dot{r}_r + F_r \quad (4.20)$$

These equations are to be solved iteratively. The solution scheme proposed by Argyris is modified to cater for the condensation. The flow chart for the programme organization is given in Fig. 12.

The implementation of the Argyris' time integration scheme with dynamic condensation is a new development carried out in the course of this analysis.

It may be pointed out here that this approach has in effect been proposed by Patel and Lynch (1983). They have analyzed the rigid body with 6 degrees of freedom and the tether system independently. The coupled dynamics was examined by first using the results of the motion analysis as the input for the dynamic analysis of the tethers and then recalculating the motion with the dynamic effects due to the tethers incorporated as a magnification of the tension term in the tether stiffness matrix. They have justified their approach by arguing that while the tether dynamics does not affect the platform motions, the platform motions affect the tether dynamics significantly.

The other aspect of numerical analysis which requires consideration is the organization of the high and low speed memory blocks. In order to use the logic effectively an array A(10000) is defined, which is used to store all the in-core variables. A number of control

variables monitor the partitioning of this memory block at various stages in the programme. The portion of arrays not needed in calculations is dumped on the slow speed devices and reread when needed. This manipulation is also used to avoid the assembly of global stiffness matrices. It can be seen from the system equations that at no stage of analysis is the stiffness matrix needed by itself in the evaluation. Since it is always compounded with a column vector before coming into the system equations, only this column vector need be stored in core.

The error bounds used in this analysis were computed from the error norms of the inertia and the displacement vectors. Based on the double precision accuracy of  $10^{-16}$  on VAX 11/780 system, they were taken as  $10^{-15}$ . The typical CPU time required for a linear analysis was 1.24 minutes. The typical CPU time required for a non-linear analysis was 34 minutes.



## CHAPTER 5

ANALYSIS OF THE RESULTS5.1 Introduction

The motions and tension forces on a typical Tension Leg Platform are computed. In order to check the validity and accuracy of the numerical process comparisons with published data are made. A parametric study of the responses is presented. Based on the findings of the parametric variations a case study has been made to evaluate the effects of the loss of tether stiffness on the behavior of a Tension Leg Platform.

The results of the frequency domain analysis are the response amplitude operators (RAO) for surge, heave, pitch motions and the cable tension variations. The results of the nonlinear analysis are the time histories for the motions and tensions. The definition sketch (Fig. 8(d)) identifies the fore and aft direction and the port and starboard side with respect to the wave direction.

5.2 Validation of the Numerical Results

The details of the platform geometry and other relevant parameters chosen in this study are presented in Appendix C. This platform is quite similar to the design AKER TPP. Kirk and Etok (1979) have presented a study of

this platform, and the numerical findings of the present study are compared with their results. The diameters of the columns are 16 m and the spacing of the corner columns is 70 m. The length of the pontoons is 54 m, and the dimensions of the hull section are 13 x 9.5 m. In the present study the rectangular section has been replaced by a tubular section of equivalent area. The diameter of the smaller columns is 3.5 m. The height of the platform center of gravity is 41.7 m above the base line. The operating draft is 35 m. The area of cross section per leg is  $46180 \text{ mm}^2$  and the Young's modulus is  $2.0 \times 10^{11} \text{ N/m}^2$ . The added mass coefficient is taken as 1.0 and the drag coefficient is taken as 0.7. The length of the cables is 125 m.

A comparison of the computed values and the added mass, natural frequencies and stiffness values reported by Kirk and Etok (1979) is presented in Table 1.

The exciting forces are compared with the results presented by Hooft (1971). Figs. 13, 14 and 15 show the plots of surge, heave and pitch forces as computed by Hooft and by the present programme. They are seen to be in good agreement.

The results of the added mass, restoring forces and exciting forces are thus adequately close for the present study.

The formulation of the time integration scheme is

checked by analyzing a single degree of freedom system problem with geometrical nonlinearity. The system has a mass of 50 Kg supported by two springs with  $EA=10^8$  N and pretension of 50 N. The length of the springs is 100 m. The mass is given an initial displacement of 20 m and the solution is found to be oscillatory. The results obtained by the Argyris formulation are compared with those obtained using the Runge-Kutta scheme. It has been shown in Fig. 16 that they are in very good agreement.

There is no data available for an exact comparison of the time histories obtained using the present formulation. However, a check on the amplitudes of the time histories confirm that they are within an acceptable range of the results obtained using the linear analysis.

### 5.3 Parametric Study

The objective of the parametric study is to vary the governing factors sequentially and to identify the trends in the variation of the responses.

Since the results of a two dimensional analysis lend themselves to clearer interpretations, a planar model is chosen for this study. The waves are assumed to be progressing in the aft and forward direction (that is the positive X axis) and the cable stiffness is varied on both cables at the aft side simultaneously. The frequency

domain analysis is carried out in five cases with each of the aft cables having 100%, 99%, 95%, 90% and 80% stiffness while the forward side cables are assumed to be intact. The nonlinear analysis is carried out for a regular wave of 10 m height and period of 8 s. The results of the three planar motions and the two tensions (forward and aft) are compared.

(i) Surge response

The values of the surge response amplitude operator obtained from the linear analysis are presented for a range of wave periods in Table 2. It can be seen that there is less than 1% change in the response for wave periods below 12 s. Even at the higher periods the change is less than 5%. Fig. 17 shows the time history obtained from the nonlinear analysis which confirms the findings of the linear analysis that the loss of stiffness has little effect on surge motions. It is therefore inferred that the surge motion is not directly affected by the loss of tether stiffness if the total tension remains constant.

(ii) Heave response

The values of the heave response amplitude operator obtained from the linear analysis for a range of wave periods are presented in Table 3. It can be seen that there is distinct pattern in the change in the response. The heave response changes from 1% to 25% for  $T=24$  s. It varies from 1.19% to 18.94% for  $T=8$  s. For the lower time periods the

response is negligible. Fig. 18 gives the time history obtained from the nonlinear analysis which indicates that the maximum response changes by 7.76% for a loss of 10% and by 15.29% for a loss of 20%. There is a significant change in the heave response due to the loss of stiffness. The effect of nonlinearities is not very pronounced.

(iii) Pitch response

The values of the pitch response amplitude operator obtained from the linear analysis are presented for a range of periods in Table 4. It can be seen that there is an increase of 2.5% to 27% for  $T=24$  s. The variation is up to 13%. Fig. 19 shows that according to the nonlinear analysis the maximum value changes by 7.3% and 16% for a loss of 10% and 20% respectively. It is inferred that the change in the pitch response is most significant and that the nonlinearities tend to reduce this variation. However the general trend is that the loss of stiffness increases the pitch motion in all cases.

(iv) Tension aft

The equilibrium tensions and the response amplitude operators obtained from the linear analysis are tabulated for the 5 cases in Table 5. The equilibrium tension changes from -1.025 to -11.91%. The responses change from -.1% up to 14% for  $T=24$  s. For  $T=8$  s the RAO changes from -.31% to

-7.137% and for  $T=4$  s the RAO changes from -1.41% to -11.29%. The nonlinear time history shows that the maximum response changes by -2.7% and 10% for a loss of 10% and 20% respectively. It may be noted that in the lower periods the response is pitch dominated, whereas in the higher periods it is heave dominated. The dynamics of the cable also affects the tension considerably as indicated in the time history in Fig. 20.

(vi) Tension forward

The values of equilibrium tensions and the response amplitude operators as per the linear analysis for the five cases are tabulated in Table 6. The equilibrium tension varies from .98% to 12.15%. The response varies from 1.1% to 28.13% at  $T=24$  s and from 1.44% to 22.36% at  $T=8$  s. The variation is between .64% to 11.4% at  $T=4$  s. Fig. 21 shows that the maximum response as per the nonlinear analysis varies by 3.29% and 18% for a loss of 10% and 20% respectively. Thus the nonlinear phenomena have a significant effect on the results. However, the general trend of increase in the response on the forward side due to the loss of stiffness on the aft side is confirmed.

(vii) The effect of wave height on the response.

Fig. 34 shows the effects of wave height on the tension history in the intact case and for a period of 8 s. The wave height is varied from 10 m to 30 m. It can readily

be seen that the effects caused by geometric nonlinearities are more for the higher wave.

(vii) Effects of wave frequency

Figure 23 shows the tension variation for a wave of 10 m height. The period is varied from 8 s to 12 s. There is significant change in the tensions both in terms of amplitude and phase. The nonlinear effects are more pronounced at higher periods or lower frequencies.

#### 5.4 Discussion

(i) A case study

Instead of reducing the stiffness on both the cables on the aft side the stiffness of only the aft starboard corner is reduced by 10%. The equilibrium tension changes from an even value of  $-0.2551 \times 10^8$  N to  $-0.2272 \times 10^8$  N on aft starboard, to  $-0.2617 \times 10^8$  N on the aft port and forward starboard corners and to  $-0.2710 \times 10^8$  on the forward port corner.

The response amplitude operators obtained from the linear analysis for the three motions are plotted in Figs. 24-26.

Fig. 24 shows that there is no change in the surge response. Figs. 25 and 26 show that the heave and pitch responses increase by about 10 to 12%. These findings are consistent with the trends shown in the parametric study.

The result also indicates a weak coupling between the six degrees of freedom. This coupling effect is caused by the asymmetry of the tether tensions. However, for the case studied the roll and yaw are very low (these values are not presented here). Figs. 27-29 show the time histories obtained from the nonlinear analysis, and they bear out the findings of the linear analysis.

The tension response amplitude operators shown in Fig. 30 indicate a reduction of 6% in the aft starboard tether which is damaged by 10%. The tension responses for the other three corners are given in Figs. 31-33. The response amplitude operator in the aft port side changes by 9% whereas both the corners on the forward side show a change of 20%. This implies that the platform has a tendency to move as a planar body for a fore and aft wave regardless of the unequal tensions, and therefore the conclusions drawn from the planar analysis are qualitatively valid. This has been confirmed by the results of the nonlinear analysis shown in Figs. 34 and 35. It may be pointed out here that the way the tension histories are plotted is a little misleading for interpretation because

- a. they indicate the tension at a given instant and not the variation of the tension from the mean value.
- b. the sign convention adopted for the nonlinear analysis takes the tension as having a minus sign.



Finally, it may be inferred from this case study that the platform has a tendency to compensate the loss of stiffness in one corner by increasing the tensions in the other three corners, with the largest share of load going on the diagonally opposite side. However, the change in the RAO does not follow this pattern. There is an equal and large increase in the RAO's on the leeward side (with respect to the incoming wave), and a marginal change in the windward side.

(ii) The natural periods of the system

The surge natural period at 57 s is high above the periods of the prevailing sea spectrum (neglecting second order effects). However, the surge response does show an increase as the wave period is increased.

The heave and pitch periods are much below the excitation spectrum. Since the platform has a very negligible response at these periods it is not possible to judge if there is any shift in the peaks.

The tether natural periods along its length are very low, since they have very small mass and high stiffness. These periods do not lie in the range of prevailing wave periods. The lateral dynamics of the tethers is in the range of the wave periods, and the results from this study have indicated that although it does not affect the platform motions, as established by Patel and Jeffries (1983), it does

affect the tension histories considerably. It will be interesting to do an eigenvalue evaluation of the tether natural frequencies and study the tension responses in that context.

(iii) Limitations of this study

The underlying assumptions made for the formulation of the problem have a strong bearing on the interpretations of the results.

It has been assumed that the total tension of the system is to remain constant for all the computations, and all the results are only valid under this condition.

The effects of vortex shedding by the tethers, and the forces caused by wind and current have not been considered for the clarity of understanding the behavior of the system.

The assumptions regarding the independence of added mass and damping terms on frequency are questionable. However, the trends shown by this analysis will not be affected significantly if these assumptions were modified.

(iv) Relevance

The relevance of the study lies in its applicability to the design and operation of the platform.

It is hardly conceivable that a designer would propose a platform having uneven stiffness. However, the operator may have to function for limited periods of time

with unequal tether stiffness, while one particular tether is being serviced. The results of this study are of relevance in such a situation.

Attempts are being made to develop reliable integrity monitoring systems for offshore platforms. A coupled elastic/rigid body analysis as developed in the present study can serve as a first step in such an effort.

The capabilities of this programme can also be utilized with very minor alterations to study other related problems such as riser dynamics and detailed fluid-cable interaction studies.

## CHAPTER 6

CONCLUSIONS

A brief summary of the study is given below:

1. The analytical methods for the development of a Tension Leg Platform are reviewed.

2. Numerical schemes for the linear and nonlinear analysis of the platform motions, tension response and lateral dynamics of the cables are formulated and implemented on a VAX 11/780 system.

3. The behavior of motion responses and tension variation on a platform with unequal tether stiffness has been studied. It has been shown that if the total tension remains constant, the surge motion is not affected by the loss of stiffness, but the heave and pitch responses are affected significantly. The tension responses are also affected directly, however, their behavior is nonlinear due to the lateral dynamics of the cables.

4. The platform has a tendency to compensate the loss of stiffness in one corner by increasing the mean tension on the diagonally opposite corner. However, if the platform is subjected to a wave progressing along the fore and aft directions, then the tension response amplitude operators increase in all the intact corners, but not in the ratio of the equilibrium tensions.

5. Recommendations: As a logical consequence of this study the following work is recommended:

- (i) An experimental verification of the results is called for.
- (ii) The effects of wave directionality on the findings ought to be investigated.
- (iii) The feasibility of developing an integrity monitoring system for the platform and cable system ought to be investigated.

## BIBLIOGRAPHY

1. Albrecht, H. G., Konig, D., Kokkinowrachos, K., "Nonlinear dynamic analysis of Tension Leg Platforms for medium and greater depths, Offshore Technology Conference, Paper #3044, Houston, 1978, pp. 7-12.
2. Argyris, J. H. and Chan, A. S. L., "Application of Finite Elements in Space and Time", Ingenieur Archive, 41, 1972, pp. 235-257.
3. Argyris, J. H., Dunne, P. C., Angelopoulos, T., "Nonlinear Oscillations using Finite-Element Technique", Computer Methods in Applied Mechanics and Engineering, 2, 1973, pp. 203-250.
4. Argyris, J. H., Dunne, P. C., Angelopoulos, T., "Dynamic response by large step integration", International Journal of Earthquake Engineering and Structural Dynamics, 2, 1973, pp. 185-203.
5. Ashford, R. A. and Wood, W. L., "Numerical integration of the motions of a tethered buoyant platform", International Journal of Numerical Methods in Engineering, 13, 1978, pp. 165-180.
6. Burke, B. G., "The analysis of motions of semisubmersible drilling vessel in waves", Offshore Technology Conference, Paper #1024, Houston, 1969, pp. 235-245.
7. Capanoglu, C., "Tension Leg Platform Design: Interaction of Naval Architectural and Structural Design Considerations", Marine Technology, Vol. 16, No. 4, Oct. 1979, pp. 343-352.
8. Chou, F. S. F., Ghosh, S., Kypke, D. A., "Analytical approach to the design of a Tension Leg Platform", Offshore Technology Conference, Paper #3883, Houston, 1980, pp. 287-296.
9. Denise, J. P. F. and Heaf, N. J., "A comparison between linear and nonlinear response of a proposed tension leg platform", Offshore Technology Conference, paper # 3555, Houston, 1979, pp. 1743-1754.
10. Dillingham, J. T., "Recent experience in Model-Scale Simulation of Tension Leg Platforms", Marine Technology, April 1984, pp. 186-200.

11. Dunsire, R. and Owen, D. G., "Model testing of TLP Systems", Third international offshore mechanics and Arctic Engineering Symposium, ASME, New Orleans, Feb. 1984, pp. 20-31.
12. Ellis, N., Tetlow, J. H., Anderson, F., Woolhead, A. L., "Hutton TLP structural configuration and design features", Offshore Technology Conference, paper #4427, Houston, 1982, pp. 557-572.
13. Faltinsen, O., and Michelson, F. C., "Motions of large structures in waves at zero Froude Number", Proceedings of Symposium on Dynamics of Marine Vehicles and Structural in Waves, London, 1974, pp. 91-106.
14. Faltinsen, O., Fylling, Van Hoof, R., Teiger, P. S., "Theoretical and experimental investigations of tension leg platform behaviour", International Conference on Behaviour of Offshore Structures, 1982, pp. 411-423.
15. Guyan, R. J., "Reduction of stiffness and mass matrices", AIAA Journal, Vol. 3, No. 2, 1965, p. 380.
16. Hong, S. T., "Tension in a taut mooring line; frequency domain analysis", Offshore Technology Conference, Paper #2069, Houston, 1974, pp. 389-400.
17. Hoof, J. P., "Oscillatory wave forces on small bodies", International shipbuilding progress, April 1970, pp. 127-135.
18. Hoof, J. P., "A mathematical method of determining hydrodynamically induced forces on a semisubmersible. Transactions, Society of Naval Architects and Marine Engineers, 1971, pp. 28-70.
19. Jeffries, E. R. and Patel, M.H., "Dynamic analysis models of Tension Leg Platforms", Offshore Technology Conference, Paper #4075, Houston, 1981, pp. 99-107.
20. Katayama, M., Unoki, K., Jiwa, E., "Response analysis of TLP with mechanical damping waves", International Conference on Behavior of Offshore Structures, 1982, pp. 497-525.
21. Kirk, C. L., and Eto, E. U., "Dynamic response of a tethered production platform in a random sea state", International Conference on Behavior of Offshore Structures, London, 1979, 2, pp. 139-163.

22. Keyser, D. R. and Mott, G. D., "The determination of wire rope tension by frequency measurements", Offshore Technology Conference, Paper # 1296, Houston, 1970, pp. 689-696.
23. Liu, D., Chen, Y. N., Shin, Y. S., Chen, P. S., "Integrated computational procedure for the hydrodynamic loads and structural responses on a TLP", Seminar on computational methods in offshore structures, ASME, 1980, pp. 89-100.
24. Lloyd, J., Potthurst, R., Winkworth, "Structural analysis of Tension Leg Platforms", Symposium of RINA Offshore Engineering Group on new generation semisubmersibles, London, 1983.
25. Lyons, G. J., Patel, M. H., Sarohia, S., "Theory and model test data for tether forces on a tethered Buoyant Platform", Offshore Technology Conference, Paper # 4643, Houston, 1983, pp. 533-543.
26. Martin, H. C., "On derivation of stiffness matrices for the analysis of large deflection and stability problems", AFF-TR-66-80, 1966.
27. Mercier, J. A., Goldsmith, R. G., Curtis, L. B., "The Hutton TLP: A preliminary design", European Offshore Petroleum Conference, London, 1980, pp. 525-534.
28. Mercier, J. A., Leverette, S. J., Bliault, A. L., "Evaluation of the Hutton TLP response to environmental loads", Offshore Technology Conference, Paper # 4429, Houston, 1983, pp. 585-601.
29. Morison, J. R., O'Brien, M. P., Johnson, J. W., Scharf, S. A., "The force exerted by surface waves on piles", Petroleum Trans. AIME, 189, 1950, pp. 149-154.
30. Natvig and Pendered, "Nonlinear motion response of floating structures to wave excitation", Offshore Technology Conference, Paper #2796, Houston, 1977, pp. 527-534.
31. Oljedirektoratet, Norway, "A state of the art review of the integrity monitoring systems being offered or under development for use in offshore structures, 1981.
32. Paulling, J. R. and Horton, E. E., "Analysis of Tension Leg Stable Platforms", Offshore Technology Conference, Paper #1263, Houston, 1970, pp. 379-390.



33. Pauling, J. R., "Time domain simulation of semisubmersible platform motions with application to tension leg platforms", Spring meeting/ STAR symposium, Society of Naval Architects and Marine Engineers, San Francisco, 1977, pp. 303-314.
34. Patel, M. H., and Lynch, E. J., "Coupled dynamics of tensioned buoyant platforms and mooring tethers", Engineering Structures, Vol. 5, Oct. 1983, pp. 299-308.
35. Rainey, R. T. C., "Dynamics of tethered platforms", The Naval Architect, May 1978, pp. 59-80.
36. Roren, E. Q. M. and Steinwik, B., "Deep water resonance problems in the mooring system of a Tension Leg platform", Offshore Structures Engineering, Gulf Publishing Co., 1977, pp. 135-149.
37. Tetlow, J. H., Bradshaw, Leece, M. J., "Hutton TLP mooring system", Offshore Technology Conference, paper #4428, Houston 1982, pp. 573-583.
38. Turner, M. J., Dill, E. H., Martin, H. R., Melosh, R. J., "Large deflection of Structures subjected to heating and external loads", J. of Aerospace Sciences, Vol. 27, Feb. 1960.
39. Standig, R. G., "Use of diffraction theory with Morison's equation to compute the wave loads and motions of offshore structures", NMI-R74, National Maritime Institute, U.K., 1979.
40. Wilson, E. L., Bathe, K. J., Numerical methods in finite element analysis, Prentice-Hall, Inc., Englewood Cliffs, N.J., 1976, p. 319.
41. Yoshida, K., Yoneya, T., Oka, N., "Snap loads on taut moored platforms", J. of Society of Naval Architects of Japan, Vol. 144, 1978.
42. Yoshida, K., Yoneya, T., Oka, N., Ozaki, M., "Motions and leg tensions of a tension leg platform", Offshore Technology Conference, Paper #4073, Houston, 1981, pp. 75-87.

Table 1: Comparison of computed results with data presented by Kirk and Etok (1979)

Item.	From literature	Computed
Displacement	$4.34 \times 10^4 \text{ m}^3$	$4.54 \times 10^4 \text{ m}^3$
Total tension	$1.0045 \times 10^8 \text{ N}$	$1.0203 \times 10^8 \text{ N}$
Surge mass and added mass	$6.4 \times 10^7 \text{ kg}$	$6.92 \times 10^7 \text{ kg}$
Heave mass and added mass	$5.6 \times 10^7 \text{ kg}$	$5.69 \times 10^7 \text{ kg}$
Pitch inertia and added inertia	$9.88 \times 10^{10} \text{ kg-m}^2$	$9.68 \times 10^{10} \text{ kg-m}^2$
Stiffness per leg in surge	$2.05 \times 10^5 \text{ N/m}$	$2.05 \times 10^5 \text{ N/m}$
Stiffness per leg in heave	$7.6 \times 10^7 \text{ N/m}$	$7.6 \times 10^7 \text{ N/m}$
Stiffness per leg in pitch	$9.3 \times 10^{10} \text{ Nm/rad}$	$9.3 \times 10^{10} \text{ Nm/rad}$
Natural period in surge	55 s	57.86 s
Natural period in heave	3.7 s	3.39 s
Natural period in pitch	4.0 s	3.9 s

Table 2: A parametric study of surge response amplitude operators

Stiffness Period	100%	99%	95%	90%	80%
	RAO				
24 s	.935	.937	.9414	.9457	.9515
16 s	.682	.6827	.6843	.686	.6879
12 s	.393	.3941	.3946	.3952	.3959
9.6 s	.07032	.07034	.07041	.07046	.07054
8 s	.1795	.17953	.17965	.17976	.1799
6.8 s	.25816	.25819	.25831	.25843	.25858
5.33 s	.04255	.04256	.04257	.04258	.04259
4.8 s	.13945	.13946	.13949	.13952	.13956
4 s	.07556	.07557	.07558	.07559	.07561

Table 3: A parametric study of heave response amplitude operators

Stiffness Period	100%	99%	95% RAO	90%	80%
24 s	.0165	.0167	.01745	.01844	.0208
16 s	.00408	.0041	.0043	.00453	.0051
12 s	.0052	.00526	.0056	.00577	.00648
9.6 s	.00805	.00812	.00845	.0089	.00995
8 s	.00586	.00573	.00595	.00626	.00697
6.8 s	.00206	.00208	.00216	.00226	.00251
5.33 s	.0003	.0003	.00031	.00032	.00035
4.8 s	.00013	.00013	.00014	.00014	.00015
4 s	.0	.0	.00001	.00001	.00003

Table 4: A parametric study of the pitch response amplitude operators

STIFFNESS Period	100%	99%	95% RMO x 10 <sup>3</sup>	90%	80%
24 s	.4	.41	.43	.45	.51
16 s	.51	.51	.54	.57	.64
12 s	.37	.38	.39	.41	.46
9.76 s	.05	.05	.05	.06	.06
8 s	.51	.52	.54	.56	.61
6.8 s	.68	.68	.70	.73	.80
5.33 s	.11	.11	.12	.12	.13
4.8 s	.39	.39	.40	.43	.44
4 s	.22	.22	.23	.23	.25

Table 5: A parametric study of the tension response amplitude operator on the aft side

Equilibrium Tensions $\times 10^8$ N	.2551	.2525	.2440	.2357	.2247
Stiffness Period	100%	99%	95%	90%	80%
	PAO $\times 10^7$ N/m				
24 s	.1492	.1492	.1489	.1484	.1471
16 s	.1290	.1289	.1287	.1284	.1274
12 s	.1126	.1126	.1128	.1129	.1131
9.5 s	.05676	.05671	.05647	.0554	.0531
8 s	.1247	.1248	.1228	.1207	.1158
6.8 s	.17	.1696	.1675	.1648	.1586
5.33 s	.02833	.02822	.02776	.02715	.02578
4.8 s	.0992	.0988	.09708	.09482	.08982
4 s	.05739	.05711	.05539	.05439	.05106

Table 6: A parametric study of the tension response amplitude operator on the forward side

Equilibrium Tensions $\times 10^3$ N	RAO $\times 10^{-10}$ N/m			
	100%	99%	95%	90%
24 s	.2551	.2576	.2665	.2754
16 s	.172	.1739	.182	.1932
12 s	.141	.142	.148	.15676
9.6 s	.0937	.0945	.09788	.1023
8 s	.0647	.0654	.06814	.0719
6.8 s	.152	.1542	.1601	.1680
5.33 s	.181	.183	.1891	.1971
4.8 s	.0301	.03039	.03125	.03236
4 s	.1001	.1007	.1032	.1065
	.0573	.05711	.0589	.06054
				.06387

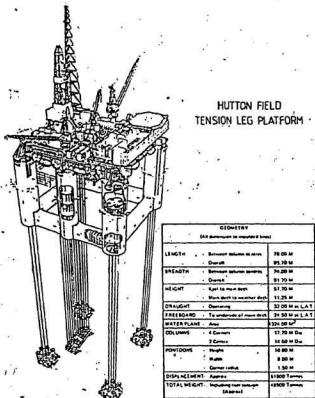


Fig. 1 Overall view of TLP with key dimensions

Taken from Ellis et. al. (1982)



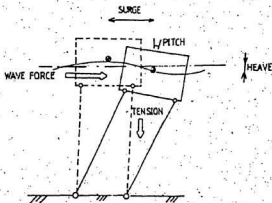


Fig. 2 Schematic representation of planar motions

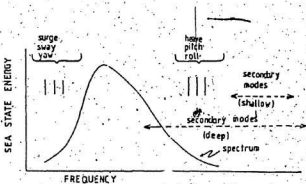


Fig. 3 Natural frequencies of a Tension Leg Platform

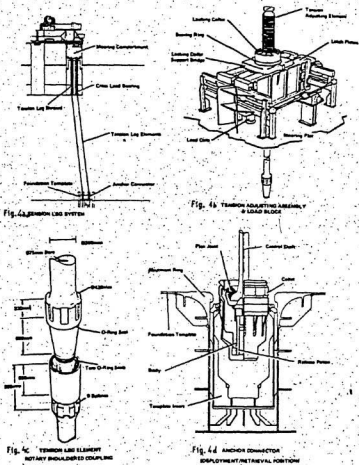


Fig. 4. Details of the mooring system

Taken from Tetlow and Leece (1982)

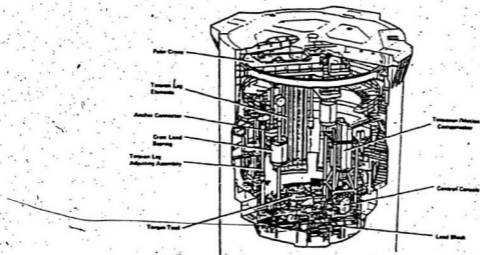


Fig. 5 Mooring compartment.

Taken from Tetlow and Leece (1982)

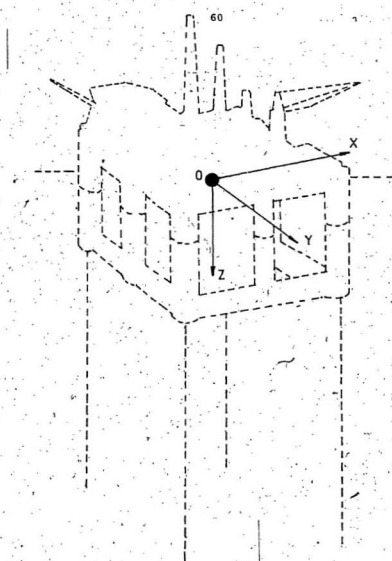


Fig 6 The linear model

OXYZ indicates the global frame of reference  
fixed at the center of gravity

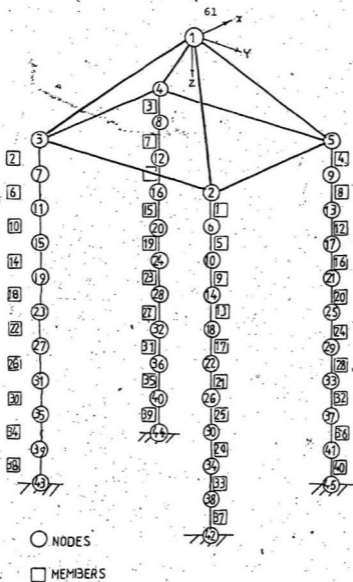


Fig. 7 The finite element model

OXYZ indicates the global frame of reference fixed at the center of gravity

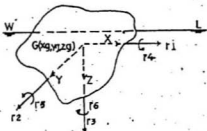


Fig. 8(a) 6 d.o.f. associated with the motion

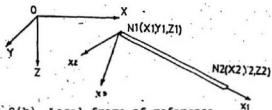


Fig. 8(b) Local frame of reference

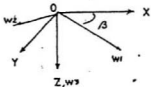


Fig. 8(c) Wave frame of reference

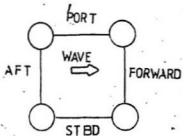


Fig. 8(d) Wave direction

Fig. 8. Definition sketches

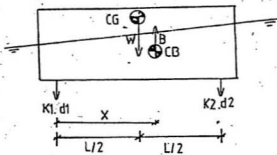


Fig. 9(a)

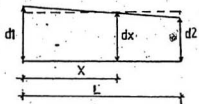


Fig. 9(b)

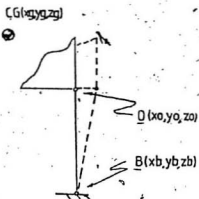


Fig. 9(c)

Fig. 9 Tether Model

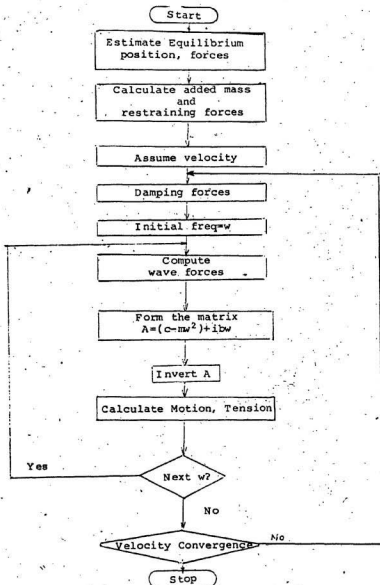


Fig. 10: Flow chart for the linear analysis algorithm



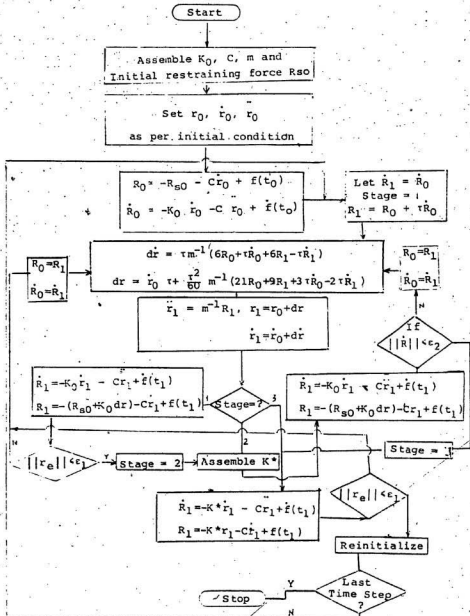
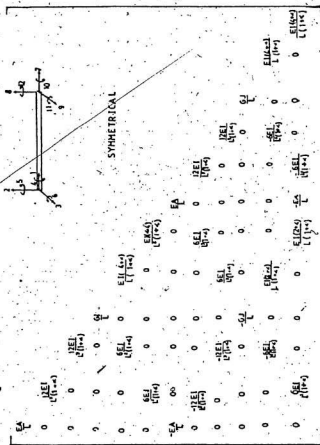


Fig. 11: Flow chart of nonlinear analysis algorithm



Note:  $E$  = Young's modulus,  $I = 12I_2$ ,  $G =$  Shear modulus,  $J =$  pol. Mom. of Inertia  
 $L =$  Moment of inertia,  $GAL = 2$  d.o.f. are constant with Fig. 8(b)

Fig. 12 Elastic stiffness matrix of a beam element

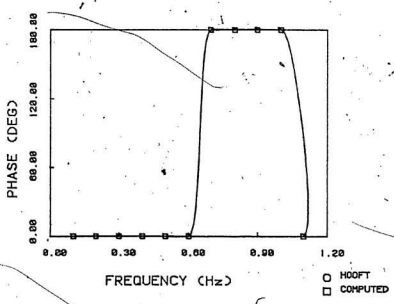
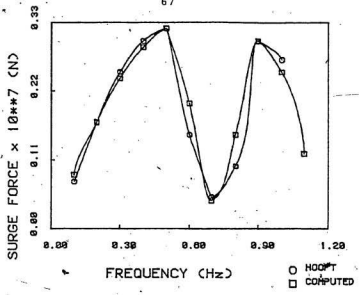


Fig- 13 Surge force versus frequency

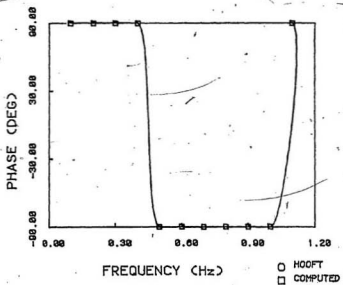
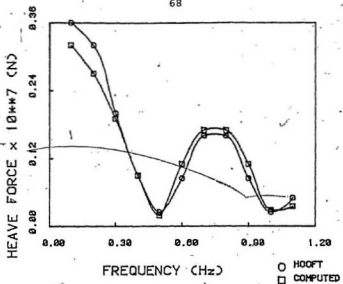


Fig. 14 Heave force versus frequency

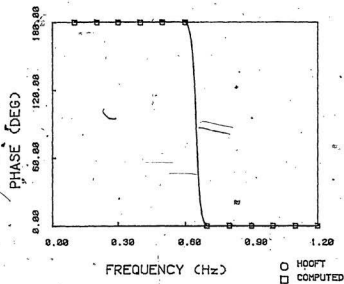
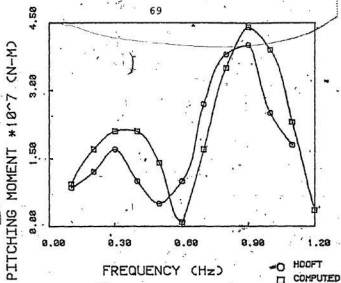
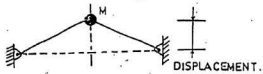


Fig. 15 Pitching moment versus frequency



- ARBYRIS
- RUNGE KUTTA

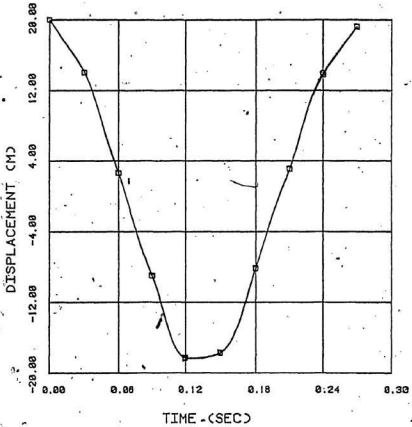


Fig. 16--Displacement versus time

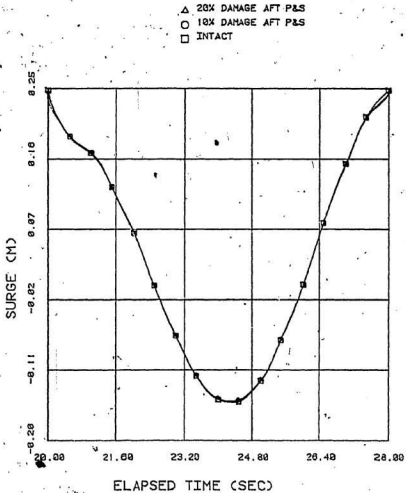


Fig. 17 Surge displacement versus time: Parametric Study.

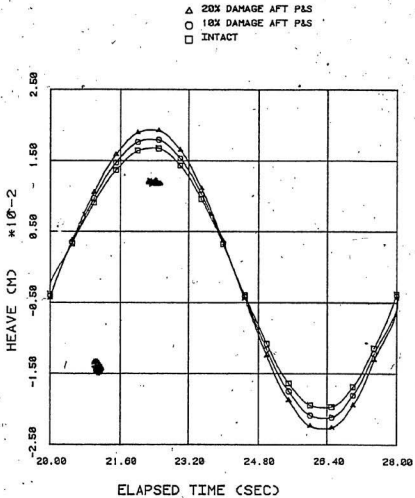


Fig. 18. Heave displacement versus time: Parametric study.



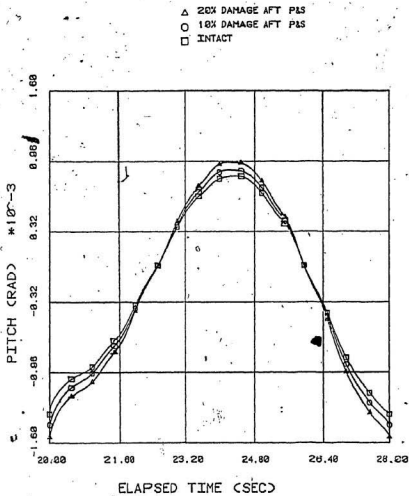


Fig. 19 Pitch motion versus time: Parametric study

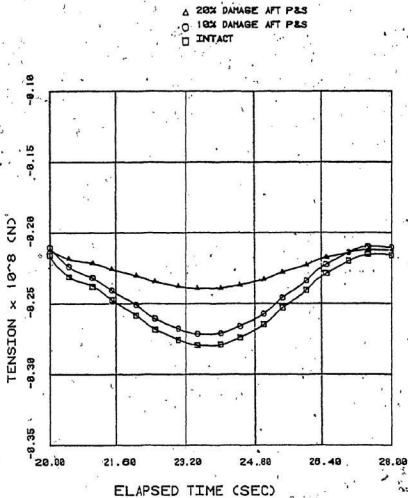


Fig. 20 Tension-aft versus time: Parametric study

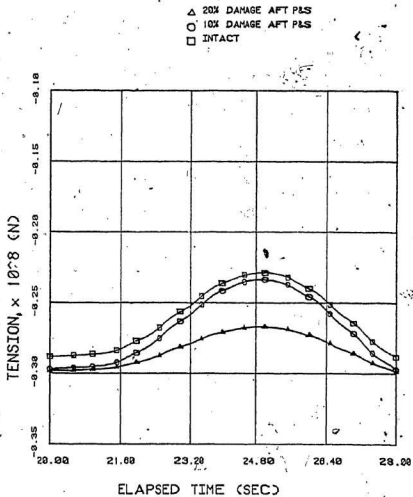


Fig. 21 Tension forward versus time; Parametric study

- + FOR TENSION FOR H = 38 m
- △ AFT TENSION FOR H = 38 m
- FOR TENSION FOR H = 18 m
- AFT TENSION FOR H = 18 m

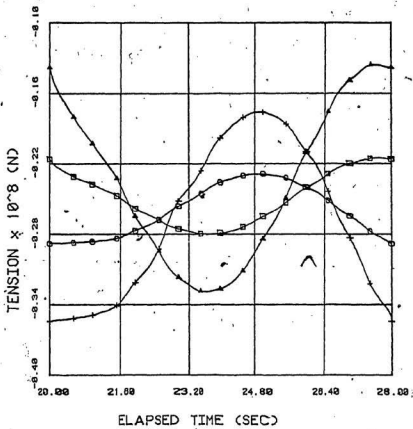


Fig. 22 Effect of wave height on tension history:  
Parametric study

- + FOR TENSION FOR T = 12 sec
- △ AFT TENSION FOR T = 12 sec
- FOR TENSION FOR T = 8 sec
- AFT TENSION FOR T = 8 sec

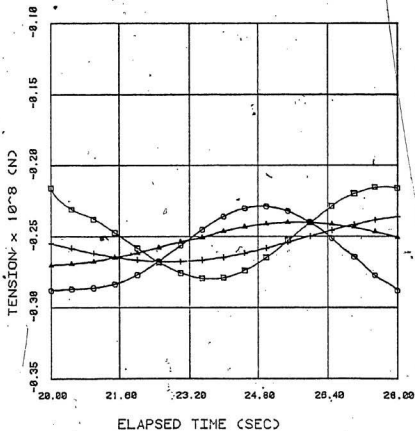


Fig. 23 Effect of wave frequency on tension history:  
Parametric study

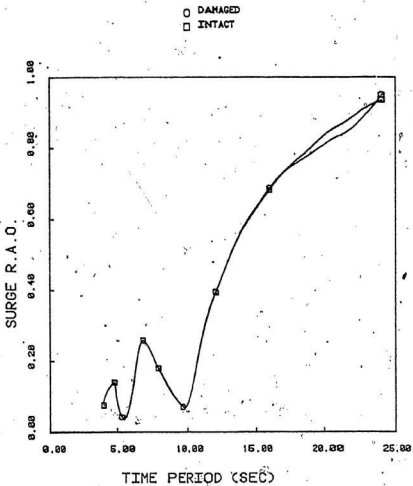


Fig. 24 Surge response amplitude operator versus time:  
A case study

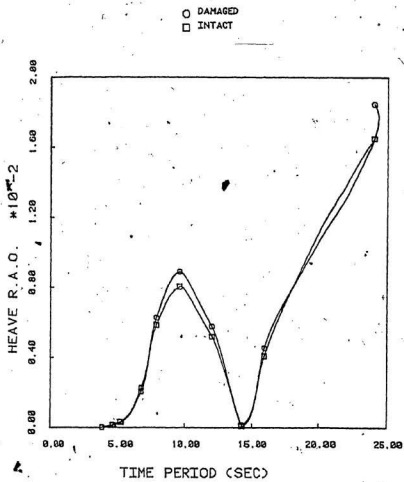


Fig. 23 Heave response amplitude operator versus time: A case study

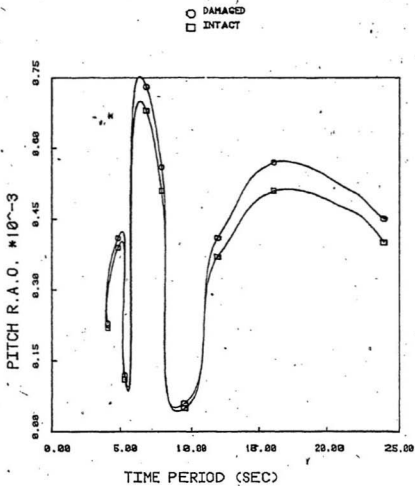


Fig. 26 Pitch response amplitude operator versus time:  
A case study



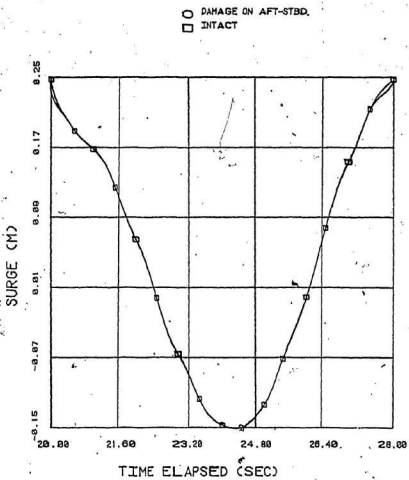


Fig. 27. Surge displacement versus time: A case study

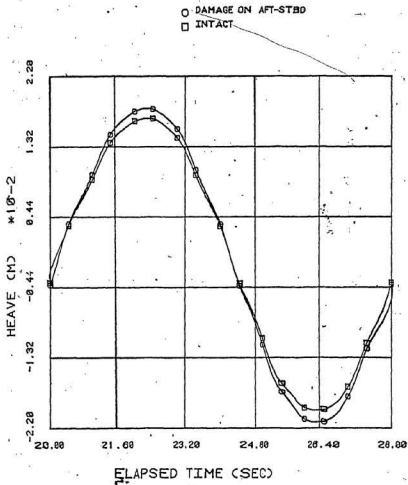


Fig. 28 Heave displacement versus time: A Case study

○ DAMAGE ON AFT-STBD  
□ INTACT

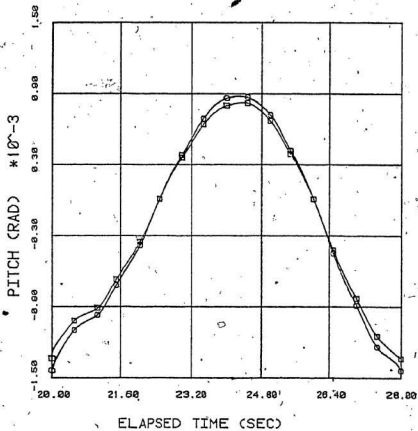


Fig. 29 Pitch motion versus time: A case study

○ DAMAGED  
□ INTACT

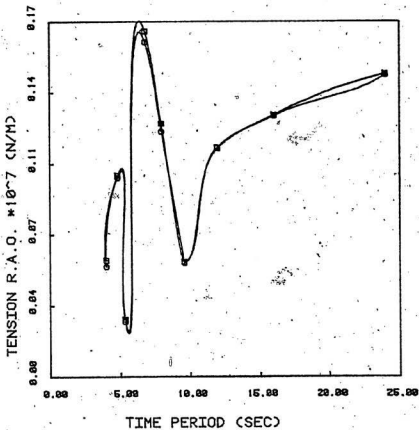


Fig. 30 Tension response amplitude operator versus time period aft starboard side

○ DAMAGED  
□ INTACT

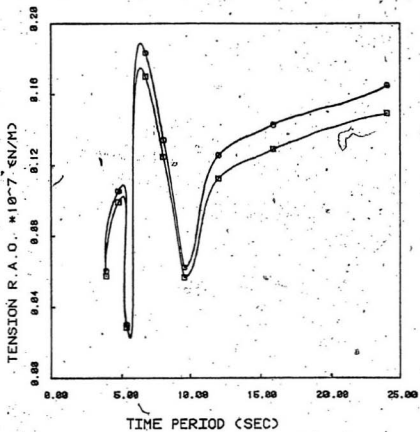


Fig. 31 Tension response amplitude operator versus time period for aft port side

○ DAMAGED  
□ INTACT

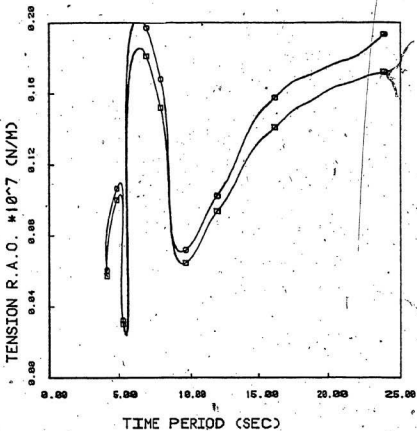


Fig. 32 Tension response amplitude operator versus time period for forward port side

○ DAMAGED  
□ INTACT

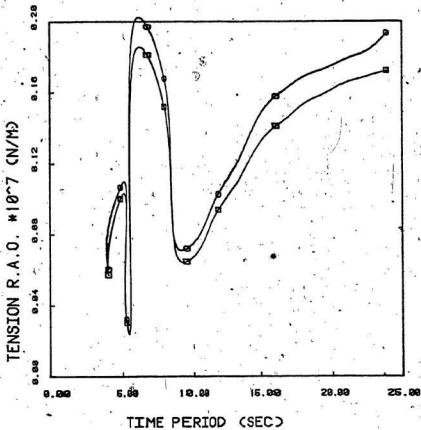


Fig. 33 Tension response amplitude operator versus time periods for forward stardboard side

- △ DAMAGE ON AFT-STBD; TENSION ON PORT  
 ○ DAMAGE ON AFT-STBD, TENSION ON STBD  
 □ INTACT AFT

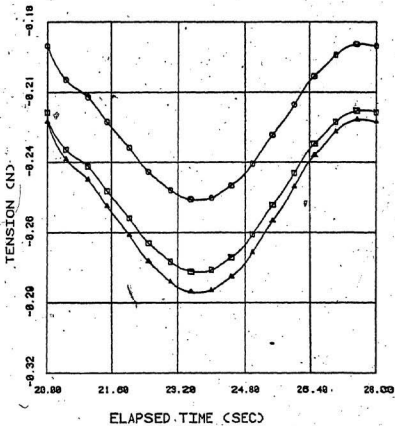


Fig. 34. Tension aft versus elapsed time



- △ DAMAGE ON AFT-STBD, TENSION ON PORT  
○ DAMAGE ON AFT-STBD, TENSION ON STBD  
□ INTACT

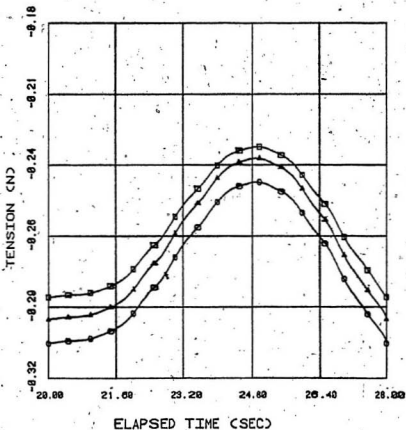


Fig. 35 Tension forward versus elapsed time

APPENDIX

APPENDIX A  
HYDRODYNAMIC ANALYSIS

A.1 The Problem

Consider a platform floating in an ocean of uniform depth  $d$  and let the free-surface be infinitely large. Fig. 8(a) shows the floating body and defines the frame of reference. If the flow conditions are assumed to be inviscid, irrotational, incompressible and acyclic, the flow field can be characterized by a single valued velocity potential  $\phi$ , such that

$$\phi(x, y, z, t) = \psi(x, y, z) \exp(i\omega t)$$

here  $(x, y, z)$  are the spatial coordinates,  $t$  is the time instant and  $\omega$  is the frequency. The potential function  $\psi$ , can be separated into 3 parts as

$$\psi = \psi_1 + \psi_2 + \psi_3$$

where

$\psi_1$  is the incident wave potential in the absence of body

$\psi_2$  is the velocity potential of the scattered waves

$\psi_3$  is the normalized velocity potential associated with the motion of the body.

All the individual potentials must satisfy the

Laplace equation in the fluid domain:

$$\nabla^2 \psi_k = 0, \quad k = 1, 2, 3$$

This equation is subject to the following boundary conditions:

(i) On the sea floor

$$\frac{\partial \phi_k}{\partial z} = 0 \text{ at } z = d \text{ for } k = 1, 2, 3$$

(ii) On the free surface

$$\frac{\partial \phi_k}{\partial z} - \frac{w^2}{g} \phi_k = 0 \text{ at } z = 0 \text{ for } k = 1, 2, 3$$

Here  $g$  is the acceleration due to gravity. The wave height and body motion are assumed to be small when compared with the wave length, water depth and body dimensions. Hence this equation can be linearized.

(iii) On the body surface

$$\frac{\partial \phi_k}{\partial n} = n_k, \quad k=3$$

$$\frac{\partial \phi_1}{\partial n} = -\frac{\partial \phi_2}{\partial n}$$

Here  $\frac{\partial}{\partial n}$  is the normal derivative in the direction of the outward normal of the body  $\bar{n}$ ,  $\bar{n}_1$  through  $\bar{n}_3$  are the generalized direction cosines. The total hydrodynamic force on the body is determined by using the Bernoulli equation derived by integrating the water pressure over the body surface.

(iv) The far field condition: In order to ensure a correct modelling of the field problem the velocity potential at a field point must tend to zero as the distance between that point and the origin tends to infinity. Physically, this

implies that all the disturbances created on the free surface ought to die out in the far field.

#### A.2 The Hydrodynamic Synthesis

The complex structure of a platform is considered as an assembly of a group of simpler bodies, whose hydrodynamic properties can be computed with relative ease. The fundamental assumption is that the hydrodynamic force on the assembled structure is equal to the sum of the forces on the component bodies. The interaction between the members is ignored. For the structure of interest, the simplified shape is taken to be an arbitrarily oriented tubular member, as shown in Figure 8(b).

#### A.3 Theoretical Analysis

Hoofst (1970) has suggested that the solution may be broken into 3 stages.

Stage 1: The hydrodynamic force on an oscillating body in still water is given by

$$F_H = - \iint_S p n_K ds$$

in which  $p$  is the pressure and  $S$  is the surface of the body.

This is expressed as

$$F_{H_j} = \sum_{k=1}^N (a_{kj} r_j + b_{kj} \dot{r}_j + c_{kj} \ddot{r}_j) \text{ for } j=1,6$$

where  $r_j$  is the motion of the body in the  $j$ th mode

$a_{kj} = -\text{Re} \rho \iint \psi_3 n_k ds$ , is the added mass

$b_{kj} = \text{Im} \rho \omega \iint \psi_3 n_k ds$ , is the hydrodynamic damping

$c_{kj}$  = Hydrostatic restoring force coefficient

Re and Im denote the real and imaginary parts of the integral.

Stage 2: The force on a fixed obstacle in waves is given by

$$F_H = i\rho \left[ \iint_S \psi_1 n_k ds - \iint_S \psi_3 \frac{\partial \psi}{\partial n} ds \right]$$

where  $\psi_1$ , the incident wave potential in the wave coordinates (see Fig. 8(c)) given by

$$\psi_1 = \frac{u_1 g a_0}{\omega} \exp(Kx - \omega t)$$

where

$a_0$  = Wave amplitude

$K$  = Wave number

$u_1 = \cosh(x+d)/\cosh(kz)$

$\omega$  = Frequency of excitation

Stage 3: After combining the first two stages it can be shown that the total hydrodynamic force on a slender member can be expressed as

$$F_H = \frac{V_j \exp(i\omega t)}{i\omega} [\omega^2 (\delta_{Kj} m_{Kj} + a_{Kj}) - b_{Kj} i\omega]$$

where

$$\delta_{Kj} = 1 \text{ if } K = j, = 0 \text{ if } K \neq j$$

$m_{Kj}$  = Mass or moment of inertia of the body

$a_{Kj}$  = Added mass

$b_{Kj}$  = Damping coefficient

It has been assumed that the added mass and the damping coefficients are independent of the frequency. Except for the Froude-Kriloff force this equation is identical to the so-called Morison's equation. Froude-Kriloff force is the undisturbed pressure force that arises from the pressure over the hull in a wave that has not been disturbed by the hull. The validity of this equation is limited to slender members, whose diameter is less than one-fifth of the wave length.

The paper by Hooft (1971) gives the detailed equations for the computation of added mass, damping forces, hydrostatic restoring forces and the wave excitation forces.

## APPENDIX B -

THE STIFFNESS COMPUTATIONB.1. The Linear Stiffness Matrix

The equations of the stiffness of a cable, whose end coordinates are  $O(x_0, y_0, z_0)$  and  $B(x_b, y_b, z_b)$  respectively, have been derived.  $T$  is the pretension in the cable,  $L$  is the length,  $E$  is the Young's modulus of the material and  $A$  is the area of cross-section. The cable geometry is shown in Fig. 9(a). The center of gravity of the structure is at  $CG(x_g, y_g, z_g)$ . The equations for the elements of the stiffness matrix are presented here.

$$K_{1j} = \frac{T}{L} P_{1j} + \left( \frac{EA-T}{L^3} \right) (B-O) Q_j; j=1, 2, 3$$

$$K_{4j} = \frac{T}{L} U_{4j} - (y_0 - y_g) K_{3j} + (z_0 - z_g) K_{2j}$$

$$K_{5j} = \frac{T}{L} U_{5j} - (z_0 - z_g) K_{1j} + (x_0 - x_g) K_{3j}$$

$$K_{6j} = \frac{T}{L} U_{6j} - (x_0 - x_g) K_{2j} + (y_0 - y_g) K_{1j}$$

For  $j=1, 2, 3, \dots, 6$ 

where

$$P_{11} = P_{22} = P_{33} = 1 \quad P_{15} = z_0 - z_g \quad P_{16} = (y_0 - y_g)$$

$$P_{26} = x_0 - x_g \quad P_{24} = -(z_0 - z_g) \quad P_{34} = y_0 - y_g \quad P_{35} = -(x_0 - x_g)$$

$$Q_1 = x_0 - x_b \quad Q_2 = y_0 - y_b \quad Q_3 = z_0 - z_b$$

$$Q_4 = (z_0 - z_g)(y_b - y_0) - (y_0 - y_g)(z_b - z_0)$$

$$Q_5 = (x_0 - x_g)(z_b - z_0) - (z_0 - z_g)(x_b - x_0)$$



$$Q_6 = (x_0 - x_g)(x_b - x_0) - (x_0 - x_g)(y_b - y_0)$$

$$U_{44} = -(z_0 - z_g)(z_b - z_0) + (y_0 - y_g)(y_b - y_0)$$

$$U_{45} = (x_0 - x_g)(y_b - y_0)$$

$$U_{46} = (x_0 - x_g)(z_b - z_0)$$

$$U_{54} = (y_0 - y_g)(x_b - x_0)$$

$$U_{55} = -(x_0 - x_g)(x_b - x_0) + (z_0 - z_g)(z_b - z_0)$$

$$U_{56} = (y_0 - y_g)(z_b - z_0)$$

$$U_{64} = (z_0 - z_g)(x_b - x_0)$$

$$U_{65} = (z_0 - z_g)(y_b - y_0)$$

$$U_{66} = (y_0 - y_g)(y_b - y_0) + (x_0 - x_g)(x_b - x_0)$$

## B.2 Nonlinear Stiffness Matrix of a Beam Element

The concept of the stiffness matrix of beam element subjected to large displacements was developed by Turner et al. (1959). This paper derived a new class of stiffness matrices for axial force members. The new stiffness matrix was shown to be dependent on the state of stress existing in the member prior to the imposition of additional disturbance.

Martin (1966) has presented a detailed formulation of the beam-column stiffness based on the energy principles in nonlinear mechanics. Two sources of nonlinearity exist for the large deflection problems. The first one is

connected with the strain-displacement equations. Even if strains remain small, rotation of the element adds nonlinear terms to the strain-displacement equations. It has been shown that if these terms are omitted, the derivations shall not yield the geometric stiffness. The second source of nonlinearity exists with respect to the equilibrium equations. If the equations, at each step, are written with respect to the deformed geometry, the formulation in effect becomes nonlinear. Nonlinearity caused by material behavior is not considered in this formulation. The total stiffness matrix is expressed as

$$[K] = [K_E] + [K_G]$$

where  $[K]$  is the total stiffness matrix of the beam,  $[K_E]$  is the elastic stiffness matrix and  $[K_G]$  is the geometric stiffness matrix.

The well known elastic stiffness matrix is shown for a beam element with 12 degrees of freedom in Fig. 12.

It has been shown that the geometric stiffness of a beam element may be approximated by the geometric stiffness of a truss element. For a plane truss with axial displacements  $V_1, V_2$ , rotations  $\theta_1, \theta_2$ , length  $L$  and with a pretension of  $T$ , the geometric stiffness matrix is given by

$$[K_G] = T \begin{matrix} & \begin{matrix} v1 & \theta1 & v2 & \theta2 \end{matrix} \\ \begin{bmatrix} 6/5L & & & \\ 1/10 & 2L/5 & & \\ -6/5L & -1/10 & 6/5L & \\ 1/10 & -L/30 & -1/10L & 2L/5 \end{bmatrix} & \begin{matrix} \\ \\ \text{symmetrical} \\ \end{matrix} \end{matrix}$$

The basis of the approximation that the geometric stiffness of a beam is identical to the geometric stiffness of a stringer is the physical reasoning that a beam-column may be viewed as a member having distinct bending and axial stiffness, and the axial stiffness is essentially that of an equivalent stringer. Furthermore, it is the initial axial loading which will have a significant influence on the overall stiffness against transverse loads, as has been borne out in a number of numerical studies. The smaller terms in the stringer stiffness matrix are ignored to arrive at the very familiar matrix for  $[K_G]$ .

$$[K_G] = \begin{matrix} & \begin{matrix} v1 & v2 \end{matrix} \\ \begin{bmatrix} T/L & -T/L \\ -T/L & T/L \end{bmatrix} & \end{matrix}$$

This approximation is valid only if a large number of elements are used to approximate the deflected shape.

The stiffness matrices discussed here have been expressed in the local frame of reference. They have to be transformed to the global frame of reference before assembling the system equation.

## APPENDIX C

## INPUT FOR THE PROGRAMME TLP1

```

12.1.02503,9.81D0
-35.0, 35.0,41.7,-35.0, 35.0, 6.7,16.0,
-35.0,-35.0,41.7,-35.0,-35.0, 6.7,16.0,
 35.0, 35.0,41.7, 35.0, 35.0, 6.7,16.0,
 35.0,-35.0,41.7, 35.0,-35.0, 6.7,16.0,
-35.0, 0.0,35.7,-35.0, 0.0, 6.7, 3.5,
 0.0, 35.0,29.2, 0.0, 35.0, 6.7, 3.5,
 0.0,-35.0,29.2, 0.0,-35.0, 6.7, 3.5,
 35.0, 0.0,35.7, 35.0, 0.0, 6.7, 3.5,
-27.0, 35.0,35.45,27.0, 35.0,35.45,12.5,
-27.0,-35.0,35.45,27.0,-35.0,35.45,12.5,
-35.0, 27.0,38.7,-35.0,-27.0,38.7, 6.0,
 35.0,-27.0,38.7, 35.0, 27.0,38.7, 6.0
36182000.,0.,0.,0.,0.,0.,
0.,36182000.,0.,0.,0.,0.,
0.,0.,36182000.,0.,0.,0.,
0.,0.,0.,0.959D11,0.,0.,
0.,0.,0.,0.,0.641D11,0.,
0.,0.,0.,0.,0.,0.867D11
0.,0.40,0.53,0.01,6.7,166.7
-35.0, 35.0,166.7,-35.0, 35.0,41.7,9.236D09,
-35.0,-35.0,166.7,-35.0,-35.0,41.7,9.236D09,
 35.0, 35.0,166.7, 35.0, 35.0,41.7,9.236D09,
 35.0,-35.0,166.7, 35.0,-35.0,41.7,9.236D09
70.,70.,102020000.,354950000.,
3.46D-02,0.04,0.00001,0.1D-5

```

C INPUT FOR THE PROGRAMME TLP2

C INPUT ON UNIT 10

ANALYSIS OF A TLP (WAVE=10M,8 S, WATER DEPTH=160M)

37,0,32,32,0,120,0.5,0.0D0,6

1,1

5,3,0.10D-15,0.10D-15,1,1

1,0,1,0,1,0,1, 0.0, 0.0, 0.0,0

2,0,1,0,1,0,1,-35.0, 35.0, 41.7,0

3,0,1,0,1,0,1,-35.0,-35.0, 41.7,0

4,0,1,0,1,0,1, 35.0,-35.0, 41.7,0

5,0,1,0,1,0,1, 35.0, 35.0, 41.7,0

6,0,1,1,1,0,1,-35.0, 35.0, 56.2,0

7,0,1,1,1,0,1,-35.0,-35.0, 56.2,0

8,0,1,1,1,0,1, 35.0,-35.0, 56.2,0

9,0,1,1,1,0,1, 35.0, 35.0, 56.2,0

10,0,1,1,1,0,1,-35.0, 35.0, 70.7,0

11,0,1,1,1,0,1,-35.0,-35.0, 70.7,0

12,0,1,1,1,0,1, 35.0,-35.0, 70.7,0

13,0,1,1,1,0,1, 35.0, 35.0, 70.7,0

14,0,1,1,1,0,1,-35.0, 35.0, 85.2,0

15,0,1,1,1,0,1,-35.0,-35.0, 85.2,0

16,0,1,1,1,0,1, 35.0,-35.0, 85.2,0

17,0,1,1,1,0,1, 35.0, 35.0, 85.2,0

18,0,1,1,1,0,1,-35.0, 35.0, 99.7,0

19,0,1,1,1,0,1,-35.0,-35.0, 99.7,0

20,0,1,1,1,0,1, 35.0,-35.0, 99.7,0

21,0,1,1,1,0,1, 35.0, 35.0, 99.7,0

22,0,1,1,1,0,1,-35.0, 35.0,114.2,0

23,0,1,1,1,0,1,-35.0,-35.0,114.2,0

24,0,1,1,1,0,1, 35.0,-35.0,114.2,0

25,0,1,1,1,0,1, 35.0, 35.0,114.2,0

26,0,1,1,1,0,1,-35.0, 35.0,128.7,0

27,0,1,1,1,0,1,-35.0,-35.0,128.7,0

28,0,1,1,1,0,1, 35.0,-35.0,128.7,0

29,0,1,1,1,0,1, 35.0, 35.0,128.7,0

30,0,1,1,1,0,1,-35.0, 35.0,143.2,0

31,0,1,1,1,0,1,-35.0,-35.0,143.2,0

32,0,1,1,1,0,1, 35.0,-35.0,143.2,0

33,1,1,1,1,1,1, 35.0, 35.0,143.2,0

34,1,1,1,1,1,1,-35.0, 35.0,157.7,0

35,1,1,1,1,1,1,-35.0,-35.0,157.7,0

36,1,1,1,1,1,1, 35.0,-35.0,157.7,0

37,1,1,1,1,1,1, 35.0, 35.0,157.7,0

1

0.69D08,0.78D08,0.529D08,1.3D11,0.97D11,0.87D11

1

0.512D07,0.5D-07,0.252D07,0.769D11,0.19D12,0.167D12

12,0,0.785,10,6.7,166.7,354950000.

-35.0, 35.0,41.7,-35.0, 35.0, 6.7,16.0,

-35.0,-35.0,41.7,-35.0,-35.0, 6.7,16.0,

35.0, 35.0,41.7, 35.0, 39.0, 6.7,16.0,

35.0,-35.0,41.7, 35.0,-35.0, 6.7,16.0,  
 -35.0, 0.0,35.7,-35.0, 0.0, 6.7, 3.5,  
 0.0, 35.0,29.2, 0.0, 35.0, 6.7, 3.5,  
 0.0,-35.0,29.2, 0.0,-35.0, 6.7, 3.5,  
 35.0, 0.0,35.7, 35.0, 0.0, 6.7, 3.5,  
 -27.0, 35.0,35.45,27.0, 35.0,35.45,12.0,  
 -27.0,-35.0,35.45,27.0,-35.0,35.45,12.0,  
 -35.0, 27.0,38.7,-35.0,-27.0,38.7, 6.0,  
 35.0,-27.0,38.7, 35.0, 27.0,38.7, 6.0

0.692D08,0.0D0,-0.851D09,  
 0.0D0,0.529D8,0.0D0,  
 -0.851D09,0.0D0,0.938D11

0.512D07,0.0D0,0:0D0,  
 0.0D0,0.252D07,0.0D0,  
 0.0D0,0.0D0,-0.366D12

1  
 1,0,0,0.,0.

9.236D09  
 9.236D09  
 9.236D09  
 9.236D09

-0.2551D08  
 -0.2551D08  
 -0.2551D08  
 -0.2551D08

C INPUT ON UNIT 11

28,2,0,3  
 0.026,0  
 1,2.0D11,0.66D11,7.85D3  
 2,2.0D01,0.66D01,0.1D-6  
 3,2.0D12,0.66D12,0.1D-6  
 0.04618,0.04618,0.04618,0.01,0.01,0.01  
 0.04618,0.04618,0.04618,0.01,0.01,0.01  
 1, 2, 6, 1,1,1,000000,000000,0  
 2, 3, 7, 1,1,1,000000,000000,0  
 3, 4, 8, 1,1,1,000000,000000,0  
 4, 5, 9, 1,1,1,000000,000000,0  
 5, 6,10, 1,1,1,000000,000000,0  
 6, 7,11, 1,1,1,000000,000000,0  
 7, 8,12, 1,1,1,000000,000000,0  
 8, 9,13, 1,1,1,000000,000000,0  
 9,10,14, 1,1,1,000000,000000,0  
 10,11,15, 1,1,1,000000,000000,0  
 11,12,16, 1,1,1,000000,000000,0  
 12,13,17, 1,1,1,000000,000000,0  
 13,14,18, 1,1,1,000000,000000,0  
 14,15,19, 1,1,1,000000,000000,0  
 15,16,20, 1,1,1,000000,000000,0

16,17,21, 1,1,1,000000,000000,0  
17,18,22, 1,1,1,000000,000000,0  
18,19,23, 1,1,1,000000,000000,0  
19,20,24, 1,1,1,000000,000000,0  
20,21,25, 1,1,1,000000,000000,0  
21,22,26, 1,1,1,000000,000000,0  
22,23,27, 1,1,1,000000,000000,0  
23,24,28, 1,1,1,000000,000000,0  
24,25,29, 1,1,1,000000,000000,0  
25,26,30, 1,1,1,000000,000000,0  
26,27,31, 1,1,1,000000,000000,0  
27,28,32, 1,1,1,000000,000000,0  
28,29,33, 1,1,1,000000,000000,0  
29,30,34, 1,1,1,000000,000000,0  
30,31,35, 1,1,1,000000,000000,0  
31,32,36, 1,1,1,000000,000000,0  
32,33,37, 1,1,1,000000,000000,0

## OUTPUT OF PROGRAMME TLPI

\*\*\*\*\*  
 MOTION ANALYSIS OF A TENSION LEG PLATFORM  
 \*\*\*\*\*

## GEOMETRY OF THE IMMERSED SECTIONS

MEMBER #	I th NODE			J th NODE			DIA
	X ORD	Y ORD	Z ORD	X ORD	Y ORD	Z ORD	
1	-35.0	35.00	42.04518	-35.00	35.000	7.04518	16.0
2	-35.0	-35.00	42.04518	-35.00	-35.000	7.04518	16.0
3	35.0	35.00	42.04518	35.00	35.000	7.04518	16.0
4	35.0	-35.00	42.04518	35.00	-35.000	7.04518	16.0
5	-35.0	0.00	36.04518	-35.00	0.000	7.04518	3.5
6	0.0	35.00	29.54518	0.00	35.000	7.04518	3.5
7	0.0	-35.00	29.54518	0.00	-35.000	7.04518	3.5
8	35.0	0.00	36.04518	35.00	0.000	7.04518	3.5
9	-27.0	35.00	35.79518	27.00	35.000	35.79518	12.5
10	-27.0	-35.00	35.79518	27.00	-35.000	35.79518	12.5
11	-35.0	27.00	39.04518	-35.00	-27.000	39.04518	6.0
12	35.0	-27.00	39.04518	35.00	27.000	39.04518	6.0

ALL DIMENSIONS IN METERS

## HYDROSTATIC PROPERTIES

DISPLACEMENT = 45446.8CUBIC METERS  
 CG IS -7.045 METERS ABOVE MEAN WL  
 BG = -28.704METERS  
 TOTAL WEIGHT = 0.354950E+09NEWTONS  
 TOTAL TENSION = 0.102029E+09NEWTONS

GM AT 45446.8CUBIC METERS(WITHOUT TETHERS)  
 GM(T) = -6.51METERS  
 GM(L) = -6.51METERS

MOTION TRANSFER FUNCTIONS  
 \*\*\*\*\*

WAVE HEADING = 0.00 DEGREE

W	T	SURGE		SWAY		HEAVE		ROLL		PITCH		YAW
		TF	P	TF	P	TF	P	TF	P	TF	P	
.40	15.7	.654	195.	0.0	90.	.00340	-90.	0.	90.	.00050	18.	0.
.41	15.3	.635	194.	0.0	90.	.00252	-90.	0.	90.	.00049	18.	0.
.42	15.0	.616	194.	0.0	90.	.00167	-90.	0.	90.	.00049	19.	0.
.43	14.6	.596	194.	0.0	90.	.00085	-90.	0.	90.	.00049	19.	0.
.44	14.3	.576	194.	0.0	90.	.00006	-90.	0.	90.	.00048	20.	0.
.45	14.0	.555	193.	0.0	90.	.00070	90.	0.	90.	.00047	20.	0.
.46	13.7	.534	193.	0.0	90.	.00143	90.	0.	90.	.00046	20.	0.
.47	13.4	.512	193.	0.0	90.	.00213	90.	0.	90.	.00045	21.	0.



.48	13.1	.490	193.	0.0	90.	.00279	90.	0.	90.	.00044	21.	0.
.49	12.8	.467	192.	0.0	90.	.00341	90.	0.	90.	.00042	21.	0.
.50	12.6	.444	192.	0.0	90.	.00400	90.	0.	90.	.00040	22.	0.
.51	12.3	.420	192.	0.0	90.	.00454	90.	0.	90.	.00038	22.	0.
.52	12.1	.396	192.	0.0	90.	.00505	90.	0.	90.	.00036	22.	0.
.53	11.9	.372	192.	0.0	90.	.00552	90.	0.	90.	.00034	23.	0.

TETHER FORCES  
\*\*\*\*\*

WAVE HEADING = 0.00 DEGREES  
EQUILIBRIUM TENSIONS IN NEWTONS

W	T	AS	AP	FS	FP
TENSION RAO IN N/M		0.2551E+08	0.2551E+08	0.2551E+08	0.2551E+08
0.40	15.708	0.1231E+07	0.1231E+07	0.1381E+07	0.1381E+07
0.41	15.325	0.1235E+07	0.1235E+07	0.1350E+07	0.1350E+07
0.42	14.960	0.1239E+07	0.1239E+07	0.1317E+07	0.1317E+07
0.43	14.612	0.1241E+07	0.1241E+07	0.1282E+07	0.1282E+07
0.44	14.280	0.1242E+07	0.1242E+07	0.1245E+07	0.1245E+07
0.45	13.963	0.1241E+07	0.1241E+07	0.1206E+07	0.1206E+07
0.46	13.659	0.1237E+07	0.1237E+07	0.1165E+07	0.1165E+07
0.47	13.368	0.1229E+07	0.1229E+07	0.1121E+07	0.1121E+07
0.48	13.090	0.1218E+07	0.1218E+07	0.1075E+07	0.1075E+07
0.49	12.823	0.1203E+07	0.1203E+07	0.1027E+07	0.1027E+07
0.50	12.566	0.1185E+07	0.1185E+07	0.9773E+06	0.9773E+06
0.51	12.320	0.1162E+07	0.1162E+07	0.9256E+06	0.9256E+06
0.52	12.083	0.1135E+07	0.1135E+07	0.8730E+06	0.8730E+06
0.53	11.855	0.1103E+07	0.1103E+07	0.8196E+06	0.8196E+06

## OUTPUT OF THE PROGRAMME TLP2

ANALYSIS OF A TLP (WAVE=10M, 8 S, DEPTH=160M)

## RESPONSE HISTORY

\*\*\*\*\*

TIME IN SEC	SURGE IN M	HEAVE IN M	PITCH IN RAD
20.50	0.189717	0.003300	-0.001028
21.00	0.168246	0.009102	-0.000911
21.50	0.124778	0.013757	-0.000676
22.00	0.065106	0.016474	-0.000352
22.50	-0.002123	0.016734	0.000012
23.00	-0.066664	0.014382	0.000361
23.50	-0.118228	0.009671	0.000640
24.00	-0.148122	0.003237	0.000801
24.50	-0.150700	-0.003982	0.000815
25.00	-0.124401	-0.010887	0.000673
25.50	-0.072161	-0.016381	0.000390
26.00	-0.001129	-0.019546	0.000006
26.50	0.078304	-0.019793	-0.000424
27.00	0.154032	-0.016971	-0.000834
27.50	0.214077	-0.011403	-0.001159
28.00	0.248482	-0.003855	-0.001346

## TENSION HISTORY

\*\*\*\*\*

TIME	AFT S	AFT P	FOR P	FOR S
20.50	-0.2322E+08	-0.2322E+08	-0.2826E+08	-0.2826E+08
21.00	-0.2391E+08	-0.2391E+08	-0.2838E+08	-0.2838E+08
21.50	-0.2481E+08	-0.2481E+08	-0.2813E+08	-0.2813E+08
22.00	-0.2580E+08	-0.2580E+08	-0.2753E+08	-0.2753E+08
22.50	-0.2671E+08	-0.2671E+08	-0.2665E+08	-0.2665E+08
23.00	-0.2740E+08	-0.2740E+08	-0.2564E+08	-0.2564E+08
23.50	-0.2776E+08	-0.2776E+08	-0.2462E+08	-0.2462E+08
24.00	-0.2770E+08	-0.2770E+08	-0.2377E+08	-0.2377E+08
24.50	-0.2723E+08	-0.2723E+08	-0.2323E+08	-0.2323E+08
25.00	-0.2640E+08	-0.2640E+08	-0.2310E+08	-0.2310E+08
25.50	-0.2531E+08	-0.2531E+08	-0.2340E+08	-0.2340E+08
26.00	-0.2416E+08	-0.2416E+08	-0.2413E+08	-0.2413E+08
26.50	-0.2308E+08	-0.2308E+08	-0.2516E+08	-0.2516E+08
27.00	-0.2227E+08	-0.2227E+08	-0.2637E+08	-0.2637E+08
27.50	-0.2186E+08	-0.2186E+08	-0.2756E+08	-0.2756E+08
28.00	-0.2194E+08	-0.2194E+08	-0.2855E+08	-0.2855E+08

ELAPSED TIME IN SEC , FORCES IN NEWTONS /



```

CALL EQL(AS,AP,FS,FP,THA,PLI,DCV,WEIGH)
DIF(3)=DCV
DIF(4)=THA
DIF(5)=PLI
DO 20 I=1,M
CALL NEWCO(I,DIF,XG,YG,ZG,XI,YI,ZI)
CALL NEWCO(I,DIF,XG,YG,ZG,XJ,YJ,ZJ)
20 CONTINUE
WRITE (2,2) (I,XI(I),YI(I),ZI(I),XJ(I),YJ(I),
ZJ(I),DI(I),I=1,M)
2 FORMAT(5X,I5,F10.5,F10.5,F10.5,F10.5,F10.5,
F10.5,F10.5)
WRITE (2,3)
WRITE (3,8)
3 FORMAT(5X,' ALL DIMENSIONS IN METERS')
8 FORMAT(/ ' SYSTEM MATRICES :',/,/, ' MASS DISRI
BUTION MATRIX')
CALL WR(6,6,AlM)
DO 30 I=1,4
CALL NEWCO(I,DIF,XG,YG,ZG,XM,YM,ZM)
30 CONTINUE
HWC=HWC -DIF(3)
HT =HT+ DIF(3)
HT1 =(0.102D01)*HT
HT2 =(0.098D01)*HT
AWP = 0.0D 00
VOL = 0.0D 00
ZMOP = 0.0D 00
XXMI = 0.0D 00
YYMI = 0.0D 00
CTX =0.0D 00
CTY =0.0D 00
UO =0.5D00
VO =UO
WO =VO
DO 50 I=1,M
IF((ZJ(I)).LE.HT1.AND.(ZJ(I)).GE.HT2)ZJ(I)=HT
CALL O(I,XI,YI,ZI,XJ,YJ,ZJ,DI,X1,X2,Y1,Y2,Z1,
Z2,D,SA,SB,SC,CA,CB,CC,ALEN,HT,L)
1 VOLA = R(D)*ALEN
ZGG = (Z1 + Z2)/0.2D 01
VOL = VOL + VOLA
ZMOP = ZMOP + VOLA*ZGG
AWP1(I) = R(D) * L
IF (SC.NE.0.0) AWP1(I) = AWP1(I) /DABS(SQ)
AWP = AWP + AWP1(I)
CTX = CTX + AWP1(I) * X2
CTY = CTY + AWP1(I) * Y2
50 CONTINUE
ZB = ZMOP/VOL
XLCF = CTX/AWP
YLCF = CTY/AWP
INERTIA OF WP ABOUT THEIR OWN AXES IGNORED
DO 100 I=1,M

```

```

YYMI = YYMI + AWP1(I)* (XJ(I) - XLCF)**2
XXMI = XXMI + AWP1(I)* (YJ(I) - ZLCF)**2
100 CONTINUE
XXMI - XXMI + AWP * YLCF ** 2
YYMI - YYMI + AWP * XLCF ** 2
BM5 = YYMI/VOL
BM4 = XXMI/VOL
GM4 = -ZB + BM4
GM5 = -ZB + BM5
HTZK = -HT
DISPL = VOL * RO * G
TENSIN = DISPL - WEIGH
WRITE (2,6)
6 FORMAT(//////////25X,' HYDROSTATIC PROPERTIES')
WRITE (2,7) VOL,HTZK,-ZB,WEIGH,TENSIN,VOL,GM4,GM5
7 FORMAT (/5X,' DISPLACEMENT = ',F10.1,'CUBIC METERS'
1/,5X,' CG IS ',F10.3,' METERS ABOVE MEAN WL',/5X,
2'BG=',F10.3,' METERS',/5X,' TOTAL WEIGHT = ',E13.6,
3'NEWTONS',/5X,' TOTAL TEN' SION = ',E13.6,' NEWTONS',
4//5X,' GM AT ',F10.1,' CUBIC METERS', '(WITHOUT TETHERS)'
5/,5X,' GM(T)=' ,F7.2,' METERS',/5X,' GM(L)=' ,F7.2,' METS'
6,///25X,' MOTION TRANSFER FUNCTIONS',/26X,25(1H*))
WRITE (2,7003) DE
495 FORMAT ( 25X,' WAVE HEADING = ',F7.2,' DEGREES')
WRITE (4,496)
496 FORMAT (/25X,' TETHER FORCES',/26X,13(1H*),//)
WRITE(4,495)DE
C
DER = DE * PI/(0.180D 03)
CD = DCOS(DER)
SD = DSIN(DER)
N = 0
499 CONTINUE
NA=0
W = WI
UV=0.0D00
VV=UV
WV=UV
C CALCULIONS START FOR FREQ. = W
C
500 CONTINUE
C WRITE (5,1002)W
DEWC = HWC-HT
CALL CAT(W,DHWC,AK,G)
TMT= 0.99999D 05
ALOP= TMT
IF(W.NE.0.0D 00)TMT = (0.6283D 01)/W
IF(AK.NE.0.0D 00)ALOP = (0.6283D 01)/AK
DO 600 I=1,6
F1(I)=0.0D00
F2(I)=0.0D00
600 IF(W.GT.WI) GO TO 2450
DO 1000 I=1,6
DO 750 J=1,6

```

```

A2M(I,J) = 0.0D 00
B(I,J) = 0.0D 00
C(I,J) = 0.0D 00
750 CONTINUE
F1(I) = 0.0D 00
F2(I) = 0.0D 00
1000 CONTINUE
C(4,4) = -(ZG-ZB)*G * VOL*RO + RO * G* XXMI
C(5,5) = -(ZG-ZB)*G * VOL*RO + RO * G* YYMI

```

C  
C  
C  
C  
C

## MEMBER PROPERTIES LOOP

```

DO 2300 I = 1, M
IF((ZJ(I)).LE.H1.AND.(ZJ(I)).GE.H2)ZJ(I)=HT
CALL O(I,XI,YI,ZI,XJ,YJ,ZJ,DI,X1,X2,Y1,Y2,ZI,
Z2,D,SA,SB,SC,CA,CB,CC,ALEN,HT,L)
C INITIALIZATION OF MATRICES
DO 1010 J = 1, 6
DO 1010 K = 1, 6
A2(J,K) = 0.0D 00
B2(J,K) = 0.0D 00
BM(J,K) = 0.0D 00
1010 CONTINUE

```

C  
C  
C

## CALCULATION OF THE RESTORING FORCE MATRIX

```

C(3,3) = C(3,3) + RO * G * AWP1(I)
C(3,4) = C(3,4) + RO * G * AWP1(I) * (Y2-YG)
C(4,3) = C(3,4)
C(3,5) = C(3,5) + RO * G * AWP1(I) * (X2-XG)
C(5,3) = C(3,5)
C(4,4) = RO * G * AWP1(I) * (Y2-YG)**2 + C(4,4)
C(5,5) = RO * G * AWP1(I) * (X2-XG)**2 + C(5,5)
C(4,6) = -(RO * G * AWP1(I) * (Y2-YG) * (X2-XG)) + C(4,6)
C(6,4) = C(4,6)

```

C  
C

## CALCULATION OF THE ADDED MASSES

```

DX = (X2-X1)/0.2D 02
DY = (Y2-Y1)/0.2D 02
DZ = (Z2-Z1)/0.2D 02
DR = ALEN / 0.2D 02
DO 1500 J = 1, 21
CALL DUN(J,X1,Y1,Z1,DX,DY,DZ,X,Y,Z,RR)
CALL ADMA(W,Z,D,L,CM)
DAD(J) = RO * CM * R(D)
ASS(J) = RR * DAD(J)
ADI(J) = RR * ASS(J)
1500 CONTINUE
CALL SIMP(DR,DAD,ADD)
CALL SIMP(DR,ASS,S)
CALL SIMP(DR,ADI,AID)
A2(1,1) = ADD * CA * CA

```

```

A2(1,2)=-ADD*SB*SA
A2(1,3)=-ADD*SC*SA
A2(2,1)= A2(1,2)
A2(3,1)= A2(1,3)
A2(2,2)= ADD*CB*CB
A2(2,3)=-ADD*SC*SB
A2(3,2)= A2(2,3)
A2(3,3)= ADD*CC*CC
A2(1,4)=-ADD*(Y1-YG)*SA*SC + ADD*(Z1-ZG)*SA*SB
A2(4,1)= A2(1,4)
A2(1,5)= -(S*SC+ADD*(X1-XG)*SA*SC+ADD*(Z1-ZG)*CA*CA)
A2(5,1)= A2(1,5)
A2(1,6)= -S*SB-ADD*(X1-XG)*SA*SB - ADD*(Y1-YG)*CA*CA
A2(6,1)= A2(1,6)
A2(2,4)= -S*SC-ADD*(Z1-ZG)*CB*CB-ADD*(Y1-YG)*SB*SC
A2(4,2)= A2(2,4)
A2(2,5)= -ADD*(Z1-ZG)*SB*SA+ADD*(X1-XG)*SB*SC
A2(5,2)= A2(2,5)
A2(2,6)= S*SA + ADD*(Y1-YG)*SB*SA +ADD*(X1-XG)*CB*CB
A2(6,2)= A2(2,6)
A2(3,4)= S*SB + ADD*(Z1-ZG)*SC*SB +ADD*(Y1-YG)*CC*CC
A2(4,3)= A2(3,4)
A2(3,5)= -S*SA-ADD*(Z1-ZG)*SC*SA-ADD*(X1-XG)*CC*CC
A2(5,3)= A2(3,5)
A2(3,6)= -ADD*(X1-XG)*SC*SB + ADD*(Y1-YG)*SC*SA
A2(4,4)= AID*(SB*SB+SC*SC)+2.*S*((Y1-YG)*SB +(Z1-ZG)
*SC)+ADD
1 *(((Y1-YG)*CC)**2 + ((Z1-ZG)*CB)**2 +2.*(Y1-YG)*(Z1-
ZG)*SB*SC)
A2(5,5)= AID*(SC*SC+SA*SA)+2.*S*((Z1-ZG)*SC +(X1-XG)
*SA)+ADD
1 *(((Z1-ZG)*CA)**2 + ((X1-XG)*CC)**2 +2.*(Z1-ZG)*(X1-
XG)*SC*SA)
A2(6,6)= AID*(SC*SC+SA*SA)+2.*S*((X1-XG)*SA +(Y1-YG)
*SB)+ADD
1 *(((X1-XG)*CB)**2 + ((Y1-YG)*CA)**2 +2.*(X1-XG)*(Y1-
YG)*SA*SB)
A2(4,6)= -AID*SA*SB-S*((X1-XG)*SB+(Y1-YG)*SA)-ADD*((
Z1-ZG)*SA
1 -(X1-XG)*SC)*(Y1-YG)*SC -(Z1-ZG)*SB) - ADD*(X1-XG)*
(Y1-YG)
A2(5,6)= -AID*SB*SC-S*((Y1-YG)*SC+(Z1-ZG)*SB)-ADD*((
X1-XG)*SB
1 -(Y1-YG)*SA)*(Z1-ZG)*SA -(X1-XG)*SC) - ADD*(Y1-YG)*
(Z1-ZG)
A2(4,5)= -AID*SC*SA-S*((Z1-ZG)*SA+(X1-XG)*SC)-ADD*((
Y1-YG)*SC
1 -(Z1-ZG)*SB)*(X1-XG)*SB -(Y1-YG)*SA) - ADD*(Z1-ZG)*
(X1-XG)
A2(5,4)= A2(4,5)
A2(6,4)= A2(4,6)
A2(6,5)= A2(5,6)
CALL NATA(A2H,A2)

```

C  
C            CALCULATION OF THE DAMPING FORCES

```

CALL DAMP(L,W,CDX,CDY,CDZ,D,RO,G,UO,V0,W0)
ACA = DABS(CA)
ACB = DABS(CB)
ACC = DABS(CC)
B2(1,1)= CDX*ACA**3
B2(2,1)--CDX*SB*SA*ACA
B2(3,1)--CDX*SC*SA*ACA
B2(1,2)--CDY*SA*SB*ACB
B2(2,2)= CDY*ACB**3
B2(3,2)--CDY*SC*SB*ACB
B2(1,3)--CDZ*SA*SC*ACC
B2(2,3)--CDZ*SB*SC*ACC
B2(3,3)= CDZ*ACC**3
DO 1750 J=1,21
CALL DUR(J,X1,Y1,Z1,DX,DY,DZ,X,Y,Z,RR)
DO 1750 K=1,6
DO 1750 KK=1,6
B4(J,K,KK)=B2(K,KK)
A4(J,K,KK)=B2(K,KK)*RR
CONTINUE
1750 CALL PV(DR,A4,BM)
DQ 2000 J=1,21
CALL DUR(J,X1,Y1,Z1,DX,DY,DZ,X,Y,Z,RR)
ABX = DABS(X-XG)
ABY = DABS(Y-YG)
ABZ = DABS(Z-ZG)
B4(J,4,1)=B2(3,1)*(Y1-YG)-B2(2,1)*(Z1-ZG)+BM(3,1)
*SB-BM(2,1)*SC
B4(J,5,1)=B2(1,1)*(Z1-ZG)-B2(3,1)*(X1-XG)+BM(1,1)
*SC-BM(3,1)*SA
B4(J,6,1)=B2(2,1)*(X1-XG)-B2(1,1)*(Y1-YG)+BM(2,1)
*SA-BM(1,1)*SB
B4(J,4,2)=B2(3,2)*(Y1-YG)-B2(2,2)*(Z1-ZG)+BM(3,2)
*SB-BM(2,2)*SC
B4(J,5,2)=B2(1,2)*(Z1-ZG)-B2(3,2)*(X1-XG)+BM(1,2)
*SC-BM(3,2)*SA
B4(J,6,2)=B2(2,2)*(X1-XG)-B2(1,2)*(Y1-YG)+BM(2,2)
*SA-BM(1,2)*SB
B4(J,4,3)=B2(3,3)*(Y1-YG)-B2(2,3)*(Z1-ZG)+BM(3,3)
*SB-BM(2,3)*SC
B4(J,5,3)=B2(1,3)*(Z1-ZG)-B2(3,3)*(X1-XG)+BM(1,3)
*SC-BM(3,3)*SA
B4(J,6,3)=B2(2,3)*(X1-XG)-B2(1,3)*(Y1-YG)+BM(2,3)
*SA-BM(1,3)*SB
B4(J,1,4)=B2(1,3)*(Y-YG)*ABY - B2(1,2)*(Z-ZG)*ABZ
B4(J,2,4)=B2(2,3)*(Y-YG)*ABY - B2(2,2)*(Z-ZG)*ABZ
B4(J,3,4)=B2(3,3)*(Y-YG)*ABY - B2(3,2)*(Z-ZG)*ABZ
B4(J,1,5)=B2(2,1)*(Z-ZG)*ABZ - B2(1,3)*(X-XG)*ABX
B4(J,2,5)=B2(2,1)*(Z-ZG)*ABZ - B2(2,3)*(X-XG)*ABX
B4(J,3,5)=B2(3,1)*(Z-ZG)*ABZ - B2(3,3)*(X-XG)*ABX
B4(J,1,6)=B2(1,2)*(X-XG)*ABX - B2(1,1)*(Y-YG)*ABY
B4(J,2,6)=B2(2,2)*(X-XG)*ABX - B2(2,1)*(Y-YG)*ABY

```



```

B4(J,3,6)=B2(3,2)*(X-XG)*ABX - B2(3,1)*(Y-YG)*ABY
B4(J,4,4)=B2(3,3)*ABY**3-B2(3,2)*(Z-ZG)*ABZ*(Y-
1 YG)+B2(2,2)*ABZ**3-B2(2,3)*(Y-YG)*(Z-ZG)*ABY
B4(J,5,5)=B2(1,1)*ABZ**3-B2(1,3)*(X-XG)*ABX*(Z-
1 ZG)+B2(3,3)*ABX**3-B2(3,1)*(Z-ZG)*ABZ*(X-XG)
B4(J,6,6)=B2(2,2)*ABX**3-B2(2,1)*(Y-YG)*ABY*(X-
2 XG)+B2(1,1)* ABY**3-B2(1,2)*(X-XG)*ABX*(Y-YG)
C
2000 CONTINUE
CALL PV(DR,B4,BH)
CALL MATA(B,BH)
2300 CONTINUE
IF(N.NE.2) GO TO 2450
WRITE (3,2311)
CALL WR(6,6,A2M)
WRITE (3,2312)
CALL WR(6,6,B)
DO 2301 J=1,6
DO 2301 K=1,6
2301 B2(J,K)=0.0D00.
DO 2302 I=1,4
AL11=DSQRT((XM(I)-XF(I))**2+(YM(I)-YF(I))**2+
(ZH(I)-ZF(I))**2)
AL22=DSQRT((XT(I)-XF(I))**2+(YT(I)-YF(I))**2+
(ZT(I)-ZF(I))**2)
TC2(I)=-TC1(I)*(AL11-AL22)/AL22
CALL CAB(I,XG,YG,ZG,XM,YM,ZM,XF,YF,ZF,TC2,TC1
,AL22,B2)
2302 CONTINUE
WRITE(3,2303)
2303 FORMAT(' MATRIX K ROPE') -
CALL WR(6,6,B2)
CALL MATA(C,B2)
WRITE (4,2310) (TC2(I),I=1,4)
WRITE (3,2313)
CALL WR(6,6,C)
WRITE (3,495)DE
2310 FORMAT (' EQUILIBRIUM TENSIONS IN NEWTONS' / ,
1 19X,'AS',11X,'AP',11X,'FS',11X,'FP',/13X,4(2X
2 ,E11.4), / ' TENSION RAO IN ', ' N/M ' )
2311 FORMAT (' ADDED MASS MATRIX' )
2312 FORMAT (' DAMPING MATRIX' )
2313 FORMAT (' RESTORING FORCE MATRIX' )
WRITE (3,2314)
2314 FORMAT (' COMPUTED WAVE FORCES' / ' W ',5X,
1 'SURGE',8X,'SWAY ',8X,'HEAVE',8X,'ROLL ',8X,
2 'PITCH',8X,'YAW' )
C
C
CALCULATION OF THE LOAD VECTOR
C
2450 DO 3500 I=1,M
IF((ZJ(I)).LE.HT1.AND.(ZJ(I)).GE.HT2)ZJ(I)=HT
DO 2525 J=1,6
F1(J)=0.0D00
F2(J)=0.0D00
2525

```

```

CALL O(I,XI,YI,ZI,XJ,YJ,ZJ,DI,XI,X2,YI,Y2,ZI,
Z2,D,SA,SB,SC,CA,CB,CC,ALen,HT,L) -
EX1 = X1*CD + Y1*SD
EX2 = X2*CD + Y2*SD
EY1 = -X1*SD + Y1*CD
EY2 = -X2*SD + Y2*CD
EZ1 = Z1
EZ2 = Z2
D3 = RO *R(D)
AD4 = W**2 *(D3 +R*(D))
DL=DSQRT((EX2-EX1)**2 +(EY2-EY1)**2 +(EZ2-EZ1)**2)
DR = DL/(O.2D02)
SA = (EX2-EX1)/DL
SB = (EY2-EY1)/DL
SC = (EZ2-EZ1)/DL
CA = DSQRT((O.1D 01)-SA**2)
CB = DSQRT((O.1D 01)-SB**2)
CC = DSQRT((O.1D 01)-SC**2)
EDX=(EX2-EX1)/(O.2D 02)
EDY=(EY2-EY1)/(O.2D 02)
EDZ=(EZ2-EZ1)/(O.2D 02)
DO. 2500 J=1,21
CALL DUN(J,EX1,EY1,EZ1,EDX,EDY,EDZ,EXX,EY,EZ,ER)
T1 = AK*(HWC-EZ)
T2 = AK*(HWC-HT)
SH1=DSINH(T1)
SH2=DSINH(T2)
CH1=DCOSH(T1)
CE = DCOS(AK*EXX)
SE = DSIN(AK*EXX)
QI(J,1)=-CE*CH1/SH2
QI(J,2)=-SE*CH1/SH2
QI(J,3)=-CE*SH1/SH2
QI(J,4)=-SE*SH1/SH2
QI(J,5)=QI(J,1)*ER
QI(J,6)=QI(J,2)*ER
QI(J,7)=QI(J,3)*ER
QI(J,8)=QI(J,4)*ER
2500 CONTINUE
DO 2600 JJ=1,8
DO 2550 J=1,21
2550 DAD(J)=QI(J,JJ)
CALL SIMP(DR,DAD,TCT3)
2600 QQ(JJ)=TCT3
XDG1 = QQ(1)*AD4*CA**2 - QQ(4)*AD4*SC*SA
XDG2 = QQ(2)*AD4*CA**2 + QQ(3)*AD4*SC*SA
YDG1 --QQ(1)*AD4*SA*SB - QQ(4)*AD4*SC*SB
YDG2 --QQ(2)*AD4*SA*SB - QQ(3)*AD4*SC*SB
F1(1)= XDG1*CD - YDG1*SD
F2(1)= XDG2*CD - YDG2*SD
F1(2)= XDG1*SD + YDG1*CD
F2(2)= XDG2*SD + YDG2*CD
F1(3)= -QQ(1)*AD4*SA*SC + QQ(4)*AD4*CC**2
F2(3)= -QQ(2)*AD4*SA*SC - QQ(3)*AD4*CC**2

```

```

AKEX = AD4*(E21*SA*SB -EY1*SA*SC)
AKEZ = AD4*(E21*SB*SA +EY1*CC*CC)
ANEX = AD4*(E21*CA*CA +EX1*SA*SC)
ANEZ = AD4*(E21*SC*SA +EX1*CC*CC)
ANEX = AD4*(EX1*SA*SB +EY1*CA*CA)
ANEZ = AD4*(EY1*SC*SA - EX1*SC*SB)
AK1 = AKEX*QQ(1) + AKEZ*QQ(4) +AD4*QQ(8)*SB
AK2 = AKEX*QQ(2) - AKEZ*QQ(3) -AD4*QQ(7)*SB
AM1 = ANEX*QQ(1) + AD4*QQ(5)*SC - ANEZ*QQ(4)
-AD4*QQ(8)*SA
AH2 = ANEX*QQ(2) + AD4*QQ(6)*SC + ANEZ*QQ(3)
+AD4*QQ(7)*SA
P1(4)=-AK1*CD - AM1*SD
P2(4)=-AK2*CD - AM2*SD
P1(5)=-AK1*SD - AM1*CD
P2(5)=-AK2*SD + AM2*CD
P1(6) = ANEZ*QQ(4) - ANEX*QQ(1) - AD4*SB*QQ(5)
P2(6) = ANEZ*QQ(3) - ANEX*QQ(2) - AD4*SB*QQ(6)
DO 3000 J=1,6
IF(ABS(P1(J)).LE.(.05D 00))P1(J)=Q.0D 00
IF(ABS(P2(J)).LE.(.05D 00))P2(J)=O.0D 00
F1(J) = F1(J)+ P1(J)
F2(J) = F2(J)+ P2(J)
3000
C
C 3500 CONTINUE
C
C CALCULATION OF LOADS DUE TO PLANE FACES
C
DO 4335 I=1,M
IF((ZJ(I)).LE.HT1.AND.(ZJ(I)).GE.HT2)ZJ(I)=HT
CALL O(I,XI,YI,ZI,XJ,YJ,ZJ,DI,X1,X2,Y1,Y2,Z1,
Z2,D,SA,SB,SC,CA,CB,CC,ALEN,HT,L)
1. KP = 1
XX=X1
YY=Y1
ZZ=Z1
AO=RO*G*(D)
T2 = AK*(HWC-HT)
4335 EXX = XI*CD +YY*SD
EY = -XX*SD+YY*CD
EZ = ZZ
T1 = AK*(HWC-EZ)
KJ=I
IF (EZ.EQ.HT)KJ=O
ACO = AO*KJ*DCOSH(T1)/DCOSH(T2)
SAK=DSIN(AK*EIX)
CAK=DCOS(AK*EIX)
P1(1)=-ACO*SA*SAK
P2(1) = ACO*SA*CAK
P1(2)=-ACO*SB*SAK
P2(2) = ACO*SB*CAK
P1(3)=-ACO*SC*SAK
P2(3) = ACO*SC*CAK
P1(4) = P1(3)*(YY-YG) -P1(2)*(ZZ-ZG)

```

```

P2(4)= P2(3)*(YY-YG) -P2(2)*(ZZ-ZG)
P1(5)= P1(1)*(ZZ-ZG) -P1(3)*(XX-XG)
P2(5)= P2(1)*(ZZ-ZG) -P2(3)*(XX-XG)
P1(6)= P1(2)*(XX-XG) -P1(1)*(YY-YG)
P2(6)= P2(2)*(XX-XG) -P2(1)*(YY-YG)
DO 4334 J=1,6
4334 F1(J)=F1(J)+P1(J)
4448 F2(J)=F2(J)+P2(J)
IF(KP.EQ.2)GO TO 4335
-KP=KP+1
XX=X2
YY=Y2
ZZ=Z2
SA = -SA
SB = -SB
SC = -SC
GO TO 4333
4335 CONTINUE
4336 CONTINUE
DO 4337 J=1,6
IF(DABS(F1(J)).LE.(0.05D00)) F1(J)=0.0D00
IF(DABS(F2(J)).LE.(0.05D00)) F2(J)=0.0D00
4337 CONTINUE
C
C
C
CALCULATION OF THE COMPLEX MOTION EQUATION
5900 DO 6000 I=1,6
DO 6000 J =1,6
RA = ((-1.*W*W)*(A1H(I,J)+A2H(I,J))+C(I,J))
RB = (1.*W)*(B(I,J))
IF(I.EQ.J)GO TO 5950
IF(DE.EQ.0.) GO TO 5910
IF(DE.EQ.90.)GO TO 5920
GO TO 5950
5910 DO 5915 K=1,3,5
IF (I.EQ.K)GO TO 5915
IF (J.EQ.K)GO TO 5915
RA=0.0D0
RB=0.0D0
5915 CONTINUE
5920 DO 5925 K=2,4,6
IF (I.EQ.K)GO TO 5925
IF (J.EQ.K)GO TO 5925
RA=0.0D0
RB=0.0D0
5925 CONTINUE
5950 IF(DABS(RA).LT.(0.1D00))RA=0.0D00
IF(DABS(RB).LT.(0.1D00))RB=0.0D00
V1(I,J)= CMPLX(RA,RB)
6000 CONTINUE
DO 7000 I=1,6
FS1=F1(I)
FS2=F2(I)
7000 FV(I,1)=CMPLX(FS1,FS2)

```

```

CALL RED(FV,AAA,APHI)
IF(N.NE.2) GO TO 7001
WRITE (3,7300) W,(AAA(I),APHI(I),I=1,5),
1 AAA(6),APHI(6)
7001 IF(W.EQ.(0.0D00))GO TO 7002
C IF(N.NE.2)GO TO 6900
C IF(W.NE.0.2) GO TO 6900
C NIT = 6
6900 CALL INVERT(V1,V2)
C IF(N.NE.2) GO TO 6901
C IF(W.NE.0.2) GO TO 6901
6901 CALL CHUL(V2,FV,DIS)
C
C NEXT FREQUENCY
7002 WAS = W
W = W + WD
NA=NA+1
C
7003 FORMAT(///25X,' WAVE HEADING =',F5.2,' DEGREE'
1//,' W ', ' T ',5X,'SURGE',7X,'SWAY',7X,'HEAVE'
2,7X,'ROLL ', ' ', 7X,' PITCH',7X,' YAW',/ 10X,5('
3 ' TF PHI'),2X,'TF')
7012 CALL RED(DIS,AAA,APHI)
UY=AAA(1)*WAS+ UV
VV=AAA(2)*WAS+ VV
WV=AAA(3)*WAS+ WV
IF(N.NE.2) GO TO 7250
C PRINTING OUT THE RESULTS
TOA=99.9
IF(WAS.NE.(0.0D00))TOA= (2.0D00)*PI/WAS
IF(WAS.EQ.(0.0D00))AAA(3)=1.0D00
DO 7100 I=4,6,1
7100 AAA(I)=AAA(I)
DO 7150 I=1,4
XMM(I)=CMLPX(XT(I),0.0D0)
YMM(I)=CMLPX(YT(I),0.0D0)
ZMM(I)=CMLPX(ZT(I),0.0D0)
CALL TENCA(I,DIS,XG,YG,ZG,XMM,YMM,ZMM,AL11)
AL22= DSQRT((XT(I)-XF(I))*2+(YT(I)-YF(I))
1 **2+(ZT(I)-ZF(I))*2)
7150 TC2(I)=(AL11)*TC1(I)/AL22
WRITE(4,7151) WAS,TOA,(TC2(I),I=1,4)
7151 FORMAT (F5.2,1X,F7.3,4(2X,E11.4))
IF(DABS(AAA(I)).LT.(0.1D-06))AAA(I)=0.0D00
WRITE(2,7200)WAS,TOA,(AAA(I),APHI(I),I=1,5),AAA(6)
7200 FORMAT (1X,F4.2,1X,F4.1,5(F8.5,1X,F4.0),F6.3)
7300 FORMAT (1X,F3.1,5(E9.2,F4.0),F8.2,F3.0)
7250 IF(W.LE.WF) GO TO 500
UO=UV/NA
VO=VV/NA
WO=WV/NA
N=N+1
IF(N.NE.3)GO TO 499
9999 STOP

```

```

C      END
C      SUBROUTINES
C      INTEGRATION USING SIMPSON'S RULE
C      SUBROUTINE SIMP(H,Q,A)
C
C      IMPLICIT REAL *8(A-H,O-Z)
C      DIMENSION Q(21)
C      I = -1
C      SUM = 0.0D 00
5      I = I + 2
C      J = I + 1
C      K = I + 2
C      SUM = SUM + Q(I) + Q(K) + (0.4D 01) * Q(J)
C      IF (I.LT.19)GO TO 5
C      A = H * SUM / (0.3D 01)
C      RETURN
C      END
C
C      FUNCTION FOR THE AREA OF A CIRCLE
C      FUNCTION R(D)
C
C      IMPLICIT REAL *8(A-H,O-Z)
C      R = (0.314159D 01) * (D**2)/(0.4D 01)
C      RETURN
C      END
C
C      SIMPLIFICATION OF THE MEMBER PROPERTIES
C      SUBROUTINE O(I,XI,YI,ZI,XJ,YJ,ZJ,DI,X1,X2,Y1,
1      Y2,Z1,Z2,D,SA,SB,SCCA,CB,CC,ALEN,HT,L)
C
C      IMPLICIT REAL *8(A-H,O-Z)
C      DIMENSION XI(1),XJ(1),YI(1),YJ(1),ZI(1),ZJ(1),DI(1)
C      X1 = XI(1)
C      X2 = XJ(1)
C      Y1 = YI(1)
C      Y2 = YJ(1)
C      Z1 = ZI(1)
C      Z2 = ZJ(1)
C      D = DI(1)
C      ALEN = DSQRT ((X2-X1)**2 + (Y2-Y1)**2 + (Z2-Z1)**2 )
C      SA = (X2-X1)/ALEN
C      SB = (Y2 - Y1)/ALEN
C      SC = ((Z2-Z1)/ALEN)
C      CA = DSQRT ( 1. - SA * SA)
C      CB = DSQRT (1.- SB*SB)
C      CC = DSQRT (1. - SC*SC)
C      L = 0
C      IF (Z2.EQ.HT) L = 1
C      RETURN
C      END
C
C      SUBROUTINE INVERT FOR INVERTING A COMPLEX MATRIX

```

```

SUBROUTINE INVERT(A,B)
C
  IMPLICIT REAL *8(A-H,O-Z)
  DIMENSION MM(6)
  COMPLEX*16 A(6,6),AC(6),TEMP,ADE,AD,B(6,6)
  N = 6
  ADE = (0.10D 01,0.0D 00)
  NN = 6
  IF(NN-1)300,350,100
100 DO 110 I=1,NN
  MM(I) = - I
110 CONTINUE
  DO 200 I =1,NN
  AX = 0.0D 00
  DO 130 L = 1,NN
  IF (MM(L).GT.0) GO TO 130
  DO 120 K = 1,NN
  IF (MM(K).GT.0) GO TO 120
  AD = A(L,K)
  AY = DABS(DREAL(AD)) + DABS(DIMAG(AD))
  IF (AX.GT.AY) GO TO 120
  LD = L
  KD = K
  AX= AY
120 CONTINUE
130 CONTINUE
  AD = A(LD,KD)
  ADE = AD
  L =-MM(LD)
  MM(LD) = MM(KD)
  MM(KD) = L
  DO 140 J =1,NN
  AC(J) = A(LD,J)
  A(LD,J) = A(KD,J)
140 A(KD,J) = AC(J)
  DO 150 K = 1,NN
  A(K,KD) = A(K,KD)/AD
150 CONTINUE
  DO 170 J=1,NN
  IF(J.EQ.KD) GO TO 170
  DO 160 K =1,NN
  A(K,J) = A(K,J) -AC(J)* A(K,KD)
160 CONTINUE
170 AC(KD) = (-0.10D 01,0.0D 00)
  DO 180 K =1,NN
  A(KD,K) = -AC(K)/AD
180 CONTINUE
200 DO 240 I=1,NN
  L = 0
  L = L+ I
220 IF (MM(L).NE.-I) GO TO 220
  MM(L) = MM(I)
  MM(I) = I
  DO 240 K =1,NN

```

```

TEMP = A(K,L)
A(K,L) = A(K,I)
240 A(K,I) = TEMP
DET = CDABS(ADE)
GO TO 300
350 A(1,1) = (0.1D 01)/(A(1,1))
DET =CDABS(A(1,1))
GO TO 300
300 DO 400 I=1,6
DO 400 J=1,6
B(I,J) = A(I,J)
400 CONTINUE
RETURN
END

```

C  
C  
C  
C

```
SUBROUTINE DUN(J,X1,Y1,Z1,DX,DY,DZ,X,Y,Z,RR)
```

```

IMPLICIT REAL *8(A-H,O-Z)
X = X1+(J-1)*DX
Y = Y1+(J-1)*DY
Z = Z1+(J-1)*DZ
RR= DSQRT((X-X1)**2 +(Y-Y1)**2 +(Z-Z1)**2)
RETURN
END

```

C  
C  
C  
C

```
SUBROUTINE ADMA(W,Z,D,L,CH)
```

```

IMPLICIT REAL *8(A-H,O-Z)
CH=0.1D 01
RETURN
END

```

C  
C  
C  
C

```
SUBROUTINE DAMP(L,W,CDX,CDY,CDZ,D,RO,G,UO,V0,W0)
```

```

IMPLICIT REAL *8(A-H,O-Z)
CX=(0.35D0)*RO*D*((8.0D0)/(3.0D0))*(0.314D01)**2
CDX=CX*UO
DDY=CX*V0
CDZ=CX*W0
RETURN
END

```

C  
C  
C  
C

```
SUBROUTINE PV(H,A4,B44)
```

```

IMPLICIT REAL *8(A-H,O-Z)
DIMENSION A4(21,6,6),B44(6,6),Q(21)

```



```

DO 2 JJ=1,6
DO 2 KK=1,6
DO 1 J=1,21
1 Q(J)=A4(J,JJ,KK)
2 CALL SIMP(H,Q,AF)
B44(JJ,KK) = AF
RETURN
END

C
C
SUBROUTINE MATA(A,B)

C
C
IMPLICIT REAL *8(A-H,O-Z)
DIMENSION A(6,6),B(6,6)
DO 1 J=1,6
DO 1 K=1,6
1 A(J,K)= A(J,K)+B(J,K)
RETURN
END

C
C
SUBROUTINE CAT(W,HWC,AK,G)

C
C
IMPLICIT REAL *8(A-H,O-Z)
SIG=(W**2)/G
A = SIG
T = 0.14D 01
10 TK = (0.5D 00)*(A +T)
THK = TANH(HWC*TK)
IF((TK-A)/TK - (0.0001D 00)) 20,20,15
15 IF(TK*THK -SIG) 18,20,25
18 A = TK
GO TO 10
25 T = TK
GO TO 10
20 AK = TK
RETURN
END

C
C
SUBROUTINE FOR COMPLEX MULTIPLICATIONS
SUBROUTINE CMUL(V2,FL,DIS)

C
IMPLICIT REAL *8(A-H,O-Z)
COMPLEX*16 V2(6,6),FL(6,1),DISS(6,1),DIS(6,1)
DO 200 I =1,6
DISS(I,1) = /((0.0D 00,0.0D 00))
DO 200 J=1,6
DISS(I,1)=DISS(I,1) + V2(I,J) * FL(J,1)
200 CONTINUE
DO 300 I =1,6
DIS(I,1) =DISS(I,1)
300 CONTINUE

```

```

RETURN
END

C
C PRINTING OF DATA
C SUBROUTINE WR(NN,MM,XX)

C IMPLICIT REAL *8(A-H,O-Z)
C DIMENSION XX(NN,MM)
C IF (MM.EQ.1)GO TO 140
149 WRITE (3,149) ((XX(I,J),J=1,MM),I=1,NN)
C FORMAT(10X,6E10.3)
C GO TO 199
140 WRITE (3,188) ((XX(I,J),J=1,MM),I=1,NN)
188 FORMAT(10X,E10.3)
199 RETURN
END

C
C SUBROUTINE RED(ZMOT,ZM,ZPHI)

C
C IMPLICIT REAL *8(A-H,O-Z)
C COMPLEX*16 ZMOT(6)
C DIMENSION ZM(6),ZPHI(6)
C DO 100 I=1,6
C ZM(I)=CDABS(ZMOT(I))
C IF(DABS(DREAL(ZMOT(I)))-LE.(0.1D-06)) GO TO 200
C ZPHI(I)=DATAN(DIMAG(ZMOT(I))/DREAL(ZMOT(I)))*
C (0.5729578D02)
1 IIF(DREAL(ZMOT(I))-LT.(0.0D00)) ZPHI(I)=ZPHI(I)+
1 0.18D03
C GO TO 100
200 ZPHI(I)=90.0D00
100 IF(DIMAG(ZMOT(I))-LT.(0.0D00)) ZPHI(I)=-90.0D00
CONTINUE
RETURN
END

C
C SUBROUTINE EQL(AS,AP,FS,FP,TTHE,TPHI,EDZ,W)

C
C IMPLICIT REAL *8(A-H,O-Z)
C READ (1,*)ALENG,ABRE,P,W,D1I,D1F,D1,ER
73 IF(ER.EQ.0.0D00)ER=0.1D-08
C N=1
C AK1 = AP +AS
C AK2 = FP+ FS
C AL = ALENG
77 AL2 = AL *(0.5D0)
C D1=D1I
78 CONTINUE
C D2 = P/(AK1+AK2)
C IF(AK1.EQ.AK2) GO TO 81

```

```

D2=(P-AK1*D1)/AK2
X=(AK2*D2*AL+W*AL2)/(P+W)
IF(AK1.GT.AK2)GO TO 79
IF(X.LT.AL2)GO TO 80
GO TO 82
79 IF(X.GT.AL2)GO TO 80
82 E=(AK1-AK2)*((D2-D1)*X+D1*AL)/(AL*P) -
1 ((O.1D01)/(AK1+AK2)) - (4.0D00)*(AL2-X)/AL)*2
IF(DABS(E).LT.(ER))GO TO 100
80 D1=D1+DI
IF(DIF.LT.D1)GO TO 1,5
GO TO 78
81 D1=D2
100 IF(N.EQ.2)GO TO 150
N=N+1
S1=D1
S2=D2
TPHI=(S2-S1)/AL
AK1=AS+FS
AK2=AP+FP
AL=ABRE
GO TO 77
150 S3=D1
S4=D2
TTHE=(S4-S3)/AL
EDZ=(S1+S2+S3+S4)/(O.4D01)
GO TO 125
115 WRITE(2,120)
120 FORMAT(' INPUT NOT IN EQUILIBRIUM')
125 CONTINUE
RETURN
END

```

C  
C  
C  
C

```
SUBROUTINE NEWCO(I,D,XG,YG,ZG,XCC,YCC,ZCC)
```

```

IMPLICIT REAL *8(A-H,O-Z)
DIMENSION D(6),XCC(1),YCC(1),ZCC(1)
XC=XCC(1)
YC=YCC(1)
ZC=ZCC(1)
DXC=D(1)+(ZC-ZG)*D(5)+(YC-YG)*D(6)
DYC=D(2)+(XC-XG)*D(6)+(ZC-ZG)*D(4)
DZC=D(3)+(YC-YG)*D(4)-(XC-XG)*D(5)
XCC(1)=XC+DXC
YCC(1)=YC+DYC
ZCC(1)=ZC+DZC
RETURN
END

```

C  
C  
C

```
SUBROUTINE TENCA(I,D,XGG,YGG,ZGG,XCC,YCC,ZCC,AL1)
```

```

C
1  IMPLICIT REAL *8(A-H,O-Z)
   COMPLEX*16 D(6),XCC(1),YCC(1),ZCC(1),XC,YC,ZC,XG,
   YG,ZG,TENC
   XG=CMPLX(XGG,0.000)
   YG=CMPLX(YGG,0.000)
   ZG=CMPLX(ZGG,0.000)
   XC=XCC(1)
   YC=YCC(1)
   ZC=ZCC(1)
   TENC= -D(3) + (YC-YG)*D(4)+(XC-XG)*D(5)
   AL1= DSQRT((DREAL(TENC))**2 + (DIMAG(TENC))**2)
   RETURN
   END

```

```

C
C
1  SUBROUTINE CAB(II,XG,YG,ZG,IX,IY,IZ,BX,BY,BZ,T0,
   T1,AL,CC)

```

```

C
C
   IMPLICIT REAL *8(A-H,O-Z)
   DIMENSION B(6,6),P1(6),C(6,6),T(3,3),CC(6,6)
   DIMENSION IX(1),IY(1),IZ(1),BX(1),BY(1),BZ(1)
   DO 7000 I=1,3
   DO 7000 J=1,3
7000  T(I,J)=0.000
   T(1,1)=-1.000
   T(2,2)=-1.000
   T(3,3)=-1.0
   XG=-GX
   YG=GY
   ZG=-GZ
   XT=-IX(II)
   YT=IY(II)
   ZT=-IZ(II)
   XB=-BX(II)
   YB=BY(II)
   ZB=-BZ(II)
   DO 10 I=1,6
   DO 10 J=1,6
10    B(I,J)=0.0000
   B(1,1)=-1.0000
   B(2,2)=B(1,1)
   B(3,3)=B(1,1)
   B(1,5)=ZT-ZG
   B(1,6)=- (YT-YG)
   B(2,4)=- (ZT-ZG)
   B(2,6)=-XT-XG
   B(3,4)=-YT-YG
   B(3,5)=- (XT-XG)
   P1(1)=XT-XB
   P1(2)=YT-YB
   P1(3)=ZT-ZB
   P1(4)=- (ZT-ZG)* (YB-YT) - (YT-YG)* (ZB-ZT)

```

```

P1(5)=(XT-XG)*(ZB-ZT)-(ZT-ZG)*(XB-XT)
P1(6)=(YT-YG)*(XB-XT)-(XT-XG)*(YB-YT)
DO 30 I=1,3
DO 30 J=1,6
IF(I.NE.1)GO TO 23
AXT=XT
AXB=XB
GO TO 25
23 IF(I.NE.2)GO TO 24
AXT=YT
AXB=YB
GO TO 25
24 AXT=ZT
AXB=ZB
25 C(I,J)=T0*B(I,J)/AL+((T0-T1)/AL**3)*(AXB-AXT)*P1(J)
30 CONTINUE
DO 1999 I=1,6
DO 1999 J=1,6
C(I,J)--C(I,J)
1999 B(I,J)=0.0DO
B(4,4)--((ZT-ZG)*(ZB-ZT)+(YT-YG)*(YB-YG))
B(4,5)=(XT-XG)*(YB-YT)
B(4,6)=(XT-XG)*(ZB-ZT)
B(5,5)--((XT-XG)*(XB-XT)+(ZT-ZG)*(ZB-ZT))
B(5,4)=(YT-YG)*(XB-XT)
B(5,6)=(YT-YG)*(ZB-ZT)
B(6,6)--((XT-XG)*(XB-XT)+(YT-YG)*(YB-YT))
B(6,4)=(ZT-ZG)*(XB-XT)
B(6,5)=(ZT-ZG)*(YB-YT)
DO 50 J=1,6
C(4,J)=T0*B(4,J)/AL + (YT-YG)*C(3,J)-(ZT-ZG)*C(2,J)
C(5,J)=T0*B(5,J)/AL + (ZT-ZG)*C(1,J)-(XT-XG)*C(3,J)
50 C(6,J)=T0*B(6,J)/AL + (XT-XG)*C(2,J)-(YT-YG)*C(1,J)
DO 7060 I=1,6
DO 7060 J=1,6
7060 B(I,J)=0.0DO
DO 7150 LA=1,4,3
LB=LA+2
DO 7150 MA=1,4,3
MB=MA-1
DO 7150 I=LA,LB
DO 7150 JM=1,3
J= JM+MB
XX=0.
DO 7151 K=1,3
7151 XX=XX + C(I,K+MB) * T(K,JM)
7150 B(I,J)=XX
DO 7152 I=1,6
DO 7152 J=1,6
7152 C(I,J)=0.0DO
DO 7160 LA=1,4,3
LB=LA-1
DO 7160 MA= 1,4,3
MB=MA + 2

```

```
DO 7160 IL=1,3
I= IL + LB
DO 7160 J= MA,MB
XX=0.
DO 7161 K=1,3
7161 XX= XX + T(K,IL) * B(K+LB,J)
C(I,J)=XX
7160 CC(I,J)=CC(I,J)+XX
RETURN
END
```



```

OPEN (UNIT=26,FILE='026.D',TYPE='NEW')
OPEN (UNIT=27,FILE='027.D',TYPE='NEW')
OPEN (UNIT=28,FILE='028.D',TYPE='NEW')
OPEN (UNIT=29,FILE='029.D',TYPE='NEW')
C   OUTPUT FILES
OPEN (UNIT= 7,FILE='07.D',TYPE='NEW')
OPEN (UNIT= 8,FILE='08.D',TYPE='NEW')
OPEN (UNIT=30,FILE='030.D',TYPE='NEW')
OPEN (UNIT=31,FILE='031.D',TYPE='NEW')
C
C   1  NUMEST=6000
      MTOT=8000
C
C   READ NODAL DATA
C
C   DEFINE CONTROL POINTS
C   A(L1)= TENSION SIZE=4
C   A(L2) =X INI   NUMNP
C   A(L3) =Y INI   NUMNP
C   A(L4) =Z INI   NUMNP
C   A(L5) =X CUR   NUMNP
C   A(L6) =Y CUR   NUMNP
C   A(L7) =Z CUR   NUMNP
C   A(L8) =EA      4
C   A(L9) =INI TENSION 4
C   N1=1
C   L1=NUMEST+1
C   CALL BREADA
C   IPRI=0
C   TT=TSTART
C   READ TOPSIDE DATA
C   CALL DREAD(MEMB)
C   SET INITIAL CONDITIONS
C   N1=1
C   N2=N1+NEQ
C   N3=N2+NEQ
C   N4=N3+NEQ
C   CALL FAINIT(A(N1),A(N2),A(N3),NEQ)
C   IPRI=INPRI
C   CALL MODGEO(A(L2),A(L3);A(L4),A(L5),A(L6),
C   1  A(L7),A(N1),ID,NUMNP,NEQ,NDOF)
C   START STIFFNESS COMPUTATION
C   NU1=17
C   NU2=18
C   NU3=19
C   CALL ELBEAM(NU1)
C   ASSEMBLY PHASE
C   MEMORY CONTROL UNITS
C   A(N1)=ro  SIZE=NEQ
C   A(N2)=vo  NEQ
C   A(N3)=ao  NEQ
C   A(N4)=V1=KEFF*D NEQ
C   A(N5)=MASS INV NEQ
C   A(N6)=DAMP NEQ

```



```

C      A(N7)=LOAD      NEQ
C      A(N8)=RO        NEQ
C      A(N9)=dRO/dt    NEQ
C      A(N10)=RB       NEQ
C      A(N11)=dRB/dt   NEQ
C      A(N12)=dr        NEQ
C      A(N13)=dr.dot   NEQ
C      A(N14)=r1       NEQ
C      A(N15)=v1       NEQ
C      A(N16)=a1       NEQ
C      A(N17)=dF/dt    NEQ
C      A(N18)=DUMMY BL NEQ
C      A(N19)=dR1/dt(L)NEQ
C      A(N20)=Rso      NEQ
      N4=N3+NEQ
      N5=N4+NEQ
      N6=N5+NEQ
      N7=N6+NEQ
      N8=N7+NEQ
      N9=N8+NEQ
      N10=N9+NEQ
      N11=N10+NEQ
      N12=N11+NEQ
      N13=N12+NEQ
      N14=N13+NEQ
      N15=N14+NEQ
      N16=N15+NEQ
      N17=N16+NEQ
      N18=N17+NEQ
      N19=N18+NEQ
      N20=N19+NEQ
      N21=N20+NEQ
C      CREATING THE MASS INV MATRIX
      CALL INMASS(A(N5),NEQ)
C      READ THE DAMP VECTOR
      REWIND 23
      READ (23,*) (A(I),I=N6,N7-1,1)
      WRITE (30,3999)
3999  FORMAT(' NEQ, N1,N2,N3,N4,N5,N6,N7,N20')
      WRITE(30,*)NEQ,N1,N2,N3,N4,N5,N6,N7,N20
C      READ THE LOAD VECTOR FOR T-TSTART AND INI GEO
      DO 4000 I=N12,N12+6
4000  A(I)=0.0D0
      L8=L7+NUMHP
      L9=L8+4
      DO 4025 I=L8,L8+3
4025  READ(10,*)A(I)
      DO 4050 I=L1,L1+3
4050  READ (10,*)A(I)
      CALL MATMUC(A(L9),A(L1),1.0D0,4)
      CALL LOADV(TT,A(N12),A(N7),A(N17),A(L8),A(L1),
1      MEMB,NEQ,NU3)
C      COMPUTE THE INITIAL GEOMETRIC STIFFNESS
      CALL GSTIP(A(L5),A(L6),A(L7),A(L1),NU2)

```

```

C      INCREMENT TT
      NEQ1=3
      NEQ2=NEQ-NEQ1
      NEQ3=NEQ-15
      K1=4
      K2=3
      K3=15
      NSTEP=1
      TOWH=TOW/5.0
      TT=TT+TOWH
      T=2*PI/W
      DO 4100 I=N8,N9-1
      A(I)=0.0
      J=I+NEQ
      A(J)=0.0D0
      J=J+NEQ
      A(J)=0.0D0
      J=J+NEQ
      A(J)=0.0D0
4100   CONTINUE
C      CALCULATION OF R0
      CALL KADDO(A(N1),A(N20),NEQ,K1)
      CALL MATADD(A(N8),A(N6),NEQ)
      CALL MATMUDL(A(N8),A(N2),NEQ)
      CALL MATADD(A(N6),A(N20),NEQ)
      CALL MATMUC(A(N8),A(N8),-1.0D0,NEQ)
      CALL MATADD(A(N8),A(N7),NEQ)
C      CALCULATION OF dR0/dt
      CALL KADDO(A(N2),A(N4),NEQ,K1)
      CALL MATADD(A(N9),A(N6),NEQ)
      CALL MATMUDL(A(N9),A(N3),NEQ)
      CALL MATADD(A(N9),A(N4),NEQ)
      CALL MATMUC(A(N9),A(N9),-1.0D00,NEQ)
      CALL MATADD(A(N9),A(N17),NEQ)
5000   CONTINUE
      NU3=26
      CALL LOADV(TT,A(N1),A(N7),A(N17),A(L8),A(L1),
1      MEMB,NEQ,NU3)
      CALL MATMUC(A(N10),A(N7),1.0,NEQ1)
      CALL MOT(TOW,A(N1),A(N2),A(N3),A(N14),A(N15),
1      A(N16),A(N8),A(N10),NEQ1)
      CALL REIN(A(N14),A(N15),A(N16),NEQ)
      CALL ZTEN(A(L1),A(L8),A(N14),A(L9),NEQ)
      IF(TT.LT.(2.0*TT)) GO TO 8000
      CALL MATMUC(A(N11),A(N9),1.0D0,NEQ)
      CALL MATMUC(A(N10),A(N9),TOW,NEQ)
      CALL MATADD(A(N10),A(N8),NEQ)
      NBOOL=-1
      NI=1
      MS=1
      CALL MATMUC(A(N21),A(N1),0.0D0,NEQ)
      GO TO 6550
6000   CONTINUE
      IF(MS.EQ.1)GO TO 6050

```

```

CALL MATMUC(A(N21),A(N12),-1.0D0,NEQ)
6050 I = K3
6100 I=I+1
      J1= I
      J2= J1+NEQ
      J3= J2+NEQ
      J4= J3+NEQ
      J5= J4+NEQ
      J6= J5+NEQ
      J7= J6+NEQ
      J8= J7+NEQ
      J9= J8+NEQ
      J10=J9+NEQ
      J11=J10+NEQ
      J12=J11+NEQ
      J13=J12+NEQ
      J14=J13+NEQ
      J15=J14+NEQ
      J16=J15+NEQ
      J17=J16+NEQ
      J18=J17+NEQ
      J19=J18+NEQ
      A(J13)=(TOW/(0.12D02))*A(J5))*
1      (6.0D0*(A(J8)+A(J10))+TOW*(A(J9)-A(J11)))
      A(J12)=(TOW*A(J2))+TOW*TOW/0.6D02)*A(J5))*
1      (0.21D2 * A(J8) + 0.3D1 *TOW* A(J9) + 9.0D0* A(J10)
2      -2.0D0 *TOW* A(J11) )
      A(J14)=A(J1)+A(J12)
      A(J15)=A(J2)+A(J13)
      A(J16)=A(J5)*A(J10)
      IF(I.NE.NEQ) GO TO 6100
C      CALL NPRI(N12,A(N12),NEQ)
      IF(NBOOL.GT.0)GO TO 7000
6550 dR1/dt =-Ko.dr1/dt - C.d2r1/dt2 + df(t1)/dt
      CALL MATMUC(A(N11+K3),A(N6+K3),1.0D0,NEQ3)
      CALL MATMUDL(A(N11+K3),A(N16+K3),NEQ3)
      CALL KADDO(A(N15),A(N4),NEQ,K1)
      CALL MATADD(A(N11+K3),A(N4+K3),NEQ3)
      CALL MATMUC(A(N11+K3),A(N11+K3),-1.0D0,NEQ3)
      CALL MATADD(A(N11+K3),A(N17+K3),NEQ3)
C      R1 =-Rso - Ko.dr -C.dr1/dt + f(t1)
      CALL MATMUC(A(N10+K3),A(N6+K3),1.0D0,NEQ3)
      CALL MATMUDL(A(N10+K3),A(N15+K3),NEQ3)
      CALL KADDO(A(N14),A(N4),NEQ,K1)
      CALL MATADD(A(N10+K3),A(N4+K3),NEQ3)
      CALL MATMUC(A(N10+K3),A(N10+K3),-1.0D0,NEQ3)
      CALL MATADD(A(N10+K3),A(N7+K3),NEQ3)
      CALL MATADD(A(N21+K3),A(N12+K3),NEQ3)
      CALL NEFN(A(N21),EPN1,NEQ)
      IF(EPN1.LE.RTOLL) GO TO 6900
      MS=MS+1
      IF(MS.EQ.NSTALL) GO TO 6800
      GO TO 6000
6800 WRITE (6,6801) TT, EPN1

```

```

6801  FORMAT(LX,' FOR TT-',F7.4,' EFN1= ',E9.2,
1'   PROG SKIPS!')
C     ASSEMBLE K1
6900  NU2=28
      CALL GSTIF(A(L5),A(L6),A(L7),A(L9),NU2)
      NBOOL= 1
7000  CONTINUE
C     R1 DOT CALCULATIONS
      CALL MATMUC(A(N19+K3),A(N11+K3),-1.0D0,NEQ3)
      CALL MATMUC(A(N11+K3),A(N11+K3),0.0D0,NEQ3)
      CALL MATADD(A(N11+K3),A(N6+K3),NEQ3)
      CALL MATMUDL(A(N11+K3),A(N16+K3),NEQ3)
      CALL KADDS(A(N15),A(N4),NEQ,K1)
      CALL MATADD(A(N11+K3),A(N4+K3),NEQ3)
      CALL MATMUC(A(N11+K3),A(N11+K3),-1.0D0,NEQ3)
      CALL MATADD(A(N11+K3),A(N17+K3),NEQ3)
C     R1 --Rso - Ko*.dr -C.drl/dt +.f(t1)
      CALL MATMUC(A(N10+K3),A(N10+K3),0.0D0,NEQ3)
      CALL MATADD(A(N10+K3),A(N15+K3),NEQ3)
      CALL MATMUDL(A(N10+K3),A(N6+K3),NEQ3)
      CALL KADDS(A(N14),A(N4),NEQ,K1)
      CALL MATADD(A(N10+K3),A(N4+K3),NEQ3)
      CALL MATMUC(A(N10+K3),A(N10+K3),-1.0D0,NEQ3)
      CALL MATADD(A(N10+K3),A(N7+K3),NEQ3)
C     ERROR CHECK
      CALL MATADD(A(N19+K3),A(N11+K3),NEQ3)
      CALL NEFN(A(N19+K3),EPN2,NEQ3)
      IF(EPN2.LE.RTOL2) GO TO 7899
      MI=MI+1
      WRITE(6,7879)TT,NSTEP,EPN2,MI,NBOOL
7879  FORMAT(' TT-',F7.4,'NSTEP=',I5,' EPN2=',E9.2,' MI=',
1     I5,'NSTAGE=',I3)
      IF (MI.EQ.NINALL)GO TO 7895
      GO TO 6000
7895  WRITE(6,7901)TT,EPN2
7899  CONTINUE
7901  FORMAT(' TT-',F7.4,' EFN=',E9.2)
8000  CONTINUE
C     PRINT COMMANDS
      IF(TT.GE.(2.5*T))GO TO 8010
      GO TO 8100
8010  IF(TT.GT.(3.5*T))GO TO 9999
      CALL TEN(A(L1),A(L9),A(N14),NEQ)
      WRITE(7,8050)TT,A(N14),A(N14+1),A(N14+2)
      WRITE(8,8060)TT,A(L1),A(L1+1),A(L1+2),A(L1+3)
8050  FORMAT(LX,F5.2,3(5X,F9.6))
8060  FORMAT(LX,F5.2,4(2X,E14.4))
8070  FORMAT(' ELAPSED TIME IN SEC , FORCES IN NEWTONS')
C     IF END OF CALCULATION
8100  NSTEP=NSTEP+1
      IF(NSTEP.GE.NSTE) GO TO 9999
C     REINITIALIZATION
      IF(TT.GE.TOW) TOWM=TOW
      TT=TT+TOWM

```

```

CALL MATHUC(A(N8),A(N10),1.0D0,NEQ)
CALL MATHUC(A(N9),A(N11),1.0D0,NEQ)
CALL MATHUC(A(N1),A(N14),1.0D0,NEQ)
CALL MATHUC(A(N2),A(N15),1.0D0,NEQ)
GO TO 5000
9999 CONTINUE
WRITE(8,8070)
STOP
END

```

C

C

C

C

## SUBROUTINE BREADA

```

IMPLICIT REAL *8(A-H,O-Z)
COMMON/JUNK/HED(12),MTOT
COMMON/SOL/NUMNP,NEQ,NUMEST,NDOP,MEMB,MODEX,INPRI
COMMON/DN/N1,N2,N3,N4,N5,N6,N7,N8,N9,N10,N11,N12,
1 N13,N14,N15,N16
COMMON/EL/NEGNL,NUMEG,NEGL,NPAR(20)
COMMON/HD/IMASSN,IDAMPN
COMMON/DL/L1,L2,L3,L4,L5,L6,L7
COMMON/NSP/NSTE,TSTART,TOW,NSTALL,NINALL,NPSTE,
1 RTOL1,RTOL2
COMMON/BL/ A(8000)
DIMENSION IDOP(6)
C HED IS THE HEADING AS PER FORMAT 12A6
READ(10,1000) (HED(I),I=1,12)
C NUMNP=NUM OF NODAL POINTS
C NEGL =NUM OF LI ELE GROUPS
C NEGNL=NUM OF NL ELE GROUPS
C MODEX=MODE OF OPERATION
C NSTE= NO OF TIME STEPS
C NDOP=NUM OF DOF PER NODE
C TOW=TIME INCREMENT
C TSTART=STARTING TIME
READ(10,*)NUMNP,NEGL,NEGNL,MEMB,MODEX,NSTE,
1 TOW,TSTART,NDOP
WRITE(30,1000) (HED(I),I=1,12)
WRITE(7,1000) (HED(I),I=1,12)
WRITE(30,1001)
WRITE(7,2000)
WRITE(8,2001)
WRITE(30,*)NUMNP,NEGL,NEGNL,MODEX,NSTE,TOW,TSTART
IF(NUMNP.EQ.0)STOP
C IMASSN NUM OF CONC NODAL MASSES
C IDAMPN NUM OF CONC NODAL DAMPERS
READ(10,*)IMASSN,IDAMPN
WRITE(30,1002)
WRITE(30,*)IMASSN,IDAMPN
C NSTALL=NUM OF ALLOWABLE STIFFNESS REF PER STEP
C NINALL=NUM OF ALLOWABLE INERTIA REFOR PER STEP
C RTOL1=TOLERANCE ON r
C RTOL2=TOLERANCE ON R

```

```

C      INPRI=INITIAL PRINTOUT STEP
C      INCPRI=PRINTOUT INTERVAL IN NUM OF STEPS
      READ(10,*)NSTALL,NINALL,RTOL1,RTOL2,INPRI,INCPRI
      WRITE(30,1003)
      WRITE(30,*)NSTALL,NINALL,RTOL1,RTOL2,INPRI,INCPRI
      NUMEG=NEGL+NEGNL
C      DEFINATION OF CONTROL VARIABLES
C      N1 IS A DUMMY IN STAGE 1
      N1=1
      L1=NUMEST+1
      L2=L1+4
      L3=L2+NUMNP
      L4=L3+NUMNP
      L5=L4+NUMNP
      L6=L5+NUMNP
      L7=L6+NUMNP
      WRITE(30,1004)
      WRITE(30,*)L1,L2,L3,L4,L5,L6,L7
      CALL BREADB(A(L2),A(L3),A(L4),NUMNP,NDOF,NEQ)
      CALL BREADC(A(N1),NEQ,NDOF)
1000   FORMAT(12A6)
1001   FORMAT('NUMNP,NEGL,NEGNL,MODEX,NSTE,TOW,TSTART,NDOF')
1002   FORMAT(' IMASN,IDAMPN')
1003   FORMAT(' NSTALL,NINALL,RTOL1,RTOL2,INPRI,INCPRI')
1004   FORMAT(' L1,L2,L3,L4,L5,L6,L7')
2000   FORMAT(/// 25X,'RESPONSE HISTORY',/25X,16(1H*),/2X,
1      'TIME',5X,' SURGE',8X,' HEAVE',8X,' PITCH',/1X,
2      'IN SEC', 5X,' IN M',10X,' IN M',9X,' IN RAD')
2001   FORMAT(/25X,'TENSION HISTORY',/25X,15(1H*),/2X,
1      'TIME',9X,'AFT S',10X,'AFT P',12X,'FOR P',9X,'FOR S')
      RETURN
      END

C
C
C      SUBROUTINE BREADB(X,Y,Z,NUMNP,NDOF,NEQ)
C
C      CALLED BY: BREADA
C      I/O OF NODAL POINT DATA AND GENERATION OF EQUATION # AND
C      STORING THEM IN AN ARRAY
C
      IMPLICIT REAL *8(A-H,O-Z)
      DIMENSION X(1),Y(1),Z(1),IDT(6),ID(6,100),IND(100)
      COMMON/BL/A(8000)
      REWIND 29
      WRITE(30,2000)
      WRITE(30,2001)
10     READ(10,*)N,(IDT(I),I=1,NDOF),X(N),Y(N),Z(N),IND(N)
      WRITE(30,2002)N,(IDT(I),I=1;6),X(N),Y(N),Z(N),IND(N)
      DO 20 I=1,NDOF
20     ID(I,N)=IDT(I)
      IF(N.NE.NUMNP)GO TO 10
      NEQ = 0
      DO 100 J=1,NUMNP

```

```

DO 100 I= 1, NDOF
KLL=IND(J)
IF(KLL.NE.0.AND.I.LE.3) GO TO 105
IF(ID(I,J))110,120,110
120 NEQ=NEQ+1
ID(I,J)=NEQ
GO TO 100
105 ID(I,J)=ID(I,KLL)
GO TO 100
110 ID(I,J)=0
100 CONTINUE
WRITE(30,2004)(N,(ID(I,N),I=1,6),N=1,NUMNP)
WRITE(29,*) ((ID(I,N),I=1,6),N=1,NUMNP)
2000 FORMAT(/23H NODAL POINT INPUT DATA )
2001 FORMAT (5HONODE,3X,24HBOUNDARY CONDITION CODES,11X,
1 23HNODAL POINT COORDINATES / 7H NUMBER,2X,1HX,4X,
2 1HY,4X,1HZ,3X2HXX,3X,2HY,3X,2HZZ,10X,1HX,10X,1HY,
3 10X,1HZ,3X,3HIND)
2002 FORMAT(1X,I4,6I5,3F11.3,I4)
2004 FORMAT (/17HEQUATION NUMBERS/
1 35H N X Y Z XX YY ZZ /(715))
RETURN
END

```

C  
C

SUBROUTINE BREADC(XMN,NEQ,NDOF)

C  
C  
C  
C  
C

```

READS CONCENTRATED NODAL MASSES AND DAMPERS
AND FINDS MASS AND DAMPING VECTORS
WRITES THEM ON UNIT 22,23
IMPLICIT REAL *8(A-H,O-Z)
COMMON/SOL/NUMNP
COMMON/MD/IMASSN,IDAMPN
DIMENSION ID(6,100),XMN(1),XMASS(6),XDAMP(6)
REWIND 29
READ (29,*) ((ID(I,N),I=1,6),N=1,NUMNP)
IF(IMASSN.EQ.0) GO TO 200
NN=6
WRITE(30,2000)
DO 80 J=1,NEQ
80 XMN(J)=0.0D0
DO 100 IN=1,IMASSN
READ(10,*) N,(XMASS(I),I=1,NN)
WRITE(30,2001)N;(XMASS(I),I=1,NN)
DO 90 J=1,NDOF
JJ=ID(J,N)
IF(JJ.EQ.0)GO TO 90
XMN(JJ)=XMN(JJ)+XMASS(J)
90 CONTINUE
100 CONTINUE
C WRITE THE NODAL MASS VECTOR ON FILE 22
REWIND 22
WRITE(22,*) (XMN(I),I=1,NEQ)

```

```

C      NODAL DAMPING
200    DO,215 I=1,NEQ
215    XMN(I)=0.000
        IF(IDAMPN.EQ.0) GO TO 300
        WRITE (30,2002)
        DO 250 IN=1, IDAMPN
        READ(10,*)M,(XDAMP(I),I=1,NN)
        DO 240 J=1, NDOF
        JJ=ID(J,N)
        IF(JJ.EQ.0)GO TO 240
        XMN(JJ)=XMN(JJ)+XDAMP(J)
240    CONTINUE
250    WRITE (30,2001) N,(XDAMP(I),I=1,NN)
        REWIND 23
        WRITE(23,*)(XMN(I),I=1,NEQ)
2000  FORMAT(1X,'NODAL MASS DATA',//3X,' NODE',6X,' XMASS',
1     3X,' YMASS',3X,'ZMASS',3X,' XINT',3X,' YINT',3X,' ZINT')
2001  FORMAT(17,6E11.3)
2002  FORMAT(1X,' NODAL DAMPER',//3X,'XDAMP',3X,'YDAMP',
1     3X,'ZDAMP',3X,'DAMPXX',3X,'DAMPYY',3X,'DAMPZZ')
300    RETURN
      END

C
C
      SUBROUTINE ELBEAM(NUI)

C
C
      IMPLICIT REAL *8(A-H,O-Z)
      COMMON/SOL/NUMNP,NEQ,NUMEST,NDOF,MEMB,NODEX
      COMMON/BL/A(8000)
      COMMON/DL/L1,L2,L3,L4,L5,L6,L7
      COMMON/DN/N1
      COMMON/EL/NEGNI,NUMEG,NEGL,NPAR(20)
      REWIND 11
      REWIND 31
      NPAR(2)=# OF BEAM ELEMENTS
      NPAR(3)=# OF ELE PROP LINES
      NPAR(4)=# OF FIXED END MOMENTS
      NPAR(5)=# OF MATERIAL PROPERTY LINES
      READ(11,*)(NPAR(I),I=2,5)
      L8=NUMNP+L7
      L9=L8+NPAR(5)
      L10=L9+NPAR(5)
      L11=L10+NPAR(5)
      L12=L11+12*NPAR(4)
      L13=L12+6*NPAR(3)
      WRITE (31,1000)
      WRITE (31,*) L8,L9,L10,L11,L12,L13,(NPAR(I),I=2,5,1)
      CALL ELREAD(NPAR(2),NPAR(3),NPAR(4),NPAR(5),A(L2),
1 A(L3),A(L4),A(L8),A(L9),A(L10),A(L12),NUMNP,NDOF,NUI)
1000  FORMAT(1X,' L8,L9,L10,L11,L12,L13,NPAR(2-5)')
      RETURN
      END
C

```



```

C      SUBROUTINE ELREAD(NBEAM,NUMETP,NUMFIX,NUMMAT,X,Y,Z,
1      E,G,RO,COPROP,NUMNP,NDOP,NU1)
C
C      CALLED BY ELBEAM      CALLS ELSTIF
C      IMPLICIT REAL *8(A-H,O-Z)
C      DIMENSION ASA(12,12),XM(12),LM(12),T(3,3),JK(6)
C      COMMON/ELST1/MELTYP,MATTYP,DL
C      COMMON/EL/NEGNL,NUMEG
1      DIMENSION X(1),Y(1),Z(1),ID(6,100),E(1),G(1),COPROP
1      (NUMETP,6),TI(3,3),TJ(3,3),TS(2,2),OD(50),WGHT(1)
1      DIMENSION R(12),S(12,12),C(12),SA(12,12),RO(1)
      REWIND 29
      READ (29,*) ((ID(I,N),I=1,6),N=1,NUMNP)
      REWIND 20
      REWIND 25
      REWIND 27
      REWIND 16
      REWIND NU1
      READ(11,*)ODC,NEXPT
      DO 3 I=NBEAM
3         OD(I)= ODC
         IF(NEXPT.EQ.0) GO TO 5900
         READ(11,*)(I,OD(I),I=1,NEXPT)
5900        CONTINUE
         WRITE (31,6000)
6000        FORMAT (' THE OD OF THE BEAMS')
         WRITE (31,*) (I,OD(I),I=1,NBEAM)
C
      NN=0
C      WRITE (31,6001)
10      NN=NN+1
6001      FORMAT (' N     E   G   RO W')
         READ(11,*) N,E(N),G(N),RO(N)
         WRITE(31,*) N,E(N),G(N),RO(N)
         IF(NN.LT.NUMMAT)GO TO 10
         WRITE(31,6002)
6002      FORMAT(' BEAM GEOMETRIC PROPERTIES','SECT AREA',3X,
1         'AXL-AR',3X,'SH AR',3X,'TORSION',3X,'INERT')
         DO 30 I=1,NUMETP
         READ (11,*)(COPROP(I,J),J=1,6)
30         WRITE(31,*) I,(COPROP(I,J),J=1,6)
         IF(NUMFIX.EQ.0) GO TO 56
         WRITE(6,6003)
6003      FORMAT(' F E DATA REQUIRED')
56         CONTINUE
         WRITE(31,6004)
6004      FORMAT('NEL,NI,NJ,NK,MATTYP,MELTYP,NEKODI,NEKODJ,INC')
         L=0
60         -KKK=0
         READ (11,*)INEL,INI,INJ,INK,IMAT,IMEL,INELKI,INELKJ,
1         INC
         IF(INEL.NE.1)GO TO 15
         NI=INI

```

```

NJ=INJ
NK=INK
15 IF(INC.EQ.0)INC=1
65 L=L+1
   KKK=KKK+1
   ML=INEL-L
C   WRITE(6,6010)L,INEL,ML
6010 FORMAT(' L,INEL,ML',3I5)
   IF(ML.EQ.0) GO TO 67
   IF(ML.GT.0) GO TO 68
   WRITE(6,6010)L,INEL,ML
66   WRITE(6,6005)INEL
6005 FORMAT(' ELEMENT INFO FAULTY AT',I5)
   STOP
67   NEL=INEL
   NI=INI
   NJ=INJ
   NK=INK
   MATTYP=IMAT
   MELTYP=IMEL
   NEKODI=INELKI
   NEKODJ=INELKJ
   GO TO 69
68   NEL=INEL-ML
   NI=IN+KKK*INCR
   NJ=JN+KKK*INCR
69   CONTINUE
74   DX=X(NJ)-X(NI)
   DY=Y(NJ)-Y(NI)
   DZ=Z(NJ)-Z(NI)
   DL=DX*DX + DY*DY +DZ*DZ
   DL=DSQRT(DL)
   IF(DL)75,75,77
75   WRITE(6,6007) NEL
6007 FORMAT(I5,' TH ELEMENT HAS ZERO LENGTH',
1      ' TERMINATION!')
   STOP
-77 WRITE(31,*)NEL,NI,NJ,NK,MATTYP,MELTYP,NEKODI,NEKODJ
C   DATA PORT HOLE SAVE
   ECON=E(MATTYP)*COPROP(MELTYP,1)
   IF(MELTYP.NZ.1)GO TO 76
   WRITE(25,*) NEL,NI,NJ,NK,NEKODI,NEKODJ,DL,ECON
C   FROM GLOBAL TO LOCAL
76   T(1,1)=DX/DL
   T(1,2)=DY/DL
   T(1,3)=DZ/DL
C   DIRECTION COSINES OF LOCAL AXES:
   A1=X(NJ)-X(NI)
   A2=Y(NJ)-Y(NI)
   A3=Z(NJ)-Z(NI)
   B1=X(NK)-X(NI)
   B2=Y(NK)-Y(NI)
   B3=Z(NK)-Z(NI)
   AA=A1*A1 +A2*A2 +A3*A3

```

```

AB=A1*B1 +A2*B2 +A3*B3
U1= AA*B1 - AB*A1
U2= AA*B2 - AB*A2
U3= AA*B3 - AB*A3
UU= DSQRT(U1*U1 + U2*U2 + U3*U3)
IF(UU.NE.0.)GO TO 40
WRITE (6,6006)INEL
6006 FORMAT(' K NODE ON THE BEAM AXIS AT ELEMENT',I5)
STOP
40 CONTINUE
T(2,1)=U1/UU
T(2,2)=U2/UU
T(2,3)=U3/UU
T(3,1)=T(1,2)*T(2,3)-T(1,3)*T(2,2)
T(3,2)=T(1,3)*T(2,1)-T(1,1)*T(2,3)
T(3,3)=T(1,1)*T(2,2)-T(1,2)*T(2,1)
C CHECK IF NEW STIFFNESS IS NEEDED
IF(NEL.GE.1)GO TO 80
IF((MT.NE.MATTYP).OR.(ME.NE.MATTYP)) GO TO 80
IF((JK(1).NE.NEKODI).OR.(JK(2).NE.NEKODJ))GO TO 80
GO TO 185
80 CONTINUE
MT=MATTYP
ME=MELTYP
JK(1)=NEKODI
JK(2)=NEKODJ
C FORM NEW STIFFNESS
C CALCULATION OF ELASTIC STIFFNESS MATRIX OF A BEAM ELEMENT
C
C WRITE(6,7505)
C7505 FORMAT(' MODULE ELSTIF')
DO 7665 I=1,12
DO 7665 J=1,12
7665 S(I,J)=0.D0
M=MELTYP
MM=MATTYP
AX=COPROP(M,1)
AY=COPROP(M,2)
AZ=COPROP(M,3)
AAX=COPROP(M,4)
AAZ=COPROP(M,5)
AAZ=COPROP(M,6)
ZY=E(MM)/(DL*DL)
EII=ZY*AAZ
EIZ=ZY*AAZ
C FORM THE ELEMENT STIFFNESS IN LOCAL COORDINATES
S(1,1)=E(MM)*AX/DL
S(4,4)=G(MM)*AAX/DL
IF(AZ.EQ.0.0) AX=0.1D-10
ACON=E(MM)*AAZ/DL
APHI=(0.12D2)*ACON/(DL*AX*G(MM))
S(2,2)=(0.12D2)*ACON/(DL*DL*(1.0 ))
S(3,3)=S(2,2)
S(5,5)=(4.0+ APHI ) * ACON / (1.0 + APHI )

```

```

S(6,6)=S(5,5)
S(2,6)=6.0D0*ACON/(DL*(1.0+APHI))
ZZ1=S(2,6)
S(3,5)=-ZZ1
DO 7102 I=1,6
J=I+6
7102 S(J,J)=S(I,I)
DO 7104 I=1,4
J=I+6
7104 S(I,J)=-S(I,I)
S(6,12)=S(6,6)*(2.0-APHI)/(1.0+APHI)
S(5,11)=S(6,12)
S(2,12)=ZZ1
S(6,8)=-ZZ1
S(8,12)=-ZZ1
S(3,11)=-ZZ1
S(5,9)=ZZ1
S(9,11)=ZZ1
DO 7106 I=2,12
K=I-1
DO 7106 J=1,K
S(I,J)=S(J,I)
7106 MODIFY ELEMENT STIFFNESSES AND ELEMENT F.E. FORCES
C FOR KNOWN ZERO MEMBER END FORCES
C
IF((JK(1)+JK(2)).EQ.0)GO TO 7145
DO 7140 K=1,2
KK=JK(K)
KD=100000
I1=6*(K-1)+1
I2=I1+5
DO 7140 I=I1,I2
IF(KK.LT.KD)GO TO 7140
SII=S(I,I)
C7125 DO 7125 N=1,12
R(N)=S(I,N)
C DO 7130 MUN=1,12
C(MUN)=S(MUN,I)/SII
C DO 7130 N=1,12
C7130 S(MUN,N)=S(MUN,N)-C(MUN)*R(N)
DO 7126 N=1,12
S(I,N)=0.0D0
S(N,I)=0.0D0
7126 CONTINUE
7135 KK=KK-KD
7140 KD=KD/10
7145 CONTINUE
C OBTAIN SA(12,12) RELATING MEMBER END FORCES LOCAL
C AND JOINT DISPLACEMENT GLOBAL
C
DO 7031 I=1,12
DO 7031 J=1,12
7031 SA(I,J)=0.0E0
DO 7150 LA=1,10,3

```

```

LB=LA +2
DO 7150 MA=1,10,3
MB=MA-1
DO 7150 I=LA, LB
DO 7150 JM=1,3
J=JM+MB
XX=0.
DO 7151 K=1,3
7151 XX=XX+S(I,K+MB)*T(K,JM)
7150 SA(I,J)=XX
C
C ELEMENT STIFFNESS ASA(12,12) ,F.E.FORCES IN GLOBAL CO.
C
DO 7032 I=1,12
DO 7032 J=1,12
7032 ASA(I,J)=0.OEO
DO 7160 LA=1,10,3
LB=LA-1
DO 7160 MA=1,10,3
MB=MA+2
DO 7160 IL=1,3
I=IL+LB
DO 7160 J=MA,MB
XX=0.
DO 7161 K=1,3
7161 XX=XX+T(K,IL)*SA(K+LB,J)
7160 ASA(I,J)=XX
C FORM MASS AND GRAVITY LOAD MATRICES
C
XXM=RO(MATTYP)*AX*DL/2.
DO 7180 MP=1,3
XM(MP)=XXM
XM(MP+6)=XXM
XM(MP+3)=XXM*DL*DL/4.OEO
XM(MP+9)=XXM*DL*DL/4.OEO
7180 CONTINUE
C
C WRITE(6,1005)
C FORM ELEMENT LOCATION MATRIX
185 CONTINUE
DO 170 M=1,6
LM(M)=ID(M,NI)
170 LM(M+6)=ID(M,NJ)
IF(MELTYP.NE.1)GO TO 9171
WRITE(25,*)((T(I,J),I=1,3),J=1,3)
WRITE(25,*)(LM(I),I=1,12)
9171 CONTINUE
NS=12
ND=12
C WRITE ELEMENT INFO ON TAPE
WRITE(NUL,*)(LM(I),I=1,ND),((ASA(I,J),I=1,NS),
1 J=1,ND)
WRITE(27,*)(LM(I),I=1,ND),(XN(I),I=1,12)
IF(NEL.EQ.1) GO TO 250

```

```

IF(NEL.NE.ITOP)GO TO 255
250 CONTINUE
WRITE(20,*)(LM(I),I-1,12),((ASA(I,J),I-1,12),J-1,12)
ITOP=NEL+1
IF(ITOP.EQ.5) ITOP=200
C CHECK FOR LAST ELEMENT
255 CONTINUE
IF(NUMEG-NEL)66,500,260
260 IF(ML.GT.0)GO TO 65
IN=INI
JN=INJ
INCR=INC
GO TO 60
500 RETURN
END

```

```

SUBROUTINE FAINIT(DISP,VEL,ACC,NEQ)

```

```

C
C
C
C
IMPLICIT REAL *8(A-H,O-Z)
COMMON/BL/A(8000)
DIMENSION DISP(1),VEL(1),ACC(1)
READ(10,*) ICON
DO 100 I=1,NEQ
DISP(I)=0.
VEL(I)=0.
100 ACC(I)=0.
IF(ICON.EQ.0)GO TO 200
DO 150 MUN=1,ICON
READ(10,*)(IM,DT,VE,AC
DISP(IM)=DISP(IM)+DT
VEL(IM)=VEL(IM)+VE
ACC(IM)=ACC(IM)+AC
150 CONTINUE
200 RETURN
END

```

```

SUBROUTINE GSTIF(X,Y,Z,AA,NU2)

```

```

C
C
C
C
IMPLICIT REAL *8(A-H,O-Z)
COMMON/EL/NEGNL,NUMEG
COMMON/BL/A(8000)
COMMON/DL/L1
DIMENSION LH(12),ASA(12,12),SA(12,24),S(12,12)
DIMENSION X(1),Y(1),Z(1),JK(6),AA(1)
DIMENSION T1(3,3),T(3,3),R(12),C(12)
REWIND 21
REWIND 25
REWIND NU2
IDCU = 0
IBMU = 0

```

```

66  READ(25,*)  NEL,NI,NJ,NK,NEKODI,NEKODJ,DLO,ECON
    READ(25,*)  ((I(I,J),I=1,3),J=1,3)
    READ(25,*)  (LM(I),I=1,12)
74  IDCU= IDCU + 1
    DX=X(NJ)-X(NI)
    DY=Y(NJ)-Y(NI)
    DZ=Z(NJ)-Z(NI)
    DL=DSQRT(DX*DX + DY*DY +DZ*DZ)
80  CONTINUE
    JK(1)=NEKODI
    JK(2)=NEKODJ
C    FORM NEW STIFFNESS
    DO 5 I=1,12
    DO 5 J=1,12
5    S(I,J)=0.
C    FORM THE ELEMENT STIFFNESS IN LOCAL COORDINATES
    IBMU=IBMU+ 1
    IF(IBMU.EQ.1)FT=AA(I)
    IF(IBMU.EQ.2)FT=AA(2)
    IF(IBMU.EQ.3)FT=AA(3)
    IF(IBMU.EQ.4)FT=AA(4)
    IF(IBMU.EQ.4)IBMU=1
    FT=FT+ ECON*(DL-DLO)/DLO
    W1=FT/DL
    S(2,2)=W1
    S(3,3)=W1
    S(8,8)=W1
    S(9,9)=W1
    S(2,8)=-W1
    S(8,2)=-W1
    S(3,9)=-W1
    S(9,3)=-W1
C  MODIFY THE STIFFNESSES FOR KNOWN ZERO MEMBER END FORCES
    IF((JK(1)+JK(2)).EQ.0)GO TO 145
    DO 140 K=1,2
    KK=JK(K)
    KD=100000
    I1=6*(K-1)+1
    I2=I1+5
    DO 140 I=I1,I2
    IF(KK.LT.KD)GO TO 140
    DO 126 N=1,12
    S(I,N)=0.0DO
    S(N,I)=0.0DO
126  CONTINUE
135  KK=KK-KD
140  KD=KD/10
145  CONTINUE
C
C  OBTAIN SA(12,12) RELATING MEMBER END FORCES LOCAL
C  AND JOINT DISPLACEMENT GLOBAL
    DO 31 I=1,12
    DO 31 J=1,12
31  SA(I,J)=0.0EO

```

```

DO 150 LA=1,10,3
LB=LA+2
DO 150 MA=1,10,3
MB=MA-1
DO 150 I=LA,LB
DO 150 JM=1,3
J=JM+MB
XX=0.
DO 151 K=1,3
151 XX=XX+S(I,K+MB)*T(K,JM)
150 SA(I,J)=XX
C
C ELEMENT STIFFNESS ASA(12,12) AND F E FORCES IN GLOBAL CO.
DO 32 I=1,12
DO 32 J=1,12
32 ASA(I,J)=0.0E0
DO 160 LA=1,10,3
LB=LA-1
DO 160 MA=1,10,3
MB=MA+2
DO 160 IL=1,3
I=IL+LB
DO 160 J=MA,MB
XX=0.
DO 161K=1,3
161 XX=XX+T(K,IL)*SA(K+LB,J)
IF(DABS(XX).LT.1.0D-9)XX=0.0
160 ASA(I,J)=XX
NS=12
ND=12
C
WRITE STIFF INFO ON TAPE
WRITE(NU2,*)(LM(I),I=1,ND),((ASA(I,J),I=1,NS),J=1,ND)
IF(NEL.EQ.1)GO TO 250
IF(NEL.NE.ITOP)GO TO 300
250 WRITE(21,*)((ASA(I,J),I=1,12),J=1,12)
ITOP=NEL+1
IF(ITOP.EQ.5) ITOP= 200
C
CHECK FOR LAST ELEMENT
300 IF(NEGNL-IDCU)500,500,66
500 RETURN
END
C
C
C
SUBROUTINE INHASS(X,NEQ)
C
C
C
IMPLICIT REAL *8(A-H,O-Z)
DIMENSION X(1),LM(12),XM(12)
COMMON/BL/A(8000)
COMMON/EL/NECNL,NUMEG
REWIND 22
READ(22,*)(X(I),I=1,NEQ)
REWIND 27
DO 150 K=1,NUMEG

```



```

READ(27,*)(LM(I),I=1,12),(XM(I),I=1,12)
DO 100 I=1,NEQ
DO 50 J=1,12
IF(LM(J).EQ.1)X(I)=X(I)+XM(J)
50 CONTINUE
100 CONTINUE
150 CONTINUE
DO 200 I=1,NEQ
IF (X(I).EQ.0.0)X(I)=0.1D-13
200 X(I)=(1.0D0)/(X(I))
RETURN
END

```

C  
C

SUBROUTINE MATADD(X,Y,NEQ)

C  
C

```

IMPLICIT REAL *8(A-H,O-Z)
DIMENSION X(1),Y(1)
COMMON/BL/A(8000)
DO 10 I=1,NEQ
10 X(I)=X(I)+Y(I)
RETURN
END

```

C  
C

SUBROUTINE MATHUC(Y,X,CONS,NEQ)

C  
C

```

IMPLICIT REAL *8(A-H,O-Z)
DIMENSION X(1),Y(1)
COMMON/BL/A(8000)
DO 10 I=1,NEQ
10 Y(I)=CONS*X(I)
RETURN
END

```

C  
C

SUBROUTINE MATHUDL(X,Y,NEQ)

C  
C

```

IMPLICIT REAL *8(A-H,O-Z)
DIMENSION X(1),Y(1)
COMMON/BL/A(8000)
DO 10 I=1,NEQ
10 X(I)=X(I)*Y(I)
RETURN
END

```

C  
C

SUBROUTINE MODGEO(X1,X2,X3,X4,X5,X6,X7,1D,  
1 NUMNP,NEQ,NDOP)

C  
C

```

      IMPLICIT REAL *8(A-H,O-Z)
      COMMON/BL/A(8000)
      DIMENSION X1(1),X2(1),X3(1),X4(1),X5(1),
1     X6(1),X7(1),ID(6,1)
      WRITE(6,1005)
      DO 400 J=1,NUMNP
      X4(J)=X1(J)
      X5(J)=X2(J)
      X6(J)=X3(J)
      DO 200 K=1,NEQ
      IF(K.GT.15)GO TO 100
      IF(ID(1,J).EQ.K)X4(J)=X4(J)+X7(K)
      IF(ID(2,J).EQ.K)X5(J)=X5(J)+X7(K)
      IF(ID(3,J).EQ.K)X6(J)=X6(J)+X7(K)
      GO TO 200
100     IF(ID(1,J).EQ.K)X4(J)=X4(J)+X7(K)
200     CONTINUE
400     CONTINUE
      RETURN
      END

```

```

C
C
C
C
      SUBROUTINE NEFN(X,CONS,NEQ)

```

```

      IMPLICIT REAL *8(A-H,O-Z)
      DIMENSION X(1)
      COMMON/BL/A(8000)
      CONS=0.0D0
10     DO 10 I=1,NEQ
      CONS=X(I)*X(I)+CONS
      CONS=DSQRT(CONS)
      RETURN
      END

```

```

C
C
C
C
      SUBROUTINE KADDS(X1,X2,NEQ,N1)

```

```

      IMPLICIT REAL *8(A-H,O-Z)
      DIMENSION X1(1),X2(1),AS(12,12),LM(12)
      COMMON/EL/NEGNL,NUMEG
      DO 10 I=N1,NEQ
10     X2(I)=0.0D0
      REWIND 17
      DO 100 K=1,NUMEG
      READ(17,*) (LM(I),I=1,12),((AS(I,J),J=1,12),I=1,12)
      DO 50 I=1,12
      DO 40 K1=N1,NEQ
      IF(LM(I).NE.K1)GO TO 40
      SUM=0.0D0
      DO 20 K2=N1,NEQ
      IF((X1(K2)).EQ.0.0D0)GO TO 20
      DO 30 J=1,12

```

```

IF(LM(J).NE.K2)GO TO 30
SUM=SUM+AS(I,J)*X1(K2)
30 CONTINUE
20 CONTINUE
X2(K1)=X2(K1)+SUM
40 CONTINUE
50 CONTINUE
100 CONTINUE
REWIND 28
DO 1100 K=1,NEGNL
READ(28,*)(LM(I),I=1,12),((AS(I,J),J=1,12),I=1,12)
DO 1050 I=1,12
DO 1040 K1=N1,NEQ
IF(LM(I).NE.K1)GO TO 1040
SUM=0.0D0
DO 1020 K2=N1,NEQ
IF(X1(K2).EQ.0.0D0)GO TO 1020
DO 1030 J=1,12
IF(LM(J).NE.K2)GO TO 1030.
SUM=SUM+AS(I,J)*X1(K2)
1030 CONTINUE
1020 CONTINUE
X2(K1)=X2(K1)+SUM
1040 CONTINUE
1050 CONTINUE
1100 CONTINUE
999 CONTINUE
RETURN
END

```

C  
C  
C  
C

SUBROUTINE KADDO(X1,X2,NEQ,N1)

```

IMPLICIT REAL *8(A-H,O-Z)
DIMENSION X1(1),X2(1),AS(12,12),LM(12)
COMMON/EL/NEGNL,NUMEG
DO 10 I=N1,NEQ
10 X2(I)=0.0D0
REWIND 17
DO 100 K=1,NUMEG
READ(17,*)(LM(I),I=1,12),((AS(I,J),J=1,12),I=1,12)
DO 50 I=1,12
DO 40 K1=N1,NEQ
IF(LM(I).NE.K1)GO TO 40
SUM=0.0D0
DO 20 K2=N1,NEQ
IF(X1(K2).EQ.0.0D0)GO TO 20
DO 30 J=1,12
IF(LM(J).NE.K2)GO TO 30
SUM=SUM+AS(I,J)*X1(K2)
30 CONTINUE
20 CONTINUE
X2(K1)=X2(K1)+SUM

```

```

40 CONTINUE
50 CONTINUE
100 CONTINUE
    REWIND 18
    DO 1100 K=1,NEGNL
    READ(18,*)(LM(I),I=1,12),((AS(I,J),J=1,12),I=1,12)
    DO 1050 I=1,12
    DO 1040 K1=N1,NEQ
    IF(LM(I).NE.K1)GO TO 1040
    SUM=0.0D0
    DO 1020 K2=N1,NEQ
    IF(X1(K2).EQ.0.0D0)GO TO 1020
    DO 1030 J=1,12
    IF(LM(J).NE.K2)GO TO 1030
    SUM=SUM+AS(I,J)*X1(K2)
1030 CONTINUE
1020 CONTINUE
    X2(K1)=X2(K1)+SUM
1040 CONTINUE
1050 CONTINUE
1100 CONTINUE
999 CONTINUE
    RETURN
    END

```

```

C
C
C
SUBROUTINE TEN(Q,R,X,NEQ)

```

```

    IMPLICIT REAL *8(A-H,O-Z)
    DIMENSION AS(12,12),DEL(12),LM(12),ASS(12,12),F(3),
1 X(1),P(1),Q(1),R(1)
    COMMON/BL/A(8000)
    REWIND 20
    REWIND 21
    DO 30 I=1,4
    READ(20,*)(LM(J),J=1,12),((AS(J,K),J=1,12),K=1,12)
    READ(21,*)((ASS(J,K),J=1,12),K=1,12)
    DO 5 II=1,12
    DEL(II)=0.0D0
    DO 3 J=1,NEQ
3 IF(LM(II).EQ.J)DEL(II)=X(J)
5 CONTINUE
    DEL(9)=DEL(3)*0.89
    DO 20 J=1,3,2
    SUM=0.0D0
    DO 20 K=1,12
    SUM=SUM+(AS(J,K)+ASS(J,K))*DEL(K)
10 CONTINUE
    F(J)=SUM
20 CONTINUE
    P(1)=DSQRT( F(1)*F(1) + F(3)*F(3))
    IF(F(3).GT.0.0D0)P(1)=-P(1)
    Q(1)=R(1)+P(1)
30 CONTINUE

```

RETURN  
END

C  
C  
C  
C

SUBROUTINE LOADV(T,DIF,ALO,PLO,TC1,TC2,M,NEQ,NU3)

IMPLICIT REAL \*8(A-H,O-Z)  
COMMON/SEV/RO,C,PI,DE,W,AK,HT,HW,HWC,TOTWT  
DIMENSION XI(12),YI(12),ZI(12),XJ(12),YJ(12),ZJ(12),  
DI(12),P1(6),P2(6),F1(6),F2(6),QI(21,8),DAD(21  
2),QQ(8),ALO(1),PLO(1)C(12,12),AWP1(12),DIF(1),LM(1  
32),B2(6,6),XM(4),XF(4),YM(4),YF(4),ZM(4),ZF(4),XT(44),  
YT(4),ZT(4),TC2(1),TC1(1),DIFF(6)CCC(3,3)  
COMMON/BL/A(8000)

REWIND 24  
READ(24,\*)(XI(I),YI(I),ZI(I),XJ(I),YJ(I),ZJ(I),D  
II(I),I=1,M)

XG=0.000  
YG=XG  
ZG=XG  
XT(1)=-35.0  
XT(2)=-35.0  
XT(3)= 35.0  
XT(4)= 35.0  
YT(1)= 35.0  
YT(2)=-35.0  
YT(3)=-35.0  
YT(4)= 35.0  
DO 5 I=1,4

XF(I)=XT(I)  
YF(I)=YT(I)  
ZT(I)=41.7  
ZF(I)=166.7  
XM(I)=XT(I)  
YM(I)=YT(I)

5 ZM(I)=ZT(I)  
CD=DCOS(DE)  
SD=DSIN(DE)  
DO 10 I=1,6  
F1(I)=0.000  
F2(I)=0.000  
10 DIFF(I)=0.000

C  
10

CALCULATION OF THE HYDROSTATIC PROPERTIES

AVP = 0.0D 00  
VOL = 0.0D 00  
ZMH = 0.0D 00  
XXMI = 0.0D 00  
YYMI = 0.0D 00  
CTX = 0.0D 00  
CTY = 0.0D 00  
DO 50 I=1,M

1 CALL O(I,XI,YI,ZI,XJ,YJ,ZJ,DI,X1,X2,Y1,Y2,Z1,  
Z2,D,SA,SB,SC,CA,CB,CC,ALEN,HT,L)

```

VOLA = R(D)*ALEN
ZGG = (Z1 + Z2)/ 0.2D 01
VOL = VOL + VOLA
ZMH = ZMH + VOLA*ZGG
AWP1(I) = R(D) * L
IF (SC.NE.0.0) AWP1(I) = AWP1(I) /DABS(SC)
AWP = AWP + AWP1(I)
CTX = CTX + AWP1(I) * X2
CTY = CTY + AWP1(I) * Y2
50 CONTINUE
BUO=VOL*G*RO
ZB = ZMH/VOL
XLCF = CTX/AWP
YLCF = CTY/AWP
C INERTIA OF WP ABOUT THEIR OWN AXES IGNORED
DO 100 I = 1,M
YYMI = YYMI + AWP1(I)*(XJ(I) - XLCF)**2
XXMI = XXMI + AWP1(I)*(YJ(I) - YLCF)**2
100 CONTINUE
XXMI = XXMI + AWP * YLCF ** 2
YYMI = YYMI + AWP * XLCF ** 2
BM5 = YYMI/VOL
BM4 = XXMI/VOL
GM4 = -ZB + BM4
GM5 = -ZB + BM5
HTZK = -HT
C CALCULATION OF THE RESTORING FORCE MATRIX
DO 750 J=1,12
DO 750 I=1,12
750 C(I,J)=0.0D0
C(4,4) = -(ZG-ZB)*G * VOL*RO + RO * G* XXMI
C(5,5) = -(ZG-ZB)*G * VOL*RO + RO * G* YYMI
DO 2300 I = 1,M
1 CALL O(I,XI,YI,ZI,XJ,YJ,ZJ,DI,X1,X2,Y1,Y2,Z1
,Z2,D,SA,SB,SC,CA,CB,CC,ALEN,HT,L)
C(3,3) = C(3,3) + RO * G* AWP1(I)
C(3,4) = C(3,4) + RO * G * AWP1(I) * (Y2-YG)
C(4,3) = C(3,4)
C(3,5) = C(3,5) + RO * G * AWP1(I) * (X2-XG)
C(5,3) = C(3,5)
C(4,4) = RO * G*AWP1(I)*(Y2-YG)**2 + C(4,4)
C(5,5) = RO * G*AWP1(I)*(X2-XG)**2 + C(5,5)
C(4,6) = -(RO * G*AWP1(I)*(Y2-YG)*(X2-XG)) + C(4,6)
C(6,4) = C(4,6)
2300 CONTINUE
DO 2301 J=1,6
DO 2301 K=1,6
2301 B2(J,K)=0.0D00
DO 2302 I=1,4
AL11=DSQRT((XH(I)-XF(I))**2+(YM(I)-YF(I))**2+(ZM(I)
1-ZF(I))**2)
AL12=DSQRT((XT(I)-XF(I))**2+(YT(I)-YF(I))**2+(ZT(I)
2-ZF(I))**2)
CALL CAB(I,XG,YG,ZG,XM,YM,ZM,XF,YF,ZF,TC2,TC1,AL22,B2)

```

```

2302 CONTINUE
DO 2350 I=1,6
DO 2350 J=1,6
C(I,J)=C(I,J)-B2(I,J)
II=0
JJ=0
IF(1.EQ.1)II=1
IF(1.EQ.3)II=2
IF(1.EQ.5)II=3
IF(J.EQ.1)JJ=1
IF(J.EQ.3)JJ=2
IF(J.EQ.5)JJ=3
IF(II.EQ.0.OR.JJ.EQ.0)GO TO 2350
CCC(II,JJ)=C(I,J)
2350 CONTINUE
REWIND 26
WRITE(26,*)((CCC(I,J),I=1,3),J=1,3)
IF(T.CE.O.O)GO TO 2401
REWIND NU3
DO 2400 I=1,12
LM(I)=0
2400 CONTINUE
LM(1)=1
LM(3)=2
LM(5)=3
WRITE(NU3,*)(LM(I),I=1,12),((C(I,J),I=1,12),J=1,12)
2401 CONTINUE
DO 2425 I=1,NEQ
ALO(I)=0.O00
2425 FLO(I)=0.O00
2450 DO 3500 I=1,M
IF((ZJ(I)).LE.HT1.AND.(ZJ(I)).GE.HT2)ZJ(I)=HT
DO 2525 J=1,6
P1(J)=0.O000
2525 P2(J)=0.O000
CALL O(I, X1,Y1, Z1,XJ, YJ,ZJ, DI,X1, X2,Y1, Y2,Z1, Z2,
1 D, SA,SB, SC,CA, CB, CC,ALEN,HT, L)
EX1 = X1*CD +Y1*SD
EX2 = X2*CD +Y2*SD.
EY1 = -X1*SD + Y1*CD
EY2 = -X2*SD + Y2*CD
EZ1 = Z1
EZ2 = Z2
D3 = RO *R(D)
AD4 = W**2 *(D3 +RO*R(D))
DL = DSQRT((EX2-EX1)**2 +(EY2-EY1)**2 +(EZ2-EZ1)**2)
DR = DL/(O.2D02)
SA = (EX2-EX1)/DL
SB = (EY2-EY1)/DL
SC = (EZ2-EZ1)/DL
CA = DSQRT((O.1D 01)-S*A**2)
CB = DSQRT((O.1D 01)-S*B**2)
CC = DSQRT((O.1D 01)-S*C**2)
EDX=(EX2-EX1)/(O.20D 02)

```

```

EDY=(EY2-EY1)/(0.2D 02)
EDZ=(EZ2-EZ1)/(0.2D 02)
DO 2500 J=1,21
CALL DUN(J,EX1,EY1,EZ1,EDX,EDY,EDZ,EXX,EY,EZ,ER)
T1 = AK*(HWC-EZ)
T2 = AK*(HWC-HT)
SH1=DSINH(T1)
SH2=DSINH(T2)
CH1=DCOSH(T1)
CE = DCOS(AK*EXX)
SE = DSIN (AK*EXX)
QI(J,1)=CE*CH1/SH2
QI(J,2)=SE*CH1/SH2
QI(J,3)=CE*SH1/SH2
QI(J,4)=SE*SH1/SH2
QI(J,5)=QI(J,1)*ER
QI(J,6)=QI(J,2)*ER
QI(J,7)=QI(J,3)*ER
QI(J,8)=QI(J,4)*ER
2500 CONTINUE
DO 2600 JJ=1,8
DO 2550 J=1,21
2550 DAD(J)=QI(J,JJ)
CALL SINY(DR,DAD,TCT3)
2600 QQ(JJ)=TCT3
XDG1 = QQ(1)*AD4*CA**2 - QQ(4)*AD4*SC*SA
XDG2 = QQ(2)*AD4*CA**2 + QQ(3)*AD4*SC*SA
YDG1 =-QQ(1)*AD4*SA*SB - QQ(4)*AD4*SC*SB
YDG2 =-QQ(2)*AD4*SA*SB - QQ(3)*AD4*SC*SB
P1(1)= XDG1*CD - YDG1*SD
P2(1)= XDG2*CD - YDG2*SD
P1(2)= XDG1*SD + YDG1*CD
P2(2)= XDG2*SD + YDG2*CD
P1(3)= -QQ(1)*AD4*SA*SC + QQ(4)*AD4*CG**2
P2(3)= -QQ(2)*AD4*SA*SC - QQ(3)*AD4*CG**2
AKEK = AD4*(EZ1*SA*SB -EY1*SA*SC)
AKEZ = AD4*(EZ1*SB*SA +EY1*CC*CC)
AMEX = AD4*(EZ1*CA*CA +EX1*SA*SC)
AMEZ = AD4*(EZ1*SC*SA +EX1*CC*CG)
ANEX = AD4*(EX1*SA*SB +EY1*CA*CA)
ANEZ = AD4*(EY1*SC*SA - EX1*SC*SB)
AK1 = AKEK*QQ(1) + AKEZ*QQ(4) +AD4*QQ(8)*SB
AK2 = AKEK*QQ(2) - AKEZ*QQ(3) -AD4*QQ(7)*SB
AM1 = AMEX*QQ(1) + AD4*QQ(5)*SC - AMEZ*QQ(4)
1 -AD4*QQ(8)*SA
AN2 = AMEX*QQ(2) + AD4*QQ(6)*SC + AMEZ*QQ(3)
2 +AD4*QQ(7)*SA
P1(4)=AK1*CD - AM1*SD
P2(4)=AK2*CD - AM2*SD
P1(5)=AK1*SD - AM1*CD
P2(5)=AK2*SD + AM2*CD
P1(6)= ANEZ*QQ(4) - ANEX*QQ(1) - AD4*SB*QQ(5)
P2(6)= ANEZ*QQ(3) - ANEX*QQ(2) - AD4*SB*QQ(6)
DO 3000 J=1,6

```



```

IF(ABS(P1(J)).LE.(0.05D 00))P1(J)=0.0D 00
IF(ABS(P2(J)).LE.(0.05D 00))P2(J)=0.0D 00
3000 F1(J) = F1(J)+ P1(J)
      F2(J) = F2(J)+ P2(J)
C
C 3500 CONTINUE
C
C CALCULATION OF LOADS DUE TO PLANE FACES
C
DO 4335 I=1,M
CALL O(I,XI,YI,ZI,XJ,YJ,ZJ,DI,X1,X2,Y1,Y2,Z1,Z2,
1 D,SA,SB,SC,CA,CB,CC,ALEN,HT,L)
KP = 1
XX=X1
YY=Y1
ZZ=Z1
AO=RO*G*R(D)
4333 T2 = AK*(HWC-HT)
      EXX = XX*CD +YY*SD
      EY = -XX*SD+YY*CD
      EZ = ZZ
      T1 = AK*(HWC-EZ)
      KJ=1
      IF (EZ.EQ.HT)KJ=0
      ACO = AO*KJ*DCOSH(T1)/DCOSH(T2)
      SAK=DSIN(AK*EXX)
      CAK=DCOS(AK*EXX)
      P1(1)=-ACO*SA*SAK
      P2(1)= ACO*SA*CAK
      P1(2)=-ACO*SB*SAK
      P2(2)= ACO*SB*CAK
      P1(3)=-ACO*SC*SAK
      P2(3)=-ACO*SC*CAK
      P1(4)= P1(3)*(YY+YG) -P1(2)*(ZZ-ZG)
      P2(4)= P2(3)*(YY+YG) -P2(2)*(ZZ-ZG)
      P1(5)= P1(1)*(ZZ-ZG) -P1(3)*(XX-XG)
      P2(5)= P2(1)*(ZZ-ZG) -P2(3)*(XX-XG)
      P1(6)= P1(2)*(XX-XG) -P1(1)*(YY-YG)
      P2(6)= P2(2)*(XX-XG) -P2(1)*(YY-YG)
DO 4334 J=1,6
4334 F1(J)=F1(J)+P1(J)
      F2(J)=F2(J)+P2(J)
4448 IF(KP.EQ.2)GO TO 4335
      KP=KP+1
      XX=X2
      YY=Y2
      ZZ=Z2
      SA = -SA
      SB = -SB
      SC = -SC
      GO TO 4333
4335 CONTINUE
4336 CONTINUE
TAB=4.0*PI/W

```

```

DO 4338 J=1,6
IF(DABS(F1(J)).LE.(0.05D00)) F1(J)=0.0D00
IF(DABS(F2(J)).LE.(0.05D00)) F2(J)=0.0D00
IF(T.GT.(2.0*TAB))GO TO 4337
F1(J)=F1(J)*T/(TAB)
F2(J)=F2(J)*T/(TAB)
4337 IF(T.LT.(2.5*T))GO TO 4338
C F1(J)=F1(J)*(T/TAB-0.24D0)
C F2(J)=F2(J)*(T/TAB-0.24D0)
4338 CONTINUE
HSA=0.0D0
DO 4500 J=1,3
I=J
IF(J.EQ.2)I=3
IF(J.EQ.3)I=5
ALO(J)=(F1(I)*DCOS(W*T)+F2(I)*DSIN(W*T))*HW
4450 PLO(J)=(-F1(I)*DSIN(W*T)+F2(I)*DCOS(W*T))*W*HW*HSA
4500 CONTINUE
RETURN
END

```

C  
C  
C  
C

SUBROUTINE SIMP(H,Q,A)

```

IMPLICIT REAL *8(A-H,O-Z)
DIMENSION Q(21)
I = -1
SUM = 0.0D 00
5 I = I + 2
J = I + 1
K = I + 2
SUM = SUM + Q(I) + Q(K) + (0.4D 01) * Q(J)
IF (I.LT.19)GO TO 5
A = H * SUM / (0.3D 01)
RETURN
END

```

C  
C  
C  
C

FUNCTION R(D)

```

IMPLICIT REAL *8(A-H,O-Z)
R = (0.314159D 01) * (D**2)/(0.4D 01)
RETURN
END

```

C  
C  
C  
C

```

SUBROUTINE O(I,XI,YI,ZI)XJ,YJ,ZJ,DI,X1,X2,Y1,Y2,Z1,
1 Z2,D,SA,SB,SC,CA,CB,CC,ALEN,RT,L)

```

```

IMPLICIT REAL *8(A-H,O-Z)
DIMENSION XI(1),XJ(1),YI(1),YJ(1),ZI(1),ZJ(1),DI(1)

```

```

X1 = XI(I)
X2 = XJ(I)
Y1 = YI(I)
Y2 = YJ(I)
Z1 = ZI(I)
Z2 = ZJ(I)
D = DI(I)
ALEN = DSQRT ((X2-X1)**2 + (Y2-Y1)**2 + (Z2-Z1)**2 )
SA = (X2-X1)/ALEN
SB = (Y2 - Y1)/ALEN
SC = ((Z2-Z1)/ALEN)
CA = DSQRT ( 1. - SA * SA)
CB = DSQRT (1.- SB*SB)
CC = DSQRT (1. - SC*SC)
L = 0
IF (Z2.EQ.HT) L = 1
RETURN
END

```

```

C
C
C
SUBROUTINE DUN(J,X1,Y1,Z1,DX,DY,DZ,X,Y,Z,RR)
C

```

```

IMPLICIT REAL *8(A-H,O-Z)
X = X1+(J-1)*DX
Y = Y1+(J-1)*DY
Z = Z1+(J-1)*DZ
RR= DSQRT((X-X1)**2 +(Y-Y1)**2 +(Z-Z1)**2)
RETURN
END

```

```

C
C
C
SUBROUTINE HATA(A,B)
C

```

```

IMPLICIT REAL *8(A-H,O-Z)
DIMENSION A(6,6),B(6,6)
DO 1 J=1,6
DO 1 K=1,6
1 A(J,K)= A(J,K)+B(J,K)
RETURN
END

```

```

C
C
C
SUBROUTINE CAT(W,G,HWC,AK)
C

```

```

IMPLICIT REAL *8(A-H,O-Z)
IF(DABS(HWC).LT.100.0)GO TO 5
GO TO 35
AK=W*W/G
SIG=(W**2)/G
A = SIG
T = 0.14D 01

```

```

10  TK = (0.5D 00)*(A +T)
    THK = TANH(HWC*TK)
    IF((TK-A)/TK - (0.0001D 00)) 20,20,15
15  IF(TK*THK -SIG) 18,20,25
18  A = TK
    GO TO 10
25  T = TK
    GO TO 10
20  AK = TK
35  CONTINUE
    RETURN
    END

```

C  
C  
C  
C

SUBROUTINE NEWCO(I,D,XG,YG,ZG,XCC,YCC,ZCC)

```

    IMPLICIT REAL *8(A-H,O-Z)
    DIMENSION D(6),XCC(1),YCC(1),ZCC(1)
    XC=XCC(1)
    YC=YCC(1)
    ZC=ZCC(1)
    DXC=D(1)+(ZC-ZG)*D(5)+(YC-YG)*D(6)
    DYC=D(2)+(XC-XG)*D(6)+(ZC-ZG)*D(4)
    DZC=D(3)+(YC-YG)*D(4)+(XC-XG)*D(5)
    XCC(1)=XC+DXC
    YCC(1)=YC+DYC
    ZCC(1)=ZC+DZC
    RETURN
    END

```

C  
C  
C  
C  
C  
C  
C

SUBROUTINE DREAD(MM)

CALLED BY AMAIN  
READS GEOMETRICAL AND WAVE DATA  
CALCULATES WAVE NUMBER

```

    IMPLICIT REAL *8(A-H,O-Z)
    COMMON/SEV/RO,G,PI,DE,W,AK,HT,HW,HWC,TOTWT
    DIMENSION XI(20),YI(20),ZI(20),XJ(20),YJ(20),
1  ZJ(20),DI(20),TC1(4),TC2(4),AC(3,3),AM(3,3)
    REWIND 16
    N1=3
    RO = 0.1025D04
    PI= 0.31415926D01
    G=0.981D01
    READ(10,*)MM,DE,W,HW,HT,HWC,TOTWT
    DHH= HWC-HT
    CALL CAT(W,G,DHH,AK)
    READ(10,*) (XI(I),YI(I),ZI(I),XJ(I),YJ(I),
2  ZJ(I),DI(I),I=1,MM)
    WRITE(24,*)(XI(I),YI(I),ZI(I),XJ(I),YJ(I),
    ZJ(I),DI(I),I=1,MM)

```

```

READ(10,*) ((AM(I,J),J=1,N1),I=1,N1)
READ(10,*) ((AC(I,J),J=1,N1),I=1,N1)
WRITE(16,*) ((AM(I,J),J=1,N1),I=1,N1)
WRITE(16,*) ((AC(I,J),J=1,N1),I=1,N1)
RETURN
END

```

C  
C

```

SUBROUTINE NPRI(N,X1,NEQQ)

```

C  
C

```

IMPLICIT REAL *8(A-H,O-Z)
DIMENSION X1(1)
COMMON/BL/A(8000)
WRITE(6,1000)N
1000 FORMAT(' ARRAY',I5)
NN=N-1
WRITE(6,*) ((NN+I),X1(I),I=1,NEQQ)
RETURN
END

```

C  
C

```

SUBROUTINE CAB(II,XG,YG,ZG,IX,IY,IZ,BX,BY,BZ,
1 TO,TI,AL,CC)

```

C  
C

```

IMPLICIT REAL *8(A-H,O-Z)
DIMENSION B(6,6),P1(6),C(6,6),T(3,3),CC(6,6)
DIMENSION IX(1),IY(1),IZ(1),BX(1),BY(1),BZ(1)
DO 7000 I=1,3
DO 7000 J=1,3
7000 T(I,J)=0.0D0
T(1,1)=-1.0D0
T(2,2)=1.0D0
T(3,3)=-1.0D0
XC=-CX
YG=GY
ZG=-GZ
XT=-IX(II)
YT=IY(II)
ZT=-IZ(II)
XB=-BX(II)
YB=BY(II)
ZB=-BZ(II)
DO 10 I=1,6
DO 10 J=1,6
10 B(I,J)=0.0D00
B(1,1)=1.0D00
B(2,2)=B(1,1)
B(3,3)=B(1,1)
B(1,5)=ZT-ZG
B(1,6)=-(YT-YG)
B(2,4)=-(ZT-ZG)
B(2,6)=XT-XG

```

```

B(3,4)=YT-YG
B(3,5)=- (XT-XG)
P1(1)=XT-XB
P1(2)=YT-YB
P4(3)=ZT-ZB
P1(4)=(ZT-ZG)*(YB-YT)-(YT-YG)*(ZB-ZT)
P1(5)=(XT-XG)*(ZB-ZT)-(ZT-ZG)*(XB-XT)
P1(6)=(YT-YG)*(XB-XT)-(XT-XG)*(YB-YT)
DO 30 I=1,3
DO 30 J=1,6
IF(I.NE.1)GO TO 23
AXT=XT
AXB=XB
GO TO .25
23 IF(I.NE.2)GO TO 24
AXT=YT
AXB=YB
GO TO .25
24 AXT=ZT
AXB=ZB
25 C(I,J)=TO*B(I,J)/AL+((TO-T1)/AL**3)*(AXB-AXT)*P1(J)
30 CONTINUE
DO 1999 I=1,6
DO 1999 J=1,6
C(I,J)=-C(I,J)
1999 B(I,J)=0.000
B(4,4)=-((ZT-ZG)*(ZB-ZT)+(YT-YG)*(YB-YG))
B(4,5)=(XT-XG)*(YB-YT)
B(4,6)=(XT-XG)*(ZB-ZT)
B(5,5)=-((XT-XG)*(XB-XT)+(ZT-ZG)*(ZB-ZT))
B(5,4)=(YT-YG)*(XB-XT)
B(5,6)=(YT-YG)*(ZB-ZT)
B(6,6)=-((XT-XG)*(XB-XT)+(YT-YG)*(YB-YT))
B(6,4)=(ZT-ZG)*(XB-XT)
B(6,5)=(ZT-ZG)*(YB-YT)
DO 50 J=1,6
C(4,J)=TO*B(4,J)/AL + (YT-YG)*C(3,J)-(ZT-ZG)*C(2,J)
C(5,J)=TO*B(5,J)/AL + (ZT-ZG)*C(1,J)-(XT-XG)*C(3,J)
50 C(6,J)=TO*B(6,J)/AL + (XT-XG)*C(2,J)-(YT-YG)*C(1,J)
DO 7060 I=1,6
DO 7060 J=1,6
7060 B(I,J)=0.000
DO 7150 LA=1,4,3
LB=LA+2
DO 7150 MA=1,4,3
MB=MA-1
DO 7150 I=LA,LB
DO 7150 JH=1,3
J= JH+MB
XX=0.
DO 7151 K=1,3
7151 XX=XX + C(I,K+MB) * T(K,JH)
7150 B(I,J)=XX
DO 7152 I=1,6

```

```

DO 7152 J=1,6
7152 C(I,J)=0.ODO
DO 7160 LA=1,4,3
LB=LA-1
DO 7160 MA= 1,4,3
MB=MA + 2
DO 7160 IL=1,3
I= IL + LB
DO 7160 J= MA,MB
XX=0.
DO 7161 K=1,3
7161 / XX= XX + T(K,IL) * B(K+LB,J)
C(I,J)=XX
7160 CC(I,J)=CC(I,J)+XX
RETURN
END

```

C

```

SUBROUTINE MOT(DT, YO, YDO, YDDO, Y, YD, YDD, FO, F, NEQ1)

```

C

```

IMPLICIT REAL*8(A-H,O-Z)
DIMENSION AT(6),BT(6),AK(6,6),AC(6,6),
1 AKK(6,7),Y(1),YO(1),YDO(1),YDD(1),
2 YDDO(1),FO(1),R(6),UD(6),
3 YD(1),AM(6,6),BM(6),BC(6),
4 BK(6,6),ATK(6,6),
5 DEF(6),F(6),DEPD(6),X(10),
6 AAC(6,6),AAK(6,6),AC1(6,6),AK1(6,6)
COMMON/BL/A(8000)
REWIND 26
REWIND 16
N1=3
N2=4

```

1

```

CONTINUE

```

C

```

READ MASS, DAMPING AND STIFFNESS MATRICES AS
INPUT DATA.

```

C

```

READ(16,*) ((AM(I,J),J=1,N1),I=1,N1)
READ(26,*) ((AC(I,J),I=1,N1),J=1,N1)
READ(16,*) ((AK(I,J),J=1,N1),I=1,N1)

```

C

```

SELECT TIME STEP DT AND CALCULATE INTEGRATION CONSTANTS

```

```

TH=1.4
THD=TH*DT
A0=6./(THD*THD)
A1=3./THD
A2=2.*A1
A3=THD/2.
A4=A0/TH
A5=A2/TH
A6=1.-3./TH
A7=DT/2.
A8=DT*DT/6.

```

C

```

INITIALISATION OF DISPLACEMENTS, VELOCITIES AND

```

C

```

AND ACCELERATIONS.
DO 2 I=1,N1
Y(I)=0.

```

```

YD(I)=0.0
DEF(I)=0.0
DEFD(I)=0.0
YDD(I)=0.0
2
C
C THE EQUATIONS ARE INTEGRATED FOR EACH TIME STEP.
DO 710 J=1,N1
AT(J)=A0*Y(J)+A2*YD(J)+2.*YDD(J)
BT(J)=A1*Y(J)+2.0*YD(J)+A3*YDD(J)
710 CONTINUE
C FORM THE EFFECTIVE STIFFNESS MATRIX
BIG=1.0E+15
BIG1=BIG
DO 712 I=1,N1
DO 712 J=1,N1
AKK(I,J)=AK(I,J)+A0*AM(I,J)+A1*AC(I,J)
IF(ABS(AKK(I,J)).GT.BIG)BIG1=ABS(AKK(I,J))
712 CONTINUE
IF((BIG1/BIG).GE.BIG)BIG=BIG*BIG1
DO 713 I=1,N1
DO 713 J=1,N1
713 AKK(I,J)=AKK(I,J)/BIG
DO 720 I=1,N1
R(I)=-FO(I)*0.4+P(I)*1.4
DO 720 J=1,N1
720 R(I)=R(I)+AM(I,J)*AT(I)+AC(I,J)*BT(I)
C DISPLACEMENT, VELOCITY AND ACCELERATION CONDITIONS
C AT THE PREVIOUS TIME STEP ARE MADE AS THE INITIAL
C CONDITIONS FOR THE PRESENT TIME STEP.
C MAKE THE LOAD TERM THE LAST TERM OF THE EFFECTIVE
C STIFFNESS MATRIX
DO 740 I=1,N1
740 AKK(I,N2)=R(I)/BIG
C SOLVE FOR DISPLACEMENTS AT TIME T+DT USING GAUSS
C ELIMINATION METHOD
DO 745 I=1,N1
DO 745 J=1,N2
745 ATK(I,J)=AKK(I,J)
CALL SOLVE(ATK,X,N1)
DO 750 I=1,N1
750 UD(I)=X(I)
C CALCULATE DISPLACEMENTS, VELOCITIES, AND ACCELERATIONS
C AT TIME T+DT
DO 760 I=1,N1
NN=I-1
YDD(I)=A4*(UD(I)-YO(I))+A5*YDO(I)+A6*YDDO(I)
YD(I)=YDO(I)+A7*(YDD(I)+YDDO(I))
Y(I)=YO(I)+DT*YDO(I)+A8*(YDD(I)+2.*YDDO(I))
760 CONTINUE
RETURN
END
C
C SUBROUTINE SOLVE(A,X,N)

```



```

      IMPLICIT REAL*8(A-H,O-Z)
      DIMENSION A(6,7),X(6)
      M=N+1
      L=N-1
      DO 12 K=1,L
      JJ=K
      BIG=ABS(A(K,K))
      KP1=K+1
C      SEARCH FOR LARGEST POSSIBLE PIVOT ELEMENT
      DO 7 I=KP1,N
      AB=ABS(A(I,K))
      IF(BIG-AB)6,7,7
6      BIG=AB
      JJ=I
7      CONTINUE
C      DECISION ON NECESSITY OF ROW INTERCHANGE
      IF(JJ-K)8,10,8
C      ROW INTERCHANGE
8      DO 9 J=K,M
      TEMP=A(JJ,J)
      A(JJ,J)=A(K,J)
      A(K,J)=TEMP
9      CALCULATION OF ELEMENTS OF NEW MATRIC
C      DO 11 I=KP1,N
10     QUOT=A(I,K)/A(K,K)
      DO 11 J=KP1,M
11     A(I,J)=A(I,J)-QUOT*A(K,J)
      DO 12 I=KP1,N
12     A(I,K)=0.
C      FIRST STEP IN BACK SUBSTITUTION
      X(N)=A(N,M)/A(N,N)
C      REMAINDER OF BACK-SUBSTITUTION PROCESS
      DO 14 NN=1,L
      SUM=0.
      I=N-NN
      IP1=I+1
      DO 13 J=IP1,N
13     SUM=SUM+A(I,J)*X(J)
14     X(I)=(A(I,M)-SUM)/A(I,I)
      RETURN
      END

```

---

```

SUBROUTINE REIN(D,V,ACN,NEQ)

```

```

C      IMPLICIT REAL *8(A-H,O-Z)
      DIMENSION D(100),V(100),ACN(100),X(4),Z(4)
      X(1)=-35.000
      X(2)=-35.000
      X(3)=35.000
      X(4)=35.000
      DO 5 I=1,4
      Z(I)= 41.7
5      NP=1+(NEQ-15)/8

```

```

CN=NF
DN=CN
I=1
J=4
10 CONTINUE
AC=DN/CN
D(J)=(D(1)+Z(I)*D(3))*AC
V(J)=(V(1)+Z(I)*D(3))*AC
ACN(J)=(ACN(1)+Z(I)*D(3))*AC
IF(J.GE.16)GO TO 25
D(J+1)=(D(2)-X(I)*D(3))*AC
V(J+1)=(V(2)-X(I)*D(3))*AC
ACN(J+1)=(ACN(2)-X(I)*D(3))*AC
25 I=I+1
IF(I.NE.5)GO TO 50
I=1
DN=DN-1.0
50 CONTINUE
IF((J+2).LT.NEQ)GO TO 100
GO TO 200
100 J=J+3
IF(J-16)10,10,150
150 J=J-1
GO TO 10
200 CONTINUE
*RETURN
END

C
C
SUBROUTINE ZTEN(A1,A2,A3,A4,NEQ)
C
IMPLICIT REAL *8(A-H,O-Z)
DIMENSION A1(4),A2(4),A3(NEQ),A4(4),AD(4)
J=2
I=0
5 I=I+1
AL(I)=125.0D0
J=J+3
AL(I)=A4(I)-A2(I)*A3(J)/AL(I)
IF(I.NE.4)GO TO 5
RETURN
END

```





